Geometry & Topology

Volume 29 (2025)

Scattering amplitudes of stable curves

JENIA TEVELEV

msp

msp

Geometry & Topology **29**:6 (2025) 3063–3128
DOI: 10.2140/gt.2025.29.3063
Published: 22 September 2025

Scattering amplitudes of stable curves

JENIA TEVELEV

Hypertree divisors on the moduli space of stable rational curves were introduced by Castravet and Tevelev (2013). Their equations appear as numerators of scattering amplitude forms for n particles in $N = 4$ Yang–Mills theory in the work of Arkani-Hamed, Bourjaily, Cachazo, Postnikov and Trnka (2016). Rather than being a coincidence, this is just the tip of the iceberg of an exciting relation between algebraic geometry and high energy physics. We interpret leading singularities of scattering amplitudes of massless particles as *probabilistic Brill–Noether theory*: the study of statistics of images of n marked points under a random meromorphic function uniformly distributed with respect to the translation-invariant volume form of the Jacobian. We focus on the maximum helicity violating case, which leads to a beautiful physics-inspired geometry for various classes of complex algebraic curves: smooth, stable, hyperelliptic, real algebraic, etc.

14D20, 14E05, 14E20, 14F10, 14H10, 14H40, 14H81, 14P05

1 Introduction

1.1 In physics, momenta of n particles satisfy the momentum conservation law, $\boldsymbol{p}_1 + \cdots + \boldsymbol{p}_n = 0$. In mathematics, meromorphic forms ω with simple poles $p_1, \dots, p_n$ (log forms) on a compact Riemann surface satisfy the residue theorem:

$$\boldsymbol{p}_1 + \cdots + \boldsymbol{p}_n = 0 \qquad \text{Res}_{p_1}\,\omega + \cdots + \text{Res}_{p_n}\,\omega = 0.$$

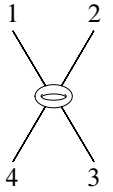

Let C be a stable projective algebraic curve with marked points $p_1, \dots, p_n$. The exact sequence

$$0 \to H^0(C, \omega_C) \to H^0(C, \omega_C(p_1 + \cdots + p_n)) \xrightarrow{\text{Res}} \mathbb{C}^n \xrightarrow{\Sigma} \mathbb{C} \to 0,$$

valid for $n \geq 1$, shows that we can always view momenta of n one-dimensional particles satisfying the momentum conservation law as residues of a form $\omega \in H^0(C, \omega_C(p_1 + \cdots + p_n))$. For a smooth curve C, ambiguities in the choice of ω can be eliminated by fixing its integrals along periods. For a nodal curve C, a local section of $\omega_C(p_1 + \cdots + p_n)$ at each node $q_1, \dots, q_r \in C$ can be identified with a log form on the normalization C^ν which has opposite residues at the points q_i^-, q_i^+ mapping to the node q_i. These residues can be viewed as momenta of "internal" or "on-shell" particles satisfying a momentum conservation law for each of the s irreducible components of C, as follows from an exact sequence

$$0 \to H^0(C^\nu, \omega_{C^\nu}) \to H^0(C, \omega_C(p_1 + \cdots + p_n)) \xrightarrow{\text{Res}} \mathbb{C}^{n+r} \xrightarrow{\Sigma_1, \dots, \Sigma_s} \mathbb{C}^s \to 0.$$

When all components of C are rational, $H^0(C^\nu, \omega_{C^\nu}) = 0$ and the datum of a log form on C is equivalent to the datum of external and internal momenta satisfying momentum conservation laws (one law for each irreducible component of C). Equivalently, this is the datum of one "edge variable" for each internal (corresponding to a node) and external (corresponding to a marked point) edge of the dual graph of C with a conservation law for each vertex of the dual graph.

1.2 Imagine a random process that gives a vector of log forms on $(C; p_1, \dots, p_n)$. What will be the probability distribution of residues? We will study the following simple random process. The first step is a random tensor product factorization

$$\omega_C(p_1 + \cdots + p_n) = L \otimes \widetilde{L} \tag{1.2.1}$$

into two line bundles, L of degree d and $\widetilde{L}$ of degree $\widetilde{d}$ (and $d + \widetilde{d} = 2g - 2 + n$). The choice of L is a choice of a point in $\text{Pic}^d\, C$ and, when C is smooth, every connected component of the Picard group has a uniform probability measure, the volume form invariant under translations by the subgroup $\text{Pic}^0\, C$ of topologically trivial line bundles. If C is not smooth then $\text{Pic}^0\, C$ contains noncompact factors $\mathbb{C}^*$ and probabilistic interpretation is less straightforward. In fact the case most related to physics literature is when all irreducible components of C are rational curves and $\text{Pic}^0\, C \simeq (\mathbb{C}^*)^g$. Noncompactness will not be an issue for us.

1.3 The second step is a choice of sections $s_\alpha \in H^0(C, L)$, $\widetilde{s}_{\widetilde{\alpha}} \in H^0(C, \widetilde{L})$ for some indices $\alpha \in I$ and $\widetilde{\alpha} \in \widetilde{I}$. Tensoring these sections gives a matrix of log forms

$$\omega_{\alpha\widetilde{\alpha}} = s_\alpha \otimes \widetilde{s}_{\widetilde{\alpha}} \in H^0(C, \omega_C(p_1 + \cdots + p_n)).$$

We focus on the case $|I| = |\widetilde{I}| = 2$, which is related to the $\mathcal{N} = 4$ Yang–Mills theory. Let $\mathbb{L} \subset \mathrm{Mat}_{2,2}$ be the subvariety of matrices of rank at most 1. The projectivization $\mathbb{P}(\mathbb{L})$ is a quadric in $\mathbb{P}^3$ isomorphic to $\mathbb{P}^1 \times \mathbb{P}^1$. Let

$$Y = \{\boldsymbol{p}_1, \dots, \boldsymbol{p}_n \in \mathbb{L} \mid \boldsymbol{p}_1 + \cdots + \boldsymbol{p}_n = 0\} \subset \mathbb{L}^n.$$

The space $\mathrm{Mat}_{2,2}$ can be viewed as the complexified 4-dimensional Minkowski space and $\mathbb{L}$ as the complexified light cone. Thus Y parametrizes complexified momenta of n massless particles in 4 dimensions satisfying the momentum conservation law. We observe that $(\mathrm{Res}_{p_1} \omega_{\alpha\widetilde{\alpha}}, \dots, \mathrm{Res}_{p_n} \omega_{\alpha\widetilde{\alpha}}) \in Y$, since each matrix $\mathrm{Res}_{p_i} \omega_{\alpha\widetilde{\alpha}}$ is proportional to the matrix $(s_\alpha(p_i)\widetilde{s}_{\widetilde{\alpha}}(p_i))$ after choosing trivializations. So this matrix has rank at most one and the residues of $\omega_{\alpha\widetilde{\alpha}}$ (at marked points and nodes) can be viewed as momenta of massless (external and internal) particles.

This construction is reversible, at least in the most physically relevant case. Namely, suppose all components of C are rational and the dual graph is 3-valent. Given massless momenta $\boldsymbol{p}_1, \dots, \boldsymbol{p}_n$ (external) and $\boldsymbol{q}_1, \dots, \boldsymbol{q}_r$ (internal) satisfying momentum conservation laws (one for each vertex of the dual graph), suppose that no two momenta adjacent to the same vertex are proportional. Then there exists a factorization (1.2.1) and sections $s_\alpha \in H^0(C, L)$, $\widetilde{s}_{\widetilde{\alpha}} \in H^0(C, \widetilde{L})$ for $\alpha, \widetilde{\alpha} = 1, 2$ such that the momenta are the residues[1] of the 2×2 matrix of log forms $(s_\alpha \otimes \widetilde{s}_{\widetilde{\alpha}})$.

1.4 We would like to focus on situations where there are no constraints on external and internal momenta, ie when a dense subset of points of Y can be obtained as residues up to a finite ambiguity. This requires imposing the condition[2]

$$n = g + 3. \tag{1.4.1}$$

1.5 We would like to study distribution of residues of the matrix $\omega_{\alpha\widetilde{\alpha}}$ but we run into a problem: there is no natural probability measure on the space of sections s_α, $\widetilde{s}_{\widetilde{\alpha}}$ unless we choose some extra data such as a hermitian metric on L. Instead of making a choice of a specific probability measure, we can design an experiment with outcomes that don't depend on sections by introducing a rational (ie defined on an

[1] Indeed, let $(\omega_{\alpha\widetilde{\alpha}})$ be the 2×2 matrix of log forms that corresponds to the momenta. Since the restriction of $\omega_C(p_1 + \cdots + p_n)$ to every irreducible component of C has degree 1, the sections $\omega_{\alpha\widetilde{\alpha}}$ globally generate the line bundle $\omega_C(p_1 + \cdots + p_n)$ and therefore give a morphism $C \to \mathbb{P}^3$ such that every irreducible component of C maps to a line. By assumption, images of marked points and nodes belong to the quadric $\mathbb{P}(\mathbb{L})$. Since a line intersecting a quadric in 3 different points belongs to it, the image of C lies on the quadric, ie the matrix of log forms has rank 1. The line bundles L and $\widetilde{L}$ are pullbacks of $\mathcal{O}_{\mathbb{P}^1 \times \mathbb{P}^1}(1, 0)$ and $\mathcal{O}_{\mathbb{P}^1 \times \mathbb{P}^1}(0, 1)$, where $\mathbb{P}(\mathbb{L}) \cong \mathbb{P}^1 \times \mathbb{P}^1$.

[2] By the Riemann–Roch theorem, $H^0(C, L)$ and $H^0(C, \widetilde{L})$ have expected dimensions $r = d + 1 - g$ and $\widetilde{r} = \widetilde{d} + 1 - g$. Rescaling all s_α by $z \in \mathbb{C}^*$ and $\widetilde{s}_{\widetilde{\alpha}}$ by z^{-1} gives the same forms $\omega_{\alpha\widetilde{\alpha}}$ and so the same residues. Thus the variety of choices $(L, \widetilde{L}, s_\alpha, s_{\widetilde{\alpha}})$ modulo $\mathbb{C}^*$ has expected dimension $g + 2r + 2\widetilde{r} - 1 = g + 2n - 1$. On the other hand, Y is a variety of dimension $3n - 4$ (assuming $n \geq 4$). Thus the condition on dimensions is $g + 2n - 1 = 3n - 4$, which is equivalent to (1.4.1).

open subset) map $\Lambda\colon Y \dashrightarrow M$ to some algebraic variety M. If Λ is independent of sections s_α and $\widetilde{s}_{\widetilde{\alpha}}$ then it descends to a rational map $\mathbf{\Lambda}\colon \mathrm{Pic}^d\, C \dashrightarrow M$ and describing a probability measure on M becomes a well-posed problem. Concretely, projecting the quadric $\mathbb{P}(\mathbb{L}) \cong \mathbb{P}^1 \times \mathbb{P}^1$ to the first or the second factor gives rational maps $\mathbb{L}^n \dashrightarrow (\mathbb{P}^1)^n$ known as spinor variables in physics. Taking a quotient by the PGL_2 action gives a rational map $(\mathbb{P}^1)^n \dashrightarrow M_{0,n}$ to the moduli space of n distinct marked points on $\mathbb{P}^1$. To summarize, we have two rational maps

$$\Lambda, \widetilde{\Lambda}\colon Y \hookrightarrow \mathbb{L}^n \dashrightarrow (\mathbb{P}^1)^n \dashrightarrow M_{0,n}.$$

The image of a point $(\mathrm{Res}_{p_1} \omega_{\alpha\widetilde{\alpha}}, \dots, \mathrm{Res}_{p_n} \omega_{\alpha\widetilde{\alpha}})$ under the map Λ (resp. $\widetilde{\Lambda}$) is given by an n-tuple $([s_1(p_i) : s_2(p_i)])_{i=1\dots,n}$ (resp. $([\widetilde{s}_1(p_i) : \widetilde{s}_2(p_i)])_{i=1\dots,n}$) of points in $\mathbb{P}^1$ modulo PGL_2. One can further compactify $M_{0,n}$ by the Grothendieck–Knudsen moduli space $\overline{M}_{0,n}$ of stable rational curves or choose a different compactification.

Requiring that Λ descends to $\mathbf{\Lambda}\colon \mathrm{Pic}^d\, C \dashrightarrow M_{0,n}$ obviously means that the expected dimension of $H^0(C, L)$, which in the physical context is known as helicity, should be equal to 2. By Riemann–Roch, this is equivalent to the requirement

$$d = g + 1. \tag{1.5.1}$$

1.6 Definition Let $(C; p_1, \dots, p_n)$ be a stable curve of genus g with $n = g + 3$ marked points. Fix a multidegree vector $\vec{d} = (d_i)$ (one degree d_i for each irreducible component of C) such that $d = \sum d_i$ satisfies (1.5.1). This gives a connected component $\mathrm{Pic}^{\vec{d}}\, C \subset \mathrm{Pic}^d\, C$. We say that a pair $(C, \vec{d})$ is *a maximum helicity violating* (*MHV*) *curve* if, for a generic line bundle $L \in \mathrm{Pic}^{\vec{d}}\, C$, we have:

(1) L is not special, ie it has exactly two linearly independent global sections,

$$H^0(C, L) = \mathbb{C}^2 \quad \text{and} \quad H^1(C, L) = 0.$$

(2) The evaluation map $\alpha\colon H^0(C, L) \otimes \mathbb{O}_C \to L$ is surjective; equivalently,

$$\varphi_L\colon C \dashrightarrow \mathbb{P}^1$$

is a morphism (which is automatic if C is smooth) and $L \simeq \varphi_L^* \mathbb{O}_{\mathbb{P}^1}(1)$.

(3) The rational *scattering amplitude map*

$$\mathbf{\Lambda}\colon \mathrm{Pic}^{\vec{d}}\, C \dashrightarrow M_{0,n}, \quad L \mapsto (\varphi_L(p_1), \dots, \varphi_L(p_n)),$$

is dominant at L, or equivalently, generically finite.

1.7 Definition The *scattering amplitude form* of an MHV curve is a unique (up to a constant multiple) nonzero $\mathrm{Pic}^{\vec{0}}\, C$-invariant holomorphic g-form

$$A \in H^0(\mathrm{Pic}^{\vec{d}}\, C, \Omega^g),$$

viewed as a multivalued meromorphic form on $M_{0,n}$.

1.8 Summary We start with a stable curve C of genus g with $n = g + 3$ marked points. The MHV experiment is a choice of a random line bundle L of degree $d = g + 1$ or, equivalently, a random meromorphic function $\varphi_L : C \to \mathbb{P}^1$ of degree d. When C is smooth, the probability distribution of L is uniform with respect to the translation-invariant volume form on the Jacobian. We study probability measures on $M_{0,n}$ that give statistics of points $\varphi_L(p_1), \dots, \varphi_L(p_n) \in \mathbb{P}^1$. This gives a family of (complexified) probability measures that depend on $4g$ complex parameters describing the input curve $(C, p_1, \dots, p_n) \in \overline{M}_{g,n}$.

1.9 Remark It is clearly superfluous to keep the notation g, d, n for quantities related by the equations (1.4.1) and (1.5.1) throughout this paper. Our excuse is that they are associated with the main players, the curve C, its Picard group and $M_{0,n}$.

1.10 Example An MHV curve of genus 0 is just $\mathbb{P}^1$ with three marked points. In this case $d = 1$ and $\operatorname{Pic}^1 C$ is a point, namely the line bundle $L = \mathbb{O}_{\mathbb{P}^1}(1)$. The map $\varphi_L : \mathbb{P}^1 \to \mathbb{P}^1$ is an isomorphism which maps p_1, p_2, p_3 to three distinct points, which can be moved to the points $0, 1, \infty$ by applying the PGL_2 action. It follows that the scattering amplitude map $\mathbf{\Lambda}$ in genus 0 is simply

$$\mathrm{pt} = \operatorname{Pic}^1 \mathbb{P}^1 \xrightarrow{\mathbf{\Lambda}} M_{0,3} = \mathrm{pt}\,.$$

1.11 Notation A connected component $\operatorname{Pic}^{\vec{d}} C$ of the Picard group is determined by multidegrees $d_s = \deg L|_{C_s}$, one for each irreducible component $C_s \subset C$. We have $d = \sum d_s$. We draw an MHV curve as an *on-shell diagram*, a dual graph of C with marked points as exterior legs. Vertices of the diagram correspond to irreducible components of C and interior edges correspond to nodes. Genus-zero components are drawn as circles, components of positive genus g_s are decorated with g_s holes. Components where the line bundle has degree $d_s = 0$ are left blank, components of degree $d_s = 1$ are shaded black, and if $d_s > 1$ then we just write d_s in or next to the component. If the curve is irreducible then we don't indicate the degree at all since it's always equal to $g + 1$.

The advantage of the on-shell diagram over the dual graph of the stable curve is that it records the multidegrees $\vec{d}$ of L. In Theorem 4.4, we will show that the locus of MHV curves is open. In particular, the set of possible on-shell diagrams is closed under edge contractions.

1.12 Example In genus 1 there are many possibilities, illustrated in Figure 1. Here $d = 2$ and $n = 4$. So the map $\varphi_L : C \to \mathbb{P}^1$ is a double cover and the scattering amplitude map $\mathbf{\Lambda}$ takes $L \in \operatorname{Pic}^2 C$ to the cross-ratio of four points

$$\varphi_L(p_1), \quad \varphi_L(p_2), \quad \varphi_L(p_3), \quad \varphi_L(p_4) \in \mathbb{P}^1.$$

It turns out that if C is a smooth elliptic curve, then $\mathbf{\Lambda} : \operatorname{Pic}^2 C \to \mathbb{P}^1$ is a double cover and the scattering amplitude form A is an integrand of an elliptic integral.

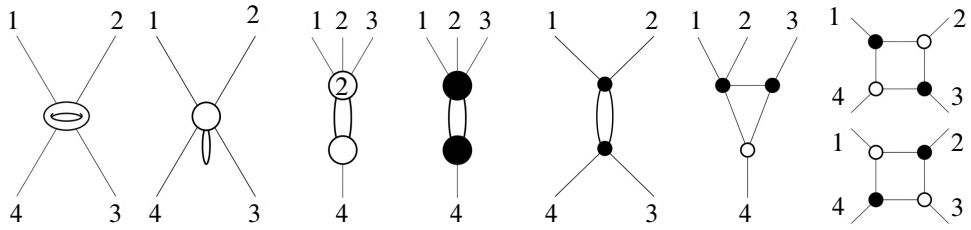

Figure 1: On-shell diagrams of MHV curves of genus 1.

The calculations in genus 0 and 1 motivate the following theorem,[3] which is explored from different points of view in subsequent sections.

1.13 Theorem *The scattering amplitude map $\mathbf{\Lambda}$ has degree 2^g for a general curve C.*

1.14 Contents of Section 2 One of the goals of the paper is to *localize* 2^g line bundles in the preimage of a general point of $M_{0,n}$, ie to describe branches of the multivalued inverse function $\mathbf{\Lambda}^{-1}$. In Theorem 2.3 we show that every smooth curve is an MHV curve. We use the theory of special divisors [Arbarello et al. 1985], which was classically developed to study the images of Abel–Jacobi maps, in particular the focus was on the $d = g-1$ case. The MHV regime $d = g+1$ is just as rich and exciting. We introduce various special divisors in $\mathrm{Pic}^{g+1} C$ as well as the *planar locus* W that parametrizes presentations of the curve C as a nodal plane curve of degree $g+1$.

1.15 Contents of Section 3 Given that all smooth curves are MHV curves, one expects a simple classification of stable MHV curves, but this is quite a delicate question, which we start to investigate in this section. These results are not central to the paper but they are used throughout. If the curve C has a node such that removing it separates C into two connected components (ie the on-shell diagram is not 2-connected), then C is not an MHV curve — the only MHV curves with compact Jacobians are smooth curves. This is known as a *one-channel factorization* in physics. If the on-shell diagram is 2-connected but not 3-connected (more precisely, if C has a two-channel factorization, see Definition 3.11), then C is separated into two components by removing two nodes, and information about the scattering amplitude can be read from the components; see Theorems 3.16 and 3.18.

1.16 Contents of Section 4 To study families of MHV curves and scattering amplitudes, we introduce the universal scattering amplitude map

$$\mathbf{\Lambda} : \mathcal{P}ic^{\mathrm{MHV}}\,\mathcal{C} \dashrightarrow M_{0,n}$$

over the locus of MHV curves $\overline{\mathcal{M}}^{\mathrm{MHV}}_{g,n} \subset \overline{\mathcal{M}}_{g,n}$. We use two open substacks in the stack of quasimaps: moduli of stable quotients [Marian et al. 2011] and moduli of presentations of slope-stable line bundles.

[3] Since the paper first appeared on the arXiv, many further interpretations and generalizations of this "Tevelev degree" have been investigated; see eg [Buch and Pandharipande 2021; Cela 2023; Cela and Lian 2023; Cela et al. 2022; Farkas and Lian 2023; Lian 2023; Lian and Pandharipande 2021].

We find a convenient polarization for MHV curves and compactify $\mathcal{P}ic^{\mathrm{MHV}}\,\mathcal{C}$ by a projective family of compactified Jacobians.

1.17 Example 1.12, continued While a smooth elliptic curve E degenerates into a wheel C of *four* projective lines, $\mathrm{Pic}^2 E$ degenerates into $\overline{\mathrm{Pic}}^{\mathrm{MHV}}C$, a wheel of *two* projective lines, the MHV components $\mathrm{Pic}^{0,1,0,1}$ and $\mathrm{Pic}^{1,0,1,0}$ represented by stacked on-shell diagrams on the right side of Figure 1. Each of these components has the same amplitude form, a phenomenon called *square move* by physicists. For any of the curves in Figure 1, the fiber of the universal scattering amplitude map is a ramified double cover of $\mathbb{P}^1$ by an irreducible curve of arithmetic genus 1 except for the four-wheel, when it becomes a reducible 2 : 1 cover

$$\overline{\mathrm{Pic}}^{\mathrm{MHV}}C = \mathbb{P}^1 \cup \mathbb{P}^1 \xrightarrow{2:1} \mathbb{P}^1 = \overline{M}_{0,4}.$$

1.18 Contents of Section 5 Scattering amplitude maps and forms of hyperelliptic curves give a new perspective on the theory of parabolic vector bundles of rank 2 on $\mathbb{P}^1$. A hyperelliptic curve C is given by the equation $y^2 = f(z)$, where f is a polynomial of degree $2g+2$ or $2g+1$ without multiple roots. This gives a double cover map

$$\varphi_h \colon C \to \mathbb{P}^1, \quad (z, y) \mapsto z.$$

Marked points $p_1, \dots, p_n$ project to points $z_1, \dots, z_n \in \mathbb{P}^1$, which we assume are different. In the study of pointed hyperelliptic curves it is often assumed that all marked points are Weierstrass points (the roots of $f(z)$), but in our approach the marked points are decoupled from the Weierstrass points. We show in Lemma 5.6 that the scattering amplitude map of hyperelliptic curves factors as

$$\mathbf{\Lambda} : \mathrm{Pic}^{g+1} C \xrightarrow{\bar{\mathbf{\Lambda}}} \mathrm{Bun}(\mathbb{P}^1; z_1, \dots, z_n) \xrightarrow{\Xi} M_{0,n},$$

where $\mathrm{Bun}(\mathbb{P}^1; z_1, \dots, z_n)$ is the moduli stack of parabolic rank 2 bundles with trivial determinant, the map $\bar{\mathbf{\Lambda}}$ associates to a line bundle $L \in \mathrm{Pic}^{g+1} C$ its pushforward $(\varphi_h)_* L$ with parabolic lines determined by marked points, and finally Ξ is a very basic birational map which can be described as follows. A projectivization of a generic parabolic vector bundle is a ruled surface $\mathbb{P}^1 \times \mathbb{P}^1$ with points $(z_1, q_1), \dots, (z_n, q_n)$ giving the parabolic structure, and the map Ξ assigns $(q_1, \dots, q_n)$ to this bundle; see Figure 2. It follows that in the hyperelliptic case the scattering amplitude map combines effects of the birational morphism Ξ, which only depends on $z_1, \dots, z_n$ but not on C, and the map $\bar{\mathbf{\Lambda}}$, which is thus a finer invariant in the hyperelliptic case. To study the scattering amplitude form as a form on the moduli space of parabolic bundles, we have to choose its projective model. We study effects of a well-known wall-crossing between projective models and the action of the Weyl group $W(D_n)$ by elementary transformations.

1.19 Contents of Section 6 In Theorem 6.2 we make another step towards proving Theorem 1.13: we show that the scattering amplitude map $\mathbf{\Lambda}$ has degree 2^g for every hyperelliptic curve C. We use beautiful results of Jacobi [1846] (amplified by Moser and then Mumford [1984]) that give an explicit model for the

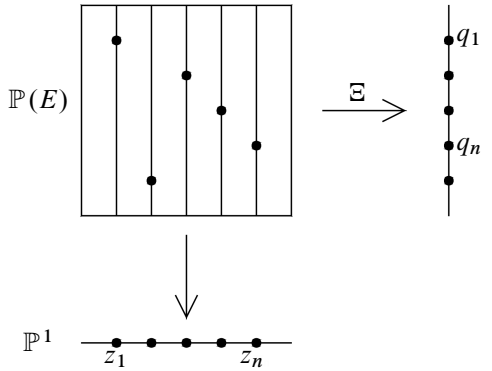

Figure 2: The map $\Xi : \mathrm{Bun}(\mathbb{P}^1; z_1, \dots, z_n) \dashrightarrow M_{0,n}$ given by $(E; V_1, \dots, V_n) \mapsto (q_1, \dots, q_n)$.

Jacobian of a hyperelliptic curve (with a removed theta-divisor) as the orbit space of conjugacy classes of 2×2 polynomial matrices. Moreover, translation-invariant vector fields on the Jacobian can be described in the form of the Lax differential equation, and this can be used to compute branches of the scattering amplitude form.

1.20 Contents of Section 7 In genus 2, where every curve is hyperelliptic, we combine methods of Section 5 with a classical observation of Halphen [1882]: a sufficiently general divisor $P = p_1 + \cdots + p_n$ of marked points on a smooth MHV curve embeds it $\varphi_P : C \hookrightarrow \mathbb{P}^3$ as a degree $n = g + 3$ space curve. This gives a way to study the scattering amplitude using geometry of $\mathbb{P}^3$. By the results of Section 5, the scattering amplitude map $\mathbf{\Lambda} : \mathrm{Pic}^3 C \dashrightarrow \overline{M}_{0,5} \simeq \mathbf{dP}_5$ into the quintic del Pezzo surface factors through the moduli space of parabolic vector bundles of rank 2, which in this case is the quartic del Pezzo surface $\mathbf{dP}_4$. In Theorem 7.6 we resolve this map by a finite morphism $\overline{\mathbf{\Lambda}} : \mathrm{Bl}_{16} \mathrm{Pic}^3 C \to \mathbf{dP}_4$ of degree 4 from the blow-up of $\mathrm{Pic}^3 C$ in 16 special points to the quartic del Pezzo surface. We show in Theorem 7.7 that whenever all marked points are Weierstrass points, $\overline{\mathbf{\Lambda}}$ becomes a well-known map: it factors as a composition of two double covers,

$$\mathrm{Bl}_{16} \mathrm{Pic}^3 C \xrightarrow{2:1} \mathrm{K3} \xrightarrow{2:1} \mathbf{dP}_4,$$

where the K3 surface is the minimal resolution of the Kummer surface. For general marked points away from the Weierstrass points, the intermediate K3 surface disappears from the picture but the degree 4 scattering amplitude morphism $\overline{\mathbf{\Lambda}}$ as well as the *double sixteen* configuration on the abelian surface survive.

1.21 Contents of Section 8 In this section we inject a measure of reality into the study of scattering amplitude forms of smooth curves. In order to obtain real probability measures, we have to turn to real algebraic geometry. The answer is beautiful for smooth real curves with the maximal number of real ovals, so called M-curves, with marked points distributed as in Figure 3: either all marked points are real and all ovals contain one marked point except for one that contains three (type A) or all but two marked points are real, one for each real oval, and the other two are complex-conjugate (type B). The main result of

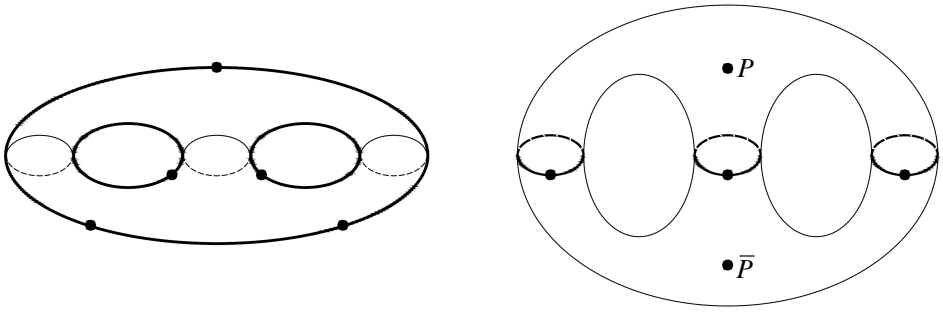

Figure 3: MHV M-curves of type A, left, and type B, right.

this section is Theorem 8.6: line bundles in every fiber of the scattering amplitude map $\mathbf{\Lambda}$ over $M_{0,n}(\mathbb{R})$ "localize" into different connected components (there are conveniently exactly 2^g of them)

$$\mathrm{Pic}_I^{g+1}\,\mathbb{R} \subset \mathrm{Pic}^{g+1}\,\mathbb{R}.$$

We use this theorem of real algebraic geometry to prove Theorem 1.13, which is a theorem of complex algebraic geometry. Back to M-curves, in Theorem 8.10 we show that the scattering amplitude map $\mathbf{\Lambda}$ gives real-analytic open immersions

$$\mathbf{\Lambda}_I : \mathrm{Pic}_I^{g+1}\,\mathbb{R} \hookrightarrow M_{0,n}(\mathbb{R})$$

from an open dense subset of every connected component of $\mathrm{Pic}^{g+1}\,\mathbb{R}$. This gives real probability measures $|A_I|$ on $M_{0,n}(\mathbb{R})$ that depend on $4g$ real parameters. For an especially nice connected component $\mathrm{Pic}_H^{g+1}\,\mathbb{R}$, which we call the *Huisman component*, the scattering amplitude map induces a real-analytic isomorphism

$$\mathbb{R}^g/\mathbb{Z}^g \simeq \mathrm{Pic}_H^{g+1}\,\mathbb{R} \xrightarrow{\mathbf{\Lambda}} (\mathbb{RP}^1)^g,$$

which gives a positive, smooth (in fact real-analytic) scattering amplitude probability measure on $(\mathbb{RP}^1)^g$; see Theorem 8.12. As an example, we study scattering amplitude probability measures in genus 2, which produces pretty probability density functions as in Figure 4.

1.22 Contents of Section 9 In this section we describe *maximally degenerate* stable MHV curves, ie curves with trivalent on-shell diagrams. By combining results from [Castravet and Tevelev 2013] and [Arkani-Hamed et al. 2015], we show that they are given by CT hypertrees: collections $\Gamma = \{\Gamma_1, \dots, \Gamma_d\}$ of triples in $\{1, \dots, n\}$ that satisfy

$$(\ddagger) \qquad \left| \bigcup_{j \in S} \Gamma_j \right| \geq |S| + 2 \quad \text{for every } S \subset \{1, \dots, d\}.$$

For example, as observed in [Castravet and Tevelev 2013], every checkerboard triangulation of a 2-sphere gives a CT hypertree, in fact two of them. Vertices of the triangulation give the indexing set $\{1, \dots, n\}$ and

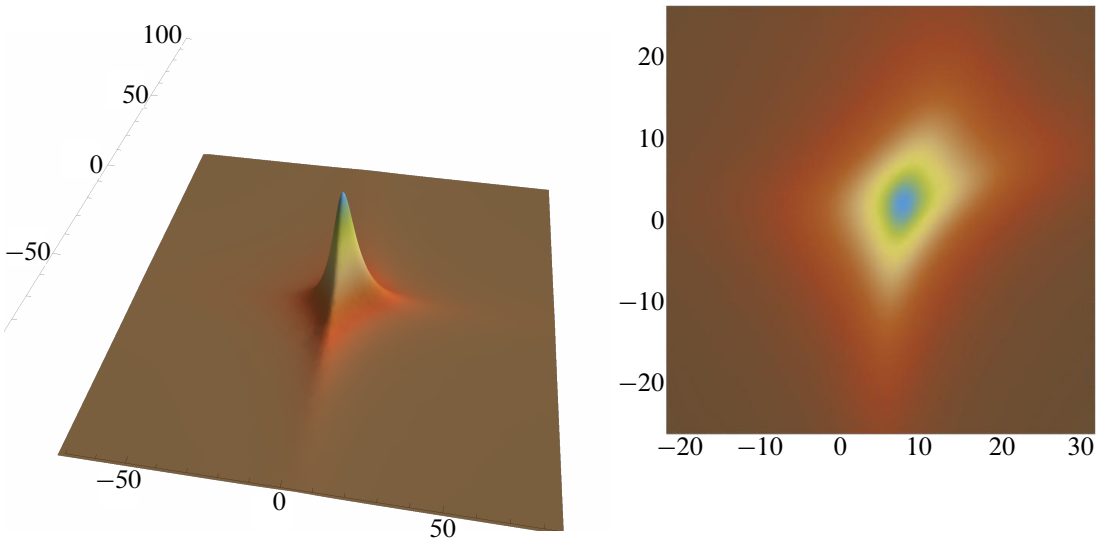

Figure 4: Scattering amplitude probability measures in genus 2.

black triangles give triples; see Figure 5. Another CT hypertree is given by white triangles. The scattering amplitude perspective uncovers geometry of spherical CT hypertrees: in Theorem 9.11 we show that they appear as stable degenerations of real MHV M-curves. Beautiful results of Tutte on arborescences associated with triangulations make an appearance in the proof.

1.23 Contents of Section 10 Here we compare our compactified Jacobian approach to a traditional Grassmannian approach of [Arkani-Hamed et al. 2016], especially in the non-MHV case.

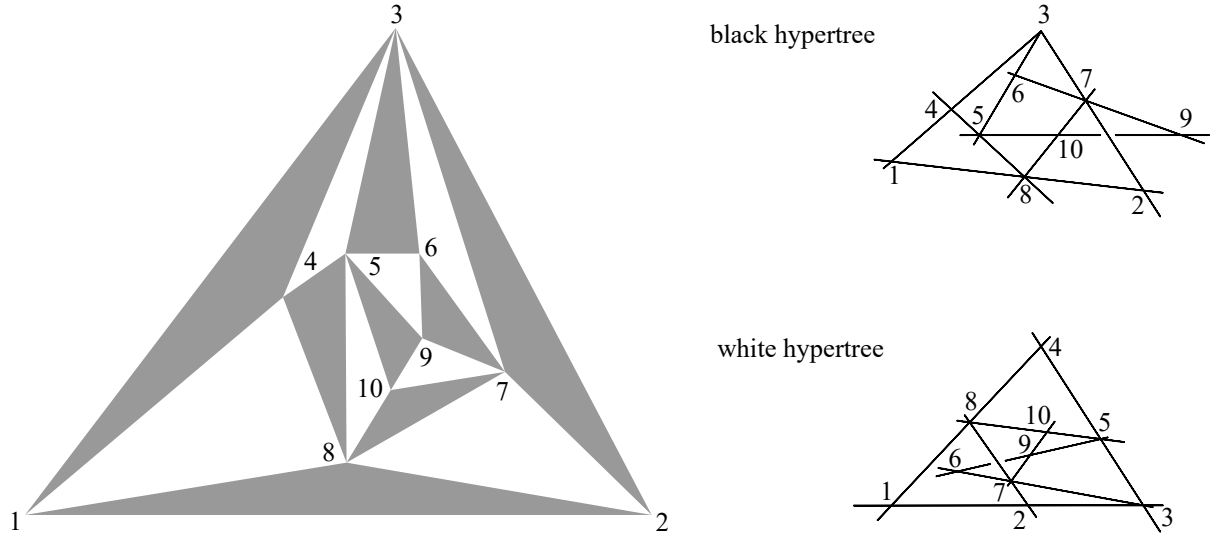

Figure 5: Two spherical CT hypertrees from the same triangulation [Castravet and Tevelev 2013].

Acknowledgements I am grateful to Ana-Maria Castravet and Rahul Pandharipande for useful discussions, and to the referee for comments and corrections. The paper started from a correspondence with Freddy Cachazo and Nick Early, who brought [Arkani-Hamed et al. 2015] to my attention. The project was supported by the NSF grants DMS-1701704 and DMS-2101726 and a Simons Fellowship.

Graphics by www.wolfram.com/mathematica and www.plainformstudio.com.

2 Massless Brill–Noether theory

2.1 Example Let C be a smooth genus-1 curve with 4 marked points $p_1, \dots, p_4$. Every line bundle $L \in \operatorname{Pic}^2 C$ gives a double cover $\varphi_L \colon C \xrightarrow{2:1} \mathbb{P}^1$ presenting C in the form $y^2 = f(x)$, where f is a polynomial of degree 3 or 4. Recall that

$$M_{0,4} \simeq \mathbb{P}^1 \setminus \{0, 1, \infty\}$$

via the cross-ratio function of four points. We compactify $M_{0,4}$ by $\overline{M}_{0,4} \simeq \mathbb{P}^1$. If we denote by $q_1, \dots, q_4$ the images of marked points $\varphi_L(p_1), \dots, \varphi_L(p_4)$ then the scattering amplitude map $\mathbf{\Lambda}$ takes $L \in \operatorname{Pic}^2 C$ to their cross-ratio function

$$\frac{q_4 - q_1}{q_2 - q_1} \cdot \frac{q_2 - q_3}{q_4 - q_3}.$$

Of course $\operatorname{Pic}^2 C \simeq C$ but not canonically. In fact $\operatorname{Pic}^2 C$ has 6 distinguished points

$$p_{ij} = \mathbb{O}(p_i + p_j), \quad \text{with } i \neq j,$$

and carries a natural degree-2 line bundle

$$\mathcal{L} = \mathbb{O}(p_{12} + p_{34}) \simeq \mathbb{O}(p_{13} + p_{24}) \simeq \mathbb{O}(p_{14} + p_{23}).$$

The images of points $p_{ij} \in \operatorname{Pic}^2 C$ under the scattering amplitude map are

$$\mathbf{\Lambda}(p_{14}) = \mathbf{\Lambda}(p_{23}) = 0, \quad \mathbf{\Lambda}(p_{13}) = \mathbf{\Lambda}(p_{24}) = 1, \quad \mathbf{\Lambda}(p_{12}) = \mathbf{\Lambda}(p_{34}) = \infty,$$

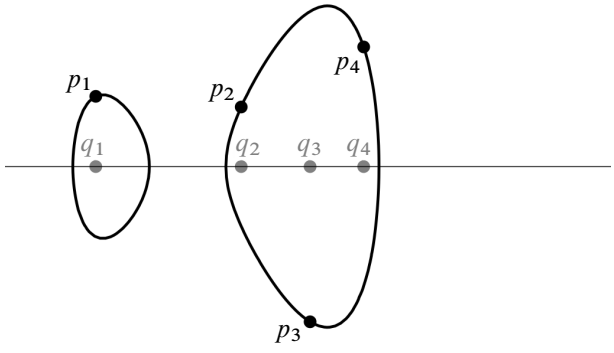

Figure 6

and $\mathbf{\Lambda}$ is the double cover

$$\varphi_{\mathcal{L}}\colon \mathrm{Pic}^2 C \xrightarrow{2:1} \mathbb{P}^1.$$

In the complex torus model $\mathrm{Pic}^2 C = \mathbb{C}/\mathbb{Z}+\mathbb{Z}\tau$, the inverse of the scattering amplitude map $\mathbf{\Lambda}$ is given by the elliptic integral

$$z = \int_{x_0}^{x} \frac{dx}{\sqrt{g(x)}},$$

where g is a degree-4 or degree-3 polynomial. To summarize:

(1) The scattering amplitude form $A(x) = dx/\sqrt{g(x)}$ has 4 branch points.

(2) The curve C is uniquely determined by the scattering amplitude form.

(3) Marked points $p_1, \dots, p_4$ are determined by $\mathbf{\Lambda}^{-1}(0)$, $\mathbf{\Lambda}^{-1}(1)$ and $\mathbf{\Lambda}^{-1}(\infty)$, but not uniquely: the action of the Klein 4-group that permutes the marked points $p_1, \dots, p_4$ in pairs is not detected by the scattering amplitude.

2.2 Remark A special case is when $p_1, \dots, p_4$ are 2-torsion points of an elliptic curve with origin p_1. We identify $\mathrm{Pic}^2 C$ with $C = \mathrm{Pic}^1 C$ by tensoring with $\mathcal{O}(p_1)$. Then $\mathcal{L}$ is identified with $\mathcal{O}(2p_1)$. The 6 points p_{ij} specialize to 3 points p_2, p_3, p_4, each with multiplicity 2. A special feature of this scattering amplitude form is that three of its branch points are at $0, 1, \infty$. The fourth one determines the j-invariant. More generally, we will see in Section 5 that scattering amplitudes of hyperelliptic curves can detect whether or not the marked points are at the Weierstrass points.

2.3 Theorem *Every smooth pointed curve $(C; p_1, \dots, p_n)$ of genus g is an MHV curve.*

Proof Recall that $n = g+3$ and $d = g+1$. We are going to use repeatedly that a generic line bundle of degree less than g is not effective [Arbarello et al. 1985]. Let L be a generic line bundle of degree $g+1$. Then $\omega_C \otimes L^*$ is also a generic line bundle. Since its degree is $(2g-2)-(g+1) = g-3 < g$, we have $h^1(L) = h^0(\omega_C \otimes L^*) = 0$, ie L is not special. This proves part (1) of Definition 1.6.

Next, we verify part (2). If $p \in C$ then $h^1(L(-p)) = h^0(\omega_C \otimes L^*(p))$. Since the degree of $\omega_C \otimes L^*(p)$ is $g-2$, it is effective only if can be written as $\mathcal{O}(x_1+\cdots+x_{g-2})$ for some points on the curve. It follows that $L \simeq \omega_C(p - x_1 - \cdots - x_{g-2})$. But the locus of these line bundles is at most $(g-1)$-dimensional, which contradicts the fact that L is generic. Thus L is globally generated.

We claim that $\varphi_L(p_i) \neq \varphi_L(p_j)$ when $i \neq j$, ie $\mathbf{\Lambda}(L) \in M_{0,n}$ for a generic L. Indeed, $h^1(L(-p_i-p_j)) = h^0(\omega_C \otimes L^*(p_i+p_j)) = 0$ since its degree is $g-1 < g$. Thus φ_L sends p_i and p_j to different points of $\mathbb{P}^1$.

To show that the scattering amplitude map $\mathbf{\Lambda}\colon \mathrm{Pic}^{g+1} C \dashrightarrow M_{0,n}$ is generically finite, we compute its differential at a generic point. Tensoring an exact sequence

$$0 \to \mathcal{O}(-P) \to \mathcal{O} \to \bigoplus_{i=1}^{g+3} \mathcal{O}_{p_i} \to 0,$$

where $P = p_1 + \cdots + p_{g+3}$, with $\varphi_L^*(T_{\mathbb{P}^1}) \simeq \mathbb{O}(L^{\otimes 2})$ gives an exact sequence

$$H^0(C, L^{\otimes 2}(-P)) \to H^0(C, \varphi_L^*(T_{\mathbb{P}^1})) \to \bigoplus_{i=1}^{g+3} H^0(p_i, \varphi_L^*(T_{\mathbb{P}^1})) \to H^1(C, L^{\otimes 2}(-P)).$$

Since $L^{\otimes 2}(-P)$ has degree $2(g+1)-(g+3) = g-1$, both ends of the sequence vanish for generic L and we have an isomorphism

$$H^0(C, \varphi_L^*(T_{\mathbb{P}^1})) \simeq \bigoplus_{i=1}^{g+3} H^0(p_i, \varphi_L^*(T_{\mathbb{P}^1})) \simeq \mathbb{C}^{g+3}.$$

In other words, every infinitesimal deformation of points $\varphi_L(p_1), \ldots, \varphi_L(p_{g+3})$ in $\mathbb{P}^1$ is induced by an infinitesimal deformation of the map $C \to \mathbb{P}^1$ which, since $H^1(C, L) = 0$, is given by an infinitesimal deformation of L and infinitesimal PGL_2 action. It follows that the differential of $\mathbf{\Lambda}$ is an isomorphism at L. □

Analyzing the special loci from the proof of Theorem 2.3 gives the following.

2.4 Amplification (planar locus W and special divisors $E, E_{ij}, R \subset \mathrm{Pic}^{g+1} C$)

(1) L is not special away from the image W of the map

$$\mathrm{Sym}^{g-3} C \to \mathrm{Pic}^{g+1} C, \quad (x_1, \ldots, x_{g-3}) \mapsto \omega_C(-x_1 - \cdots - x_{g-3}).$$

(2) L is basepoint-free away from the image E of the map

$$C \times \mathrm{Sym}^{g-2} C \to \mathrm{Pic}^{g+1} C, \quad (p, x_1, \ldots, x_{g-2}) \mapsto \omega_C(p - x_1 - \cdots - x_{g-2}).$$

(3) $\mathbf{\Lambda}(L)$ is in $M_{0,n}$ when L is away from E and the images E_{ij} for $1 \le i < j \le n$ of the maps

$$\mathrm{Sym}^{g-1} C \to \mathrm{Pic}^{g+1} C, \quad (x_1, \ldots, x_{g-1}) \mapsto \omega_C(-x_1 - \cdots - x_{g-1} + p_i + p_j).$$

(4) Let $\Theta \subset \mathrm{Pic}^{2g+2}$ be the image of the map

$$\mathrm{Sym}^{g-1} C \to \mathrm{Pic}^{2g+2} C, \quad (x_1, \ldots, x_{g-1}) \mapsto \mathbb{O}(x_1 + \cdots + x_{g-1} + p_1 + \cdots + p_{g+3}).$$

The scattering amplitude map $\mathbf{\Lambda}$ is unramified away from E, E_{ij} and the locus $R = m^{-1}(\Theta)$, where m is the map

$$m\colon \mathrm{Pic}^{g+1} C \to \mathrm{Pic}^{2g+2} C, \quad L \mapsto L^{\otimes 2}.$$

(5) $W \subset E \cap \bigcap_{i \neq j} E_{ij}$ has codimension 3 in $\mathrm{Pic}^{g+1} C$.

(6) E_{ij} and Θ are theta-divisors.

(7) E is a theta-divisor if C is hyperelliptic, otherwise $E \equiv (g-1)\Theta$.

(8) The divisor R is algebraically equivalent to 4Θ.

Proof Recall that theta-divisors are defined up to translation by an element of $\mathrm{Pic}^0 C$ and are not preserved by any nonzero translation. The locus of effective divisors in $\mathrm{Pic}^{g-1} C$ is "the" theta-divisor. Thus everything follows from the proof of Theorem 2.3, except for the calculation of the class of the ramification divisor R, which follows from the theorem of the cube, and the class of the "difference divisor" E. If C is hyperelliptic then $\omega_C(p-x_1-\cdots-x_{g-2}) \sim K_C-(g-2)h+p+x_1+\cdots+x_{g-2}$, where h is the hyperelliptic divisor, and so E is the translate of the theta-divisor. If C is not hyperelliptic, the class of E in the Neron–Severi group was computed in [Farkas et al. 2003, Proposition 3.7(b)]. □

2.5 Remark (i) As pointed out by the referee, [Farkas et al. 2003, Proposition 3.7] studies the image of the difference map

$$\psi_{b,a}\colon \mathrm{Sym}^b C\times \mathrm{Sym}^a C\to \mathrm{Pic}^{b-a} C,\quad (p_1,\dots,p_b)\times(x_1,\dots,x_a)\mapsto \mathbb{O}_C(p_1+\cdots+p_b-x_1-\cdots-x_a)$$

only under the assumption that $1\le b\le a\le \frac{1}{2}(g-1)$, which is stronger than ours ($b=1$, $a=g-2$). However, their argument works verbatim in our case. We only need to show that $\psi_{1,g-2}$ is birational onto its image if C is not hyperelliptic. Arguing by contradiction, take two different points in a fiber, $p_1-x_1-\cdots-x_{g-2}\sim p_1'-x_1'-\cdots-x_{g-2}'$, for a general $(g-1)$-tuple $p_1,x_1,\dots,x_{g-2}$. Then $p_1+x_1'+\cdots+x_{g-2}'\sim p_1'+x_1+\cdots+x_{g-2}$. If these divisors are different, then by Riemann singularity theorem and dimension count, $\dim \mathrm{Sing}\,\Theta\ge g-3$, which contradicts Martens' theorem since C is not hyperelliptic. Thus these divisors are the same, and so $p_1=x_i$ for some i, which contradicts generality.

(ii) Divisors E, E_{ij} and R all provide natural polarizations of $\mathrm{Pic}^{g+1} C$. Note especially that E is independent of the marked points $p_1,\dots,p_n$.

2.6 Loci E and E_{ij} After choosing a compactification of $M_{0,n}$, for example $\overline{M}_{0,n}$, the scattering amplitude map (as any rational map) will extend generically along divisors E and E_{ij}. Line bundles $L\in E$ have base locus but (away from W) still determine meromorphic functions $\varphi_L\colon C\to\mathbb{P}^1$. However, moving base points doesn't change φ_L but changes L and as a result $\mathbf{\Lambda}$ contracts E to a locus of smaller dimension, most dramatically to a point $o\in M_{0,n}$ in the hyperelliptic case (see Corollary 5.13). This produces a singularity in the scattering amplitude probability measure. By contrast, divisors E_{ij} are largely harmless: extension of $\mathbf{\Lambda}$ maps E_{ij} to the locus in the compactification of $M_{0,n}$ where two marked points in $\mathbb{P}^1$ come together, for example to the boundary divisor Δ_{ij} in the case of $\overline{M}_{0,n}$. Here is an example of a different and very ergonomic compactification.

2.7 Lemma *Fix three indices, for example $g+1, g+2, g+3$. The scattering amplitude map induces a generically finite rational map*

$$\mathbf{\Lambda}\colon \mathrm{Pic}^{g+1} C \dashrightarrow M_{0,n}\xrightarrow{\pi_1,\dots,\pi_g} (\overline{M}_{0,4})^g\simeq(\mathbb{P}^1)^g, \tag{2.7.1}$$

where $\pi_i\colon M_{0,n}\to\overline{M}_{0,4}$ for $i=1,\dots,g$ is the forgetful morphism given by the indices i, $g+1$, $g+2$ and $g+3$. A general line bundle $L\in\mathrm{Pic}^{g+1} C$ is mapped by π_i to the cross-ratio of the points $\varphi_L(p_i)$, $\varphi_L(p_{g+1})$, $\varphi_L(p_{g+2})$, $\varphi_L(p_{g+3})$. Let $L\in\mathrm{Pic}^{g+1} C\setminus\{R\cup E\}$. If the points $\varphi_L(p_{g+1})$, $\varphi_L(p_{g+2})$ and $\varphi_L(p_{g+3})$ are different, then (2.7.1) is regular and unramified at L.

Proof Identical to the last paragraph of the proof of Theorem 2.3. □

2.8 Locus W We call W the *planar locus*: generically along W, φ_L is a morphism

$$\varphi_L : C \to \mathbb{P}^2. \tag{2.8.1}$$

If C is a general curve, φ_L realizes it as a degree-$(g+1)$ plane curve with $\frac{1}{2}g(g-3)$ nodes away from the marked points $p_1, \dots, p_n$. Generically along W, the scattering amplitude map is resolved by the blow-up

$$\mathbf{\Lambda} : G = \mathrm{Bl}_W \operatorname{Pic}^{g+1} C \dashrightarrow M_{0,n}. \tag{2.8.2}$$

In the language of Brill–Noether theory [Arbarello et al. 1985], G parametrizes pencils of divisors on C of degree $g+1$. Let

$$\widehat{W} \subset G$$

be an exceptional divisor over W. The map $\widehat{W} \to W$ is a $\mathbb{P}^2$-bundle (generically along W). Generically along $\widehat{W}$, the map $\mathbf{\Lambda}$ of (2.8.2) can be described as follows: a point $(L, p) \in \widehat{W}$ gives both a "planar realization" (2.8.1) and a point $p \in \mathbb{P}^2$. Projecting points

$$\varphi_L(p_1), \dots, \varphi_L(p_n) \in \mathbb{P}^2$$

from p gives points $q_1, \dots, q_n \in \mathbb{P}^1$. The class of $(q_1, \dots, q_n)$ in $M_{0,n}$ is the image of (L, p) under $\mathbf{\Lambda}$. By [Castravet and Tevelev 2012, Theorem 3.1], $\mathbf{\Lambda}(D_W) \subset \overline{M}_{0,n}$ is a divisor covered by surfaces

$$S = \mathrm{Bl}_{\varphi_L(p_1),\dots,\varphi_L(p_n)} \mathbb{P}^2 \tag{2.8.3}$$

for general $L \in W$ unless points $\varphi_L(p_1), \dots, \varphi_L(p_n)$ lie on a conic, in which case the conic is contracted to a point.

2.9 Lemma *The multivalued scattering amplitude form A on $M_{0,n}$ has branches that vanish along the divisor $\mathbf{\Lambda}(D_W)$ with multiplicity 2.*

Proof Equivalently, we claim that the pullback of the scattering amplitude form A on $\operatorname{Pic}^{g+1} C$ to G vanishes to the order 2 along $\widehat{W}$. But W has codimension 3 and for a blow-up $\pi : G = \mathrm{Bl}_W X \to X$ with exceptional divisor $\widehat{W}$, one has $\pi^* K_X = K_G(-k\widehat{W})$, where $k = \operatorname{codim}_W X - 1$. □

2.10 Example W is empty in genus 1 and 2. For a curve of genus 3,

$$W = \{K\} \in \operatorname{Pic}^4 C,$$

and $\varphi_K : C \to \mathbb{P}^2$ is an embedding of C as a quartic curve if C is not hyperelliptic and a $2:1$ map to a conic in $\mathbb{P}^2$ if C is hyperelliptic. If C is a general quartic (resp. hyperelliptic) curve then S as in (2.8.3) is a general smooth (resp. nodal) cubic surface. This is related to the fact that $M_{0,6}$ has another projective model, the Segre cubic threefold in $\mathbb{P}^4$, and S is its hyperplane section. At the moment little is known about divisors $\mathbf{\Lambda}(\widehat{W}) \subset M_{0,n}$ for $g > 3$.

3 One- and two-channel factorization

3.1 Recall that the on-shell diagram is the dual graph of C decorated with degrees of $L \in \mathrm{Pic}^{\vec{d}}\, C$ on its irreducible components. If C is an MHV curve then none of these degrees are negative since L is globally generated. However, some of the degrees can be equal to 0. The corresponding components are contracted by the map $\varphi_L : C \to \mathbb{P}^1$. The union of irreducible components where $L \in \mathrm{Pic}^{\vec{d}}\, C$ has degree 0 can be written as a disjoint union of maximal connected components

$$C_1^{(0)}, \dots, C_r^{(0)}.$$

The following lemma is essentially from [Arkani-Hamed et al. 2015]:

3.2 Lemma *If C is an MHV curve then each connected component $C_i^{(0)}$ is a curve of arithmetic genus* 0 *(ie a tree of $\mathbb{P}^1$'s) with at most one marked point.*

Proof The restriction of a generic line bundle L to each $C_i^{(0)}$ is a globally generated, on the other hand generic, line bundle of degree 0. Therefore this restriction is a trivial line bundle and so the genus of each $C_i^{(0)}$ is zero. Since φ_L contracts each $C_i^{(0)}$, it can contain at most one marked point, otherwise $\mathbf{\Lambda}$ is not dominant. □

3.3 Remark One can substitute each tree $C_i^{(0)}$ of rational components with any other fixed curve of arithmetic genus zero with the same number of marked points (ie zero or one) and the same number of "outbound" points (where $C_i^{(0)}$ is connected to the rest of the curve C). This doesn't change the scattering amplitude. In the language of on-shell diagrams, Lemma 3.2 says that a subgraph of degree 0 vertices is a disjoint union of r connected trees of white circles with at most one marked point on each tree. Each of these trees can be substituted with one white *megacircle* without changing the scattering amplitude.

The following fact is very useful.

3.4 Lemma *Let C be an MHV curve. Choose two points $x, y \in C$ (not necessarily marked points). Then either x and y belong to the same rational component $C_i^{(0)}$ of Section 3.1, or*

$$\varphi_L(x) \neq \varphi_L(y)$$

for a general line bundle $L \in \mathrm{Pic}^{\vec{d}}\, C$.

Proof Let L be a general line bundle in $\mathrm{Pic}^{\vec{d}}\, C$. It gives a morphism $\varphi_L : C \to \mathbb{P}^1$. Suppose x and y are not in the same component $C_i^{(0)}$ (clearly contracted by φ_L) but $\varphi_L(x) = \varphi_L(y) = 0 \in \mathbb{P}^1$. Conditions (1) and (2) in Definition 1.6 of an MHV curve are open in $\mathrm{Pic}^{\vec{d}}\, C$. We claim that L can be deformed to force $\varphi_L(x) \neq \varphi_L(y)$. Let $g : C' \to C$ be a morphism and let $D, D' \subset C'$ be divisors defined as follows:

(1) If x is a smooth point of C and its irreducible component A containing x is not contracted by φ_L, then $C' = C$ and $D = m[x]$, where $\varphi_L^*(0) = m[x] + \cdots$ and $D' = m[x']$, where $x' \in A$ is a general point.

(2) If x is a node of C and irreducible components A and B passing through x are not contracted by φ_L (it could be that $A = B$) then C' is a partial normalization of C obtained by separating the node x, D is a divisor supported at $g^{-1}(x)$ such that $(\varphi_L \circ g)^*(0) = D + \cdots$ and D' is a general effective divisor on C' with the same multidegree as D.

(3) Finally, if $x \in C_i^{(0)}$, and letting C' be $\overline{C \setminus C_i^{(0)}}$, then D is a divisor supported at $g^{-1}(C_i^{(0)})$ such that $(\varphi_L \circ g)^*(0) = D + \cdots$ and D' is a general effective divisor on C' with the same multidegree as D.

Let $L_0 \in \mathrm{Pic}^{\vec{0}} C$ be a line bundle such that $g^* L_0 \simeq \mathbb{O}_{C'}(D' - D)$, which exists since $g^* : \mathrm{Pic}(C) \to \mathrm{Pic}(C')$ is surjective in all three cases. We can assume that $\varphi_{L \otimes L_0}(y) = 0$. We claim that $\varphi_{L \otimes L_0}(x) \neq 0$. Indeed, let s be a global section of L that vanishes at x and y and let s_0 be a rational section of L_0 such that $(g^* s_0) = D' - D$. Then $g^*(s_0 s)$ has no poles and doesn't vanish along D, and therefore $s_0 s$ is a global section of $L_0 \otimes L$ that vanishes at y but not at x. □

There are two more restrictions on MHV curves:

3.5 Lemma *Let $(C, \vec{d})$ be an MHV curve with a connected subcurve A of arithmetic genus p, and $L \in \mathrm{Pic}^{\vec{d}} C$ a generic line bundle.*

(1) *If $p > 0$, then $\deg L|_A \geq p + 1$.*

(2) *If $\deg L|_A = p + 1$, then A contains at most $p + 3$ marked points.*

Proof Indeed, $L|_A$ is both globally generated and generic, thus $\deg L|_A \geq p + 1$. This proves (1). Let $N_A \subset \{1, \ldots, n\}$ be the subset of marked points that belong to A and let n_A be its cardinality. If $\deg L|_A = p + 1$, then $\varphi_{L|_A}$ is a map $A \to \mathbb{P}^1$. The scattering amplitude map $\mathbf{\Lambda}$ is dominant, therefore the induced map $\mathrm{Pic}^{\vec{d}_A} A \to M_{0,n_A}$ that sends $L|_A$ to the configuration of points $\varphi_{L|_A}(p_i)$ for $i \in N_A$ must be dominant as well. It follows that $n_A \leq p + 3$. This proves (2). □

3.6 Corollary *Figure 1 lists all MHV curves with $g = 1$ (up to permuting markings).*

Proof A dual graph of a nodal curve of arithmetic genus 1 is a graph of genus 1, ie a genus 1 vertex or a cycle (perhaps reduced to a loop) with trees attached. By Lemma 3.5, the degree of the cycle is 2, so all trees have degree 0. By Lemma 3.2, there are actually no trees, so the on-shell diagram is a cycle. This leaves diagrams from Figure 1. □

3.7 Example Let C be an irreducible nodal curve of arithmetic genus 1 with 4 marked points $p_1, \ldots, p_4$. We view C as $\mathbb{P}^1$ with 0 and ∞ identified. Marked points $p_1, \ldots, p_4 \in \mathbb{C}^* \subset \mathbb{P}^1$. For $x, y \in \mathbb{C}^*$, the line bundle $L = \mathbb{O}([x] + [y]) \in \mathrm{Pic}^2 C$ determines the map

$$\varphi_L : C \xrightarrow{2:1} \mathbb{P}^1, \quad p \mapsto \frac{p}{(p - x)(p - y)}.$$

(Note that $\varphi_L(0)=\varphi_L(\infty)$.) It is easy to see that $\mathbb{O}([x]+[y])\simeq\mathbb{O}([x']+[y'])$ if and only if $xy=x'y'=z$ in $\mathbb{C}^*$. This gives an identification of $\mathrm{Pic}^2 C\simeq\mathbb{C}^*$. The map

$$\mathbf{\Lambda}:\mathrm{Pic}^2 C\to\overline{M}_{0,4}\simeq\mathbb{P}^1,\quad \mathbf{\Lambda}(L)=\lambda=[\varphi_L(p_1):\varphi_L(p_2);\varphi_L(p_3):\varphi_L(p_4)],$$

is the cross-ratio of points varying with L. Using invariance of the cross-ratio,

$$\begin{aligned}\mathbf{\Lambda}(L)&=\left[\frac{p_1}{(p_1-x)(p_1-y)}:\frac{p_2}{(p_2-x)(p_2-y)};\frac{p_3}{(p_3-x)(p_3-y)}:\frac{p_4}{(p_4-x)(p_4-y)}\right]\\&=\left[\frac{(p_1-x)(p_1-y)}{p_1}:\frac{(p_2-x)(p_2-y)}{p_2};\frac{(p_3-x)(p_3-y)}{p_3}:\frac{(p_4-x)(p_4-y)}{p_1}\right]\\&=\left[p_1-(x+y)+\frac{z}{p_1}:p_2-(x+y)+\frac{z}{p_2};p_3-(x+y)+\frac{z}{p_3}:p_4-(x+y)+\frac{z}{p_4}\right]\\&=\left[p_1+\frac{z}{p_1}:p_2+\frac{z}{p_2};p_3+\frac{z}{p_3}:p_4+\frac{z}{p_4}\right]=\lambda.\end{aligned}$$

Thus $\lambda=\mathbf{\Lambda}(z)$ extends to a map $\mathbb{P}^1\xrightarrow{2:1}\mathbb{P}^1$ that sends $0,\infty$ to $[p_1:p_2;p_3:p_4]$. The target $\mathbb{P}^1$ is the $\overline{M}_{0,4}$ and the source $\mathbb{P}^1$ is a new feature of the stable curve case, the normalization of the *compactified Jacobian* $\overline{\mathrm{Pic}^2 C}$, in this case a nodal cubic. The 1-form dz/z of $\overline{\mathrm{Pic}^2 C}$ is invariant under the group action of $\mathbb{C}^*\cong\mathrm{Pic}^{\vec{0}} C$ on $\overline{\mathrm{Pic}^2 C}$. As a form on $\overline{\mathrm{Pic}^2 C}$, the amplitude has log poles at its boundary point, but as a form of λ, the pole is located at $[p_1:p_2;p_3:p_4]\notin\{0,1,\infty\}$. To summarize:

(1) The scattering amplitude form is

$$A(\lambda)=\frac{d\lambda}{(\lambda-\lambda_0)\sqrt{f_2(\lambda)}},$$

with the log pole

$$\lambda_0=[p_1:p_2;p_3:p_4]\notin\{0,1,\infty\},$$

where f_2 is a polynomial of degree 2 with roots $\mathbf{\Lambda}(\pm\sqrt{p_1p_2p_3p_4})$.

(2) The marked points $p_1,\dots,p_4$ are determined modulo the action of the Klein 4-group that permutes them in pairs. Specifically,

$$\mathbf{\Lambda}^{-1}(0)=\{p_1p_4,p_2p_3\},\quad \mathbf{\Lambda}^{-1}(1)=\{p_1p_3,p_2p_4\},\quad \mathbf{\Lambda}^{-1}(\infty)=\{p_1p_2,p_3p_4\}.$$

3.8 Next we consider various situations when the curve C can be separated into two connected components A and B by nodes. We will use the following notation:

(1) g_A and g_B for the arithmetic genus of components A and B.

(2) d_A and d_B for the degree of $L_A=L|_A$ and $L_B=L|_B$. We have $d_A+d_B=d$.

(3) N_A and N_B for the subsets of marked points on A and B and n_A and n_B for their cardinalities. We have $n_A+n_B=n$.

3.9 One-channel factorization Let C be a nodal curve with a separating node. In other words, the on-shell diagram of C is not 2-connected. This is related to a one-channel factorization in physics where virtual particles are interchanged through the separating node. The following lemma is well-known in physics.

3.10 Lemma *A curve with a separating node is never an MHV curve. In particular, the only MHV curves with compact Jacobians are smooth curves.*

Proof We argue by contradiction. Let the node separate C into components A and B. Note that $g_A+g_B=g$. If $g_A>0$ and $g_B>0$, then $d_A\geq g_A+1$ and $d_B\geq g_B+1$ by Lemma 3.5; thus $g+1\geq g+2$, a contradiction. If $g_A=g$ and $g_B=0$ (or vice versa) then $d_A=g+1$ and $d_B=0$ by Lemma 3.5. But B contains at least two marked points, which contradicts Lemma 3.2. □

3.11 Definition (two-channel factorization) Suppose that C can be separated into A and B by two nodes but not by one node. In other words, the on-shell diagram of C is 2-connected but not 3-connected. We say that C has a *two-channel factorization* unless A (or B) is a $\mathbb{P}^1$ with a marked point and L has degree 0 on it.

3.12 Example Let $(C; p_1, p_2, p_3, p_4)$ be a curve obtained by gluing two copies of $\mathbb{P}^1$ at 0 and ∞, with p_1, p_2 on the first component and p_3, p_4 on the second. This is an example of a two-channel factorization. The MHV component of the Picard group is $\mathrm{Pic}^{1,1} C$. Every line bundle $L\in\mathrm{Pic}^{1,1} C$ can be written as $\mathcal{O}([x]+[x'])$, where x is a point of the first component and x' of the second (away from the nodes of C). Consider the map

$$\varphi_L : C \xrightarrow{2:1} \mathbb{P}^1, \quad p\mapsto \begin{cases} a+\dfrac{b}{p-x} & \text{on the first component,}\\[2mm] a'+\dfrac{b'}{p-x'} & \text{on the second component,}\end{cases}$$

where $a=a'$ and $bx'=b'x$ so that φ_L is regular. It is easy to see that $\mathcal{O}([x]+[x'])\simeq\mathcal{O}([y]+[y'])$ if and only if $x/x'=y/y'=z$. This gives an identification $\mathrm{Pic}^{1,1} C\simeq\mathbb{C}^*$.

We are studying the scattering amplitude map $\mathbf{\Lambda}:\mathrm{Pic}^{1,1} C\to\overline{M}_{0,4}\simeq\mathbb{P}^1$ given by the cross-ratio of points $\varphi_L(p_1),\dots,\varphi_L(p_4)$ varying with L. Using invariance of the cross-ratio,

$$\begin{aligned}\lambda &= \left[a+\frac{b}{p_1-x} : a+\frac{b}{p_2-x}; a+\frac{b'}{p_3-x'} : a+\frac{b'}{p_4-x'}\right]\\ &= \left[\frac{b}{p_1-x} : \frac{b}{p_2-x}; \frac{b'}{p_3-x'} : \frac{b'}{p_4-x'}\right] = \left[\frac{x}{p_1-x} : \frac{x}{p_2-x}; \frac{x'}{p_3-x'} : \frac{x'}{p_4-x'}\right]\\ &= \left[\frac{p_1}{x} : \frac{p_2}{x}; \frac{p_3}{x'} : \frac{p_4}{x'}\right] = \left[p_1 : p_2; zp_3 : zp_4\right] = \frac{zp_4-p_1}{p_2-p_1}\cdot\frac{p_2-zp_3}{zp_4-zp_3}.\end{aligned}$$

As in Example 3.7, we view the map $\mathbf{\Lambda}$ as the map from the compactified Jacobian:

$$\overline{\mathrm{Pic}^{1,1} C} = \mathbb{P}^1_z/_{\{0=\infty\}} \xrightarrow{2:1} \mathbb{P}^1_\lambda = \overline{M}_{0,4}.$$

The difference from Example 3.7 is that $\mathbf{\Lambda}(0) = \mathbf{\Lambda}(\infty) = \infty$. In particular, the scattering amplitude form, which is the $\mathrm{Pic}^{0,0} C$-invariant form dz/z written as a multivalued form of λ, has a log pole at ∞. Explicitly, from the above, we have

$$\lambda z(p_2 - p_1)(p_4 - p_3) = (zp_4 - p_1)(p_2 - zp_3). \tag{3.12.1}$$

Solving (3.12.1) for z using the quadratic formula gives, after algebraic manipulations,

$$\frac{dz}{z} = (p_1 - p_2)(p_4 - p_3)\frac{d\lambda}{\sqrt{f_2(\lambda)}},$$

where $f_2(\lambda)$ is the discriminant of this quadratic equation.

3.13 Lemma *Suppose $(C, \vec{d})$ is an MHV curve with a two-channel factorization into components A and B by nodes x and y. Let $L \in \mathrm{Pic}^{\vec{d}} C$ be a generic line bundle. Then*:

(1) $d_A = g_A + 1$, $d_B = g_B + 1$.

(2) $n_A = g_A + 3$, $n_B = g_B + 1$ (Case I), *or* $n_A = g_A + 2$, $n_B = g_B + 2$ (Case II).

(3) $H^0(A, L_A) = H^0(B, L_B) = 2$ *and* $H^1(A, L_A) = H^1(B, L_B) = 0$.

(4) L_A *and* L_B *are globally generated.*

(5) $\varphi_L(x) \neq \varphi_L(y)$. *In particular, neither A nor B contains a degree* 0 *rational component $C_i^{(0)}$ with both x and y as in Lemma 3.4.*

Proof Let $L \in \mathrm{Pic}^{\vec{d}} C$ be a generic line bundle. Consider a partial normalization map

$$\nu\colon A \sqcup B \to C$$

and an exact sequence

$$0 \to \mathbb{O}_C \to \nu_*(\mathbb{O}_A \oplus \mathbb{O}_B) \xrightarrow{\alpha} \mathbb{O}_x \oplus \mathbb{O}_y \to 0,$$

where $\alpha(f, g) = (f(x) - g(x), f(y) - g(y))$. Since $H^1(C, L) = 0$, tensoring with L gives $H^1(A, L_A) = H^1(B, L_B) = 0$. Since restrictions L_A and L_B are globally generated and neither A nor B is a $\mathbb{P}^1$ with a marked point and degree 0, we get

$$d_A = g_A + 1, \quad d_B = g_B + 1, \quad H^0(A, L_A) = H^0(B, L_B) = 2. \tag{3.13.1}$$

Next we consider the restriction map $H^0(A, L_A) \to \mathbb{C}^2$ at points x and y. We claim that it is an isomorphism (and the same for B) and in particular $\varphi_L(x) \neq \varphi_L(y)$. If not, let $s_A \in H^0(A, L_A)$ be a nonzero section that vanishes at x and y. Extension of this section by 0 on B gives a section s_1 in $H^0(C, L)$. Let $s_2 \in H^0(C, L)$ be a linearly independent section. Then the morphism $\varphi_L\colon C \xrightarrow{[s_1:s_2]} \mathbb{P}^1$ contracts B to a point. Thus all components of B have degree 0, which contradicts (3.13.1).

Finally, we study distribution of marked points among components A and B. By Lemma 3.5(2), $n_A \leq g_A + 3$ and $n_B \leq g_B + 3$. Up to symmetry, there are only two possible cases, namely (I) and (II). □

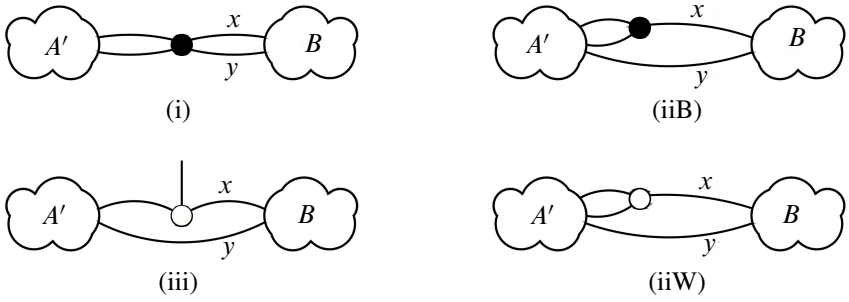

Figure 7

3.14 Amplification The proof of the lemma shows how to build the map $\varphi_L : C \to \mathbb{P}^1$. We start with the maps $\varphi_{L_A} : A \to \mathbb{P}^1$ and $\varphi_{L_B} : B \to \mathbb{P}^1$ that each map x and y to different points. Without loss of generality, we can assume that

$$\varphi_{L_A}(x) = \varphi_{L_B}(x) = 0 \quad \text{and} \quad \varphi_{L_A}(y) = \varphi_{L_B}(y) = \infty.$$

The maps φ_{L_A} and φ_{L_B} then glue and give a map $\varphi : C \to \mathbb{P}^1$, which corresponds to *some* line bundle L that restricts to L_A and L_B. The restriction map

$$\mathrm{Pic}^{\vec{d}}\, C \to \mathrm{Pic}^{\vec{d}_A}\, A \times \mathrm{Pic}^{\vec{d}_B}\, B$$

has kernel $\mathbb{C}^*$. Changing L by an element $z \in \mathbb{C}^*$ gives a map φ_{zL} such that

$$\varphi_{zL}|_A = \varphi_L|_A \quad \text{and} \quad \varphi_{zL}|_B = z\varphi_L|_B.$$

3.15 Curves A and B do not have to be stable. Suppose that A is not stable (analysis for B is the same). Then A contains a rational component that in C is attached to x or y (or both) which has less than 3 special points (marked points or nodes) once x and y are separated. Since C doesn't have a 1-channel factorization, A can't have a rational component with 1 special point (in A) attached to both x and y. Thus A is at least semistable. We list the remaining possibilities in Figure 7:

(i) A contains a 4-pointed $\mathbb{P}^1$ without marked points attached to x and y and to the rest of the subcurve A' at 2 points. Then $d_{A'} \geq g_A$ by Lemma 3.5(1) if $g_A > 1$, or by Lemma 3.2 and $n_A = 2$ if $g_{A'} = 0$. Then $d_{A'} + d_{\mathbb{P}^1} = g_A + 1$ and $d_{\mathbb{P}^1} \geq 1$ since $\varphi_L(x) \neq \varphi_L(y)$. Thus $\mathbb{P}^1$ has degree 1.

(iiW) A contains a 3-pointed $\mathbb{P}^1$ of degree 0 without marked points attached to the rest of the subcurve A' at 2 points and also to x (or y).

(iiB) A contains a 3-pointed $\mathbb{P}^1$ of degree 1 without marked points attached to the rest of the subcurve A' at 2 points and also to x (or y).[4]

(iii) A contains a 3-pointed $\mathbb{P}^1$ with a marked point attached to the rest of the subcurve A' at one point and also to x (or y). This $\mathbb{P}^1$ must have degree 0 by Lemma 3.5(1).

[4]By Lemma 3.5(1), this $\mathbb{P}^1$ can't have degree > 1.

3.16 Theorem *A curve C with a two-channel factorization such that $n_A = g_A + 3$ and $n_B = g_B + 1$ is an MHV curve if and only if*:

(1) *The stabilization $\widetilde{A}$ of A with its n_A marked points is an MHV curve that does not contain a degree 0 rational component $C_i^{(0)}$ as in Section 3.1 with both x and y.*

(2) *The curve $\widetilde{B}$ obtained by adding to B two extra marked points in addition to its n_B marked points (at the nodes separating A from B) is an MHV curve.*

A (multivalued) inverse of the map $\mathbf{\Lambda}$ at a general point $(p_1, \dots, p_n) \in M_{0,n}$ can be found as follows. Take $L_A \in \mathbf{\Lambda}_A^{-1}((p_i)_{i\in N_A})$. Then $p' = \varphi_{L_A}(x) \neq \varphi_{L_A}(y) = p''$. Take $L_B \in \mathbf{\Lambda}_B^{-1}(p', (p_i)_{i\in N_B}, p'')$. Finally, we can find L using Amplification 3.14.

Proof If A is stable then it is an MHV curve. Indeed, by Amplification 3.14 we have a commutative diagram

$$\begin{array}{ccc} \mathrm{Pic}^{\vec{d}}\, C & \xrightarrow{\mathbf{\Lambda}} & M_{0,n} \\ {\scriptstyle \mathrm{Res}_A\colon L\mapsto L_A}\big\downarrow & & \big\downarrow{\scriptstyle \pi_A} \\ \mathrm{Pic}^{\vec{d}_A}\, A & \xrightarrow{\mathbf{\Lambda}_A} & M_{0,n_A} \end{array} \tag{3.16.1}$$

where π_A is the forgetful map, and so the rational map $\mathbf{\Lambda}_A$ is dominant. If A is not stable then we claim that its stabilization $\widetilde{A}$ is an MHV curve. Indeed, cases (i) and (iiB) of Section 3.15 are impossible because the remaining part A' would have genus $g_A - 1$, degree g_A, but will contain $g_A + 3$ points, in contradiction with Lemma 3.5(2). In the remaining cases (iiW) and (iii) of Section 3.15, $\widetilde{A}$ is obtained by contracting a $\mathbb{P}^1$ (or two $\mathbb{P}^1$, one attached to x and another to y), both of degree 0. It follows that the map $\varphi_L|_A$ factors through $\widetilde{A}$ and we can argue as in the case when A is stable.

3.17 Claim *The curve $\widetilde{B}$ obtained by adding x and y to B as extra marked points is MHV.*

Proof Indeed, $\widetilde{B}$ is clearly stable and we have already checked conditions (1) and (2) in Definition 1.6 of an MHV curve.[5] We need to check that

$$\mathbf{\Lambda}_{\widetilde{B}}\colon \mathrm{Pic}^{\vec{d}_B}\, B \to M_{0,n_B+2}$$

is dominant. We use the fact that $\mathbf{\Lambda}$ is dominant, and diagram (3.16.1). Fix a general line bundle L_A on A and fix n_A points $\mathbf{\Lambda}_A(L_A) \subset \mathbb{P}^1$. Since these points include three different points in $\mathbb{P}^1$, no automorphisms of PGL_2 preserve them. We adjust homogeneous coordinates on $\mathbb{P}^1$ so that $\varphi_{L_A}(x) = 0$ and $\varphi_{L_A}(y) = \infty$. Thus $\mathbf{\Lambda}(L)$ for $L \in \mathrm{Res}_A^{-1}(L_A)$ is determined by points $\varphi_L(p_i)$ for $i \in N_B$. Since $\mathbf{\Lambda}|_{\mathrm{Res}_A^{-1}(L_A)}$ is a dominant map from a semiabelian variety of dimension $n_B = g_B + 1$, we see that the following locus of points is dense:

$$\{\varphi_L(p_i)\}_{i\in N_B} \subset (\mathbb{P}^1)^{n_B}.$$

[5] We will not use this but note that if B is not stable then case (iii) of Section 3.15 is impossible because attaching this 3-pointed $\mathbb{P}^1$ to A instead of B creates a subcurve of genus g_A, degree $g_A + 1$ with $g_A + 4$ marked points, which contradicts Lemma 3.5(2).

The map $\mathbf{\Lambda}_{\widetilde{B}}$ sends L_B to an isomorphism class of the (n_B+2)-tuple of points $(0, \varphi_L(p_i)_{i\in N_B}, \infty)$ in $\mathbb{P}^1$, equivalently to the class of $\{\varphi_L(p_i)\}_{i\in N_B}$ modulo $\mathbb{C}^*$. Therefore, $\mathbf{\Lambda}_{\widetilde{B}}$ is dominant. □

It remains to show that if A and B are as in the theorem then C is an MHV curve, and to construct a multivalued inverse of the scattering amplitude map $\mathbf{\Lambda}$. Start with a point $(p_1, \dots, p_n) \in M_{0,n}$. Since $\widetilde{A}$ is an MHV curve, we can find a line bundle L_A such that $\mathbf{\Lambda}_A(L_A) = (p_i)_{i\in N_A}$. We lift L_A to a line bundle on A. By Lemma 3.4, $p' = \varphi_{L_A}(x) \neq \varphi_{L_A}(y) = p''$. Since $\widetilde{B}$ is an MHV curve, we can find L_B such that $\mathbf{\Lambda}_B(L_B) = (p', (p_i)_{i\in N_A}, p'')$. We finish using Amplification 3.14. □

When $n_A = g_A + 2$, $n_B = g_B + 2$ (as in Example 3.12), our result is less precise.

3.18 Theorem *Suppose that C is an MHV curve with a two-channel factorization such that $n_A = g_A+2$ and $n_B = g_B+2$ which does not admit an alternative two-channel factorization as in Theorem 3.16. Then*:

(1) *The curve $\widetilde{A}$ obtained by adding to A an extra marked point (at one of the nodes separating A from B) and stabilizing is an MHV curve that does not contain a degree-0 rational component $C_i^{(0)}$ as in Section 3.1 with both x and y.*

(2) *The same for B.*

Proof Suppose that A is not stable. In cases (i) and (iii) of Section 3.15, the curve admits an alternative two-channel factorization of type considered in Theorem 3.16. Namely, in case (i) (resp. (iii)) we move the 4-pointed (resp. the 3-pointed) $\mathbb{P}^1$ to B. This gives a two channel factorization such that $n_{A'} = g_{A'} + 3$ and $n_{B'} = g_{B'} + 1$. So we will assume that neither (i) nor (iii) occurs for either A or B.

3.19 Claim *We can choose extra points p and q for A and B at one of the points x or y such that curves $\widetilde{A}$ and $\widetilde{B}$ obtained by stabilization are MHV curves.*

Indeed, if A or B is not stable and case (iiB) occurs, we would have to add an extra point to that $\mathbb{P}^1$. Note that (iiB) can only occur at one point of A, x or y, and the same for B. Indeed, otherwise A' has genus $g_A - 2$, degree $g_A - 1$ and $g_A + 2$ marked points, which contradicts Lemma 3.10(2).

If (iiB) does not occur, we are going to decide where to add an extra point later in the proof of the claim. We stabilize the curves if (iiW) occurs but the extra point p is not attached to the corresponding 3-pointed $\mathbb{P}^1$. The curves $\widetilde{A}$ and $\widetilde{B}$ are of course stable and we have already checked conditions (1) and (2) in the definition of an MHV curve. We just need to check that $\mathbf{\Lambda}_{\widetilde{A}}$ and $\mathbf{\Lambda}_{\widetilde{B}}$ are dominant. Since the situation is symmetric, we only consider $\widetilde{A}$. Suppose first that (iiB) occurs. From the commutative diagram (3.16.1), the map $\mathbf{\Lambda}_A$ is dominant. Note that an extra point p doesn't impose any conditions and can be anywhere in $\mathbb{P}^1$. Thus $\mathbf{\Lambda}_{\widetilde{A}}$ is dominant as well. Next we suppose that (iiB) does not occur. For a general line bundle $L_A \in \mathrm{Pic}^{\vec{d}_A} A$, the n_A points $\varphi_{L_A}(p_i)_{i\in N_A}$ are distinct, and as we vary L_A, span an (n_A-3)-dimensional open locus in M_{0,n_A}. It suffices to show that adding $\varphi_{L_A}(x)$ (or $\varphi_{L_A}(y)$)

gives the locus of dimension $n_A - 2 = g_A$. Equivalently, we claim that adding both $\varphi_{L_A}(x)$ and $\varphi_{L_A}(y)$ gives the locus of dimension g_A. We argue by contradiction. If this is not the case then $\varphi_{L_A}(x)$ and $\varphi_{L_A}(y)$ are determined by positions of points $\varphi_{L_A}(p_i)_{i\in N_A}$ up to a finite ambiguity. Positions of n_B points $\varphi_{L_B}(p_i)_{i\in N_B}$ are then determined by $g_B + 1$ parameters as in Amplification 3.14. Thus the locus of images of marked points has dimension at most $g_A + g_B < g$, which contradict the fact that Λ is dominant. □

4 Compactified Jacobians of MHV curves

4.1 In this section we will globalize the scattering amplitude map by the diagram

$$\begin{array}{ccc} \mathcal{P}ic_0^{\mathrm{MHV}}\,\mathscr{C} & \xrightarrow{\ \boldsymbol{\Lambda}\ } & M_{0,n} \\ \big\downarrow & & \\ \overline{\mathcal{M}}_{g,n}^{\mathrm{MHV}} & & \end{array}$$

where $\overline{\mathcal{M}}_{g,n}^{\mathrm{MHV}} \subset \overline{\mathcal{M}}_{g,n}$ is an open locus of MHV curves, $\mathcal{P}ic^{\mathrm{MHV}}\,\mathscr{C}$ is a universal MHV Picard family over it, $\mathcal{P}ic_0^{\mathrm{MHV}}\,\mathscr{C} \subset \mathcal{P}ic^{\mathrm{MHV}}\,\mathscr{C}$ is an open locus and $\boldsymbol{\Lambda}$ is the universal scattering amplitude map. We also compactify $\mathcal{P}ic^{\mathrm{MHV}}\,\mathscr{C}$ by a projective family $\overline{\mathcal{P}ic}^{\mathrm{MHV}}\mathscr{C}$ of compactified Jacobians. Recall that $n = g + 3$ and $d = g + 1$.

4.2 Consider the stack $\mathfrak{Q}_{g,n,d}$ of *quasimaps* [Ciocan-Fontanine and Kim 2010] of C to $\mathbb{P}^1$. Its sections over a scheme S are triples $(\mathscr{C}, \mathscr{L}, \alpha)$, where $\mathscr{C} \to S$ is a family of semistable curves of genus g with n marked points, $\mathscr{L}$ is a line bundle on $\mathscr{C}$ of relative degree d, and $\alpha\colon \mathcal{O}_{\mathscr{C}}^{\oplus 2} \to \mathscr{L}$ is a homomorphism which does not vanish on each fiber. The morphism

$$\nu\colon \mathfrak{Q}_{g,n,d} \to \overline{\mathcal{M}}_{g,n}$$

sends $\mathscr{C}$ to its stabilization. The stack $\mathfrak{Q}_{g,n,d}$ (and its higher-rank analogues) contains many useful open proper separated substacks.

4.3 Definition Let $\overline{\mathcal{M}}_{g,n}^{\mathrm{MHV}} \subset \overline{\mathcal{M}}_{g,n}$ be the locus of families of stable curves such that all their geometric fibers are MHV curves for some choice of $\vec{d}$. Let $\mathfrak{Q}_{g,n,d}^{\mathrm{MHV}} \subset \mathfrak{Q}_{g,n,d}$ be the locus of families of quasimaps such that, for any geometric fiber (C, L, α), the curve C is stable and (L, α) satisfies Definition 1.6(1)–(3).

4.4 Theorem (1) *$\overline{\mathcal{M}}_{g,n}^{\mathrm{MHV}}$ is an open substack of $\overline{\mathcal{M}}_{g,n}$.*

(2) *$\mathfrak{Q}_{g,n,d}^{\mathrm{MHV}}$ is an open substack of the proper and separated Deligne–Mumford stack $\overline{Q}_{g,n,d}$ of stable quotients as defined in* [Marian et al. 2011].

(3) *The morphism $\nu\colon \mathfrak{Q}_{g,n,d}^{\mathrm{MHV}} \to \overline{\mathcal{M}}_{g,n}^{\mathrm{MHV}}$ is smooth, of relative dimension n.*

(4) *Consider the action of* GL_2 *on* $\mathcal{Q}^{\mathrm{MHV}}_{g,n,d}$ *via its action on* $\mathbb{O}_{\mathscr{C}}^{\oplus 2}$. *The stabilizer of every point is the diagonal torus* $\mathbb{C}^*$. *The quotient stack* $\mathcal{P}ic_0^{\mathrm{MHV}}\mathscr{C} := [\mathcal{Q}^{\mathrm{MHV}}_{g,n,d}/\mathrm{PGL}_2]$ *is an open substack in the rigidified Picard stack of pairs* (C, L), *where* L *is a degree-*d *line bundle on* C.

(5) *For* $1 \le i < j \le n$, *let* $\Delta_{ij} \subset (\mathbb{P}^1)^n$ *be diagonals. We have a commutative diagram*

$$\begin{array}{ccc}
\mathcal{Q}^{\mathrm{MHV}}_{g,n,d} & \longrightarrow & (\mathbb{P}^1)^n \setminus \bigcup_{i,j} \Delta_{ij} \\
\big\downarrow /\mathrm{PGL}_2 & & \big\downarrow /\mathrm{PGL}_2 \\
\mathcal{P}ic_0^{\mathrm{MHV}}\mathscr{C} & \xrightarrow{\boldsymbol{\Lambda}} & M_{0,n} \\
\big\downarrow & & \\
\overline{\mathcal{M}}^{\mathrm{MHV}}_{g,n} & &
\end{array}$$

Proof Dualizing the homomorphism $\alpha\colon \mathbb{O}_C^{\oplus 2} \to L$ gives an exact sequence

$$0 \to L^* \to \mathbb{O}_C^{\oplus 2} \xrightarrow{q} Q \to 0. \tag{4.4.1}$$

The moduli space of stable quotients $\overline{Q}_{g,n,d}$ parametrizes data (4.4.1) such that Q is locally free at the nodes and at the marked points and has positive degree along all strictly semistable components of C. All these conditions are clearly satisfied in our case, in fact $q = \alpha$. From [Marian et al. 2011], we conclude that:

(1) There is a universal curve $\mathscr{C}$ over $\overline{Q}_{g,n,d}$ with n sections, and a universal quotient

$$0 \to \mathcal{S} \to \mathbb{O}_{\mathscr{C}}^{\oplus 2} \to \mathcal{Q} \to 0$$

over $\mathscr{C}$ with an invertible sheaf $\mathcal{S}$.

(2) The map $\nu\colon \overline{Q}_{g,n,d} \to \overline{\mathcal{M}}_{g,n}$ that sends $\mathscr{C}$ to its stabilization is proper.

(3) Evaluating sections $q(1,0)$ and $q(0,1)$ at the marked points $p_1, \dots, p_n$ gives evaluation maps $\mathrm{ev}_i\colon \overline{Q}_{g,n,d} \to \mathbb{P}^1$, which we combine into one morphism

$$\overline{Q}_{g,n,d} \to (\mathbb{P}^1)^n.$$

(4) All structures above are equivariant under PGL_2.

(5) $\overline{Q}_{g,n,d}$ has a 2-term obstruction theory relative to ν, given by $\mathrm{RHom}(\mathcal{S}, \mathcal{Q})$.

In particular, ν is smooth at (C, q) if $\mathrm{Ext}^1(S, Q) = 0$, which in our case follows from the short exact sequence (4.4.1) and $H^1(C, L) = 0$. Since $\nu\colon \mathcal{Q}^{\mathrm{MHV}}_{g,n,d} \to \overline{\mathcal{M}}_{g,n}$ is smooth, its image $\overline{\mathcal{M}}^{\mathrm{MHV}}_{g,n}$ is open. □

4.5 Next we show that $\mathcal{P}ic_0^{\mathrm{MHV}}\mathscr{C}$ is separated (note that the quotient by a free action of an algebraic group is often not separated). We will introduce a natural polarization A on MHV curves and study slope-stability of line bundles L with respect to it. It is well-known that slope stability on reducible curves

boils down to *Gieseker's basic inequality*: for any proper subcurve $Y \subset C$, we need to show

$$\left| d_Y - a_Y \frac{d_C}{a_C} \right| < \tfrac{1}{2}\#Y, \tag{4.5.1}$$

where

$$d_Y = \deg L|_Y, \quad a_Y = \deg A|_Y \quad \text{and} \quad \#Y := |Y \cap \overline{X \setminus Y}|.$$

Classically, the most studied case was $d_C = g-1$, $A = \omega_C$, and no marked points. This is a convenient choice because $d_C/a_C = \frac{1}{2}$. In the MHV Brill–Noether theory, when $d_C = g+1$ and marked points are present, an equally convenient choice is a fractional polarization

$$A = \omega_C + \frac{4}{n}(p_1 + \cdots + p_n),$$

which also gives $d_C/a_C = \frac{1}{2}$. The $\mathbb{Q}$-line bundle A is ample as long as C is stable curve without rational tails (subcurves of arithmetic genus 0 attached to the rest of the curve at one point), which doesn't happen for MHV curves by Lemma 3.10.

4.6 Lemma *A line bundle is A-stable if and only if*

$$d_Y > g_Y - 1 + \frac{2}{n} n_Y \tag{4.6.1}$$

for every proper connected subcurve $Y \subset C$, where g_Y is the arithmetic genus of Y and n_Y is the number of marked points on it. For semistability, the inequality is not strict.

Proof For every proper subcurve $Y \subset C$, we have to check that

$$\left| d_Y - \tfrac{1}{2} a_Y \right| < \tfrac{1}{2}\#Y.$$

For the complementary subcurve $Y^c := \overline{X \setminus Y}$, we have $d_Y - \frac{1}{2}a_Y = -d_{Y^c} + \frac{1}{2}a_{Y^c}$. Thus we just have to show that $\frac{1}{2}a_Y - d_Y < \frac{1}{2}\#Y$ for every proper subcurve Y, in fact for every proper connected subcurve, which is equivalent to (4.6.1). □

4.7 Lemma *For an MHV curve C, every line bundle $L \in \mathrm{Pic}^{\mathrm{MHV}} C$ is A-stable.*

Proof To verify (4.6.1), we consider several cases.

(1) If $d_Y \geq g_Y + 2$, the equation (4.6.1) is automatic.

(2) If $d_Y = g_Y + 1$, the equation (4.6.1) holds unless $n_Y = n$, in which case $g_Y = g$ by Lemma 3.5 and therefore $Y = C$ by Lemma 3.10, a contradiction.

(3) If $d_Y \leq g_Y$, then $d_Y = g_Y = 0$ by Lemma 3.5 and thus $n_Y \leq 1$ by Lemma 3.2. Equation (4.6.1) follows.

This finishes the proof. □

4.8 Corollary *The family $\mathcal{P}ic_0^{\mathrm{MHV}}\mathscr{C}$ over $\overline{\mathcal{M}}_{g,n}^{\mathrm{MHV}}$ is compactified by a projective (and hence separated) family $\overline{\mathcal{P}ic}^{\mathrm{MHV}}\mathscr{C}$ of compactified Jacobians. Its geometric points represent* gr*-equivalence classes of A-semistable admissible sheaves on an MHV curve C.*

4.9 Amplification If all irreducible components of C are rational, then $\overline{\mathcal{P}ic}^{\mathrm{MHV}}\mathcal{C}$ is a stable toric variety of an algebraic torus $\mathrm{Pic}^0 C \simeq (\mathbb{C}^*)^g$ and can be described as follows. Choose one on-shell diagram for C, ie endow each vertex i of the dual graph Γ of C with degree d_i such that $\sum d_i = d$. For every vertex $i \in \Gamma$,

(1) e_i is the number of edges (count each loop twice);

(2) l_i is the number of legs, ie the number of marked points on the corresponding irreducible component of C;

(3) θ_i is the Oda–Seshadri number [1979], in our case

$$\theta_i = -d_i + \frac{4l_i}{dn} + \frac{n(e_i-2)}{2d}.$$

Let C_0 and C_1 be spaces of chains of the graph Γ (with arbitrary coefficients). Let

$$\partial\colon C_1 \to C_0$$

be the differential and let H_1 be the first homology group. We can view $\theta = (\theta_i)$ as a vector in $C_0(\Gamma, \mathbb{Q})$. Consider the tiling of the affine space $\partial^{-1}(\theta) \subset C_1(\Gamma, \mathbb{Q})$ by the hyperplanes $x_i = \frac{1}{2} + \mathbb{Z}$, where x_i are the natural coordinates on C_1 (one coordinate for each edge of the graph). This affine space is parallel to the homology group $H_1(\Gamma, \mathbb{Q})$ and the tiling has to be viewed modulo the action of $H_1(\Gamma, \mathbb{Z})$. Irreducible components of the compactified Jacobian are given by the g-dimensional polytopes of the tiling and the rest of the tiling determines how they are glued.

Proof Follows from [Simpson 1994] and [Oda and Seshadri 1979], see also [Alexeev 2004]. □

4.10 Example Let $C = C_1 \cup \cdots \cup C_4$ be the following curve of arithmetic genus 1: the wheel of four $\mathbb{P}^1$'s with marked points $p_i \in C_i$ for $i = 1, \ldots, 4$. The Picard group has two MHV components:

$$\mathrm{Pic}^{\mathrm{MHV}} C = \mathrm{Pic}^{1,0,1,0} C \cup \mathrm{Pic}^{0,1,0,1} C.$$

Consider the first component. Since L has degree 0 on components C_2 and C_4, the map $\varphi_L\colon C \to \mathbb{P}^1$ contracts them to points, say $\varphi_L(C_2) = 0$ and $\varphi_L(C_4) = \infty$. The restriction of φ_L to C_1 and C_3 is an isomorphism. Thus φ_L is completely determined by points $x = \varphi_L(p_1)$ and $y = \varphi_L(p_3)$. We have an identification

$$\mathrm{Pic}^{1,0,1,0} C \simeq \mathbb{C}^*, \quad z = \frac{y}{x}.$$

The scattering amplitude map $\mathbf{\Lambda}\colon \mathrm{Pic}^{1,0,1,0} C \to \overline{M}_{0,4} \simeq \mathbb{P}^1$ is given by the cross-ratio of points $\varphi_L(p_1), \ldots, \varphi_L(p_4)$ varying with L. This map is an isomorphism:

$$\lambda = [x:0; y:\infty] = \frac{\infty - x}{0 - x} \cdot \frac{0 - y}{\infty - y} = z.$$

The scattering amplitude form is $dz/z = d\lambda/\lambda$ with log poles at 0 and ∞. Next we compute the compactified Jacobian. There are 2 types of stable line bundle and 4 types of semistable line bundle

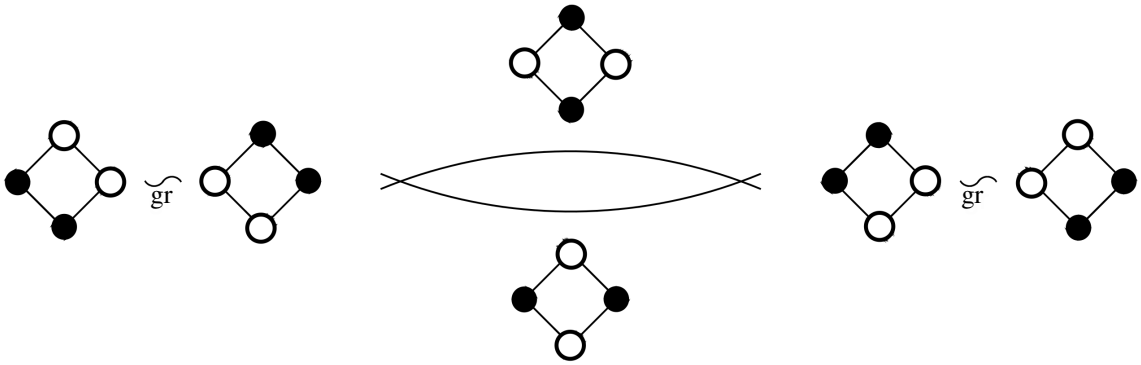

Figure 8: MHV compactified Jacobian in genus 1.

(in two gr-equivalence classes); see Figure 8. Stable components are $\mathbb{P}^1$'s and gr-equivalence classes of semistable line bundles correspond to their intersection points in the compactified Jacobian

$$\overline{\mathrm{Pic}}^{\mathrm{MHV}}C = \overline{\mathrm{Pic}}^{1,0,1,0}C \cup \overline{\mathrm{Pic}}^{0,1,0,1}C = \mathbb{P}^1 \cup \mathbb{P}^1.$$

One can visualize topology on $\overline{\mathrm{Pic}}^{\mathrm{MHV}}C$ through "chip-firing" of black chips.

4.11 Remark The MHV condition implies A-stability, but the converse is not true. For example, curves with 1-channel factorization can have A-stable line bundles. Moreover, even the compactified Jacobian of an MHV curve will typically contain non-MHV components contracted by the scattering amplitude map $\mathbf{\Lambda}$ to loci of smaller dimension either in $M_{0,n}$ or in its boundary (for some compactification of $M_{0,n}$). Nevertheless, we view A-stability and MHV conditions as close.

4.12 Example Consider a genus 2 curve with 5 rational components, each with a marked point; see the left of Figure 9 for on-shell diagrams of all possible stable line bundles. There are no strictly semistable

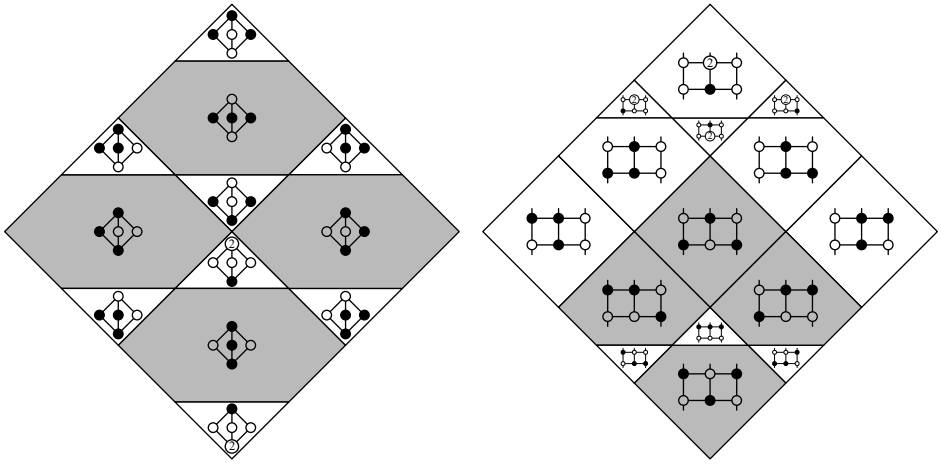

Figure 9: MHV compactified Jacobians in genus 2.

line bundles in this case. The compactified Jacobian contains 4 MHV (shaded gray) and 8 non-MHV irreducible components. They are glued in an alternating fashion, MHV to non-MHV, according to Figure 9, which is a fundamental parallelogram of a tiling of a 2-torus: components adjacent to a side of the parallelogram intersect components adjacent to the opposite side. The compactified Jacobian is a stable toric surface of the algebraic torus $\mathrm{Pic}^0 C \simeq (\mathbb{C}^*)^2$ with polygons representing its irreducible components, which are toric surfaces. MHV components are isomorphic to $\mathrm{Bl}_3 \mathbb{P}^2$ (hexagons) and non-MHV components are isomorphic to $\mathbb{P}^2$ (triangles). Crossing each of the six walls corresponds to firing a black chip across the corresponding edge of the on-shell diagram. There are two types of non-MHV components, with or without an irreducible component where L has degree 2. Under the scattering amplitude map, surfaces of the first type contract to curves intersecting the interior of $M_{0,5}$, and surfaces of the second type contract to curves in the boundary.

4.13 Example Another genus 2 example is on the right of Figure 9. There are 4 MHV components (shaded gray) and 11 non-MHV components, which are all mapped to the boundary of $M_{0,5}$ by the scattering amplitude map. Three of the MHV components are isomorphic to $\mathrm{Bl}_2 \mathbb{P}^2$ (pentagons) and one to $\mathbb{P}^1 \times \mathbb{P}^1$.

5 Scattering via moduli of parabolic bundles

5.1 Let C be a smooth hyperelliptic curve of genus $g \geq 2$ with a hyperelliptic involution $p \mapsto \tau(p)$ (whenever it exists, the hyperelliptic involution is unique). The quotient by τ is the double cover $\varphi_h : C \xrightarrow{2:1} \mathbb{P}^1$ associated with the line bundle

$$h = \mathcal{O}(p + \tau(p)) \in \mathrm{Pic}^2 C \quad \text{for } p \in C.$$

Let $p_1, \dots, p_n \in C$ be distinct marked points, where $n = g + 3$. In our approach the marked points are decoupled from $2g + 2$ Weierstrass points (fixed points of the hyperelliptic involution). To simplify the analysis, we make an assumption:

5.2 Assumption Points $\varphi_h(p_1), \dots, \varphi_h(p_n)$ are different, ie $p_i \neq \tau(p_j)$ for $i \neq j$. Thus the special feature of the hyperelliptic case is the existence of a well-defined point

$$o(p_1, \dots, p_n) = (z_1, \dots, z_n) = (\varphi_h(p_1), \dots, \varphi_h(p_n)) \in M_{0,n}, \tag{5.2.1}$$

that shouldn't be confused with the scattering amplitude map

$$\mathbf{\Lambda} : \mathrm{Pic}^{g+1} C \dashrightarrow M_{0,n}, \quad L \mapsto (\varphi_L(p_1), \dots, \varphi_L(p_n)).$$

5.3 Let $\mathrm{Bun}(\mathbb{P}^1; z_1, \dots, z_n)$ be the smooth algebraic stack of *quasiparabolic vector bundles* F on $\mathbb{P}^1$ of rank 2 with trivial determinant [Pauly 1996]. Recall that a quasiparabolic structure on a vector bundle

is a choice of a line $V_i \subset F|_{z_i}$ over each marked point. This data determines a ruled surface $\mathbb{P}(F) \to \mathbb{P}^1$ of even degree, and points

$$q_i = \mathbb{P}(V_i) \subset \mathbb{P}(F|_{z_i}) \quad \text{for } i = 1, \dots, n.$$

5.4 Definition There is a standard morphism of stacks

$$\bar{\mathbf{\Lambda}} : \mathrm{Pic}^{g+1} C \to \mathrm{Bun}(\mathbb{P}^1; z_1, \dots, z_n), \quad L \mapsto F = (\varphi_h)_* L.$$

To see that $(\varphi_h)_* L$ gives an object of $\mathrm{Bun}(\mathbb{P}^1; z_1, \dots, z_n)$, we check that its determinant vanishes. It suffices to check that $(\varphi_h)_* \mathbb{O}$ has determinant of degree $-(g+1)$. As with any double cover, we have $(\varphi_h)_* \mathbb{O} \simeq \mathbb{O} \oplus \mathcal{M}^{-1}$, where $\mathcal{M}^{\otimes 2} \simeq \mathbb{O}(B)$, where B is a branch divisor. But the number of branch points is $2g+2$; cf [Hartshorne 1977, Exercise IV.2.6].

To define parabolic lines, note that $F|_{z_i} = L|_{p_i} \oplus L|_{\tau(p_i)}$ (or $L_{p_i}/\mathfrak{m}_{p_i}^2$ if p_i is a Weierstrass point). The line $V_i \subset F|_{z_i}$ is the kernel of the surjection $F|_{z_i} \to L|_{p_i}$.

5.5 A generic parabolic bundle F is a trivial bundle[6] $\mathbb{P}^1 \times \mathbb{C}^2$ with lines $\{z_i\} \times V_i$ for $V_i \subset \mathbb{C}^2$. The corresponding ruled surface is the product $\mathbb{P}^1 \times \mathbb{P}^1$ with points $(z_1, q_1), \dots, (z_n, q_n) \in \mathbb{P}^1 \times \mathbb{P}^1$, where $q_i = \mathbb{P}(V_i)$. Thus we have a birational map $\Xi : \mathrm{Bun}(\mathbb{P}^1; z_1, \dots, z_n) \dashrightarrow M_{0,n}$ defined as in Figure 2.

5.6 Lemma *The scattering amplitude map of a hyperelliptic curve C is a composition*

$$\mathbf{\Lambda} : \mathrm{Pic}^{g+1} C \xrightarrow{\bar{\mathbf{\Lambda}}} \mathrm{Bun}(\mathbb{P}^1; z_1, \dots, z_n) \xrightarrow{\Xi} M_{0,n}.$$

The bundle $\bar{\mathbf{\Lambda}}(L)$ has splitting type $\mathbb{O} \oplus \mathbb{O}$ away from the theta-divisor E of Amplification 2.4.

Proof By Grothendieck's theorem, $(\varphi_h)_* L \simeq \mathbb{O}(-s) \oplus \mathbb{O}(s)$ for some s. We require that $s = 0$, which is equivalent to the following conditions (i) and (ii):

(i) $H^0(\mathbb{P}^1, F) = H^0(C, L) = 2$, ie L is not special. This happens outside of the locus W of Amplification 2.4.

(ii) $\mathrm{RHom}(F, \mathbb{O}(-1)) = 0$. By Grothendieck–Serre duality, this is equivalent to the vanishing of $\mathrm{RHom}(L, \mathbb{O}(-h + K + 2h)) = R\Gamma(L^*(K+h))$. This means that L has to be away from the theta-divisor

$$K + h - x_1 - \cdots - x_{g-1} = h + \tau(x_1) + \cdots + \tau(x_{g-1}) \in \mathrm{Pic}^{g-1} C,$$

where we use that $K \sim (g-1)h$. In fact this theta-divisor is the divisor E of Amplification 2.4, which contains W.

[6] Indeed, the trivial vector bundle on $\mathbb{P}^1$ does not deform, therefore these parabolic bundles are parametrized by a nonempty open substack of $\mathrm{Bun}(\mathbb{P}^1; z_1, \dots, z_n)$. On the other hand, all parabolic bundles of rank 2 and degree 0 can be deformed to a parabolic bundle with trivial F.

Choosing a basis s_1, s_2 of $H^0(C, L)$ is equivalent to choosing a splitting $F \simeq \mathbb{O} \oplus \mathbb{O}$. The scattering amplitude map $\mathbf{\Lambda}$ is given by $\big([s_1(p_1) : s_2(p_1)], \dots, [s_1(p_n) : s_2(p_n)]\big)$, which is equal to the slopes of $V_1, \dots, V_n$ inside $\mathbb{C}^2$. Thus $\mathbf{\Lambda} = \Xi \circ \overline{\mathbf{\Lambda}}$. □

5.7 Stability In view of Lemma 5.6, in the hyperelliptic case the scattering amplitude map combines effects of the birational morphism Ξ, which as we will see only depends on the point $o = (z_1, \dots, z_n)$ in $M_{0,n}$ and the map $\overline{\mathbf{\Lambda}}$, which is a finer invariant in the hyperelliptic case. Moreover, the divisor E of $\mathrm{Pic}^d C$ is mapped to a divisor by $\overline{\mathbf{\Lambda}}$ but is collapsed to the point o by $\mathbf{\Lambda}$, which creates a singularity for the probability measure; see the discussion of the real case in Section 8. However, at the moment the target of $\overline{\mathbf{\Lambda}}$ is the stack of quasiparabolic bundles. To make $\overline{\mathbf{\Lambda}}$ more concrete, we will choose a projective model for the stack (at the price of making $\overline{\mathbf{\Lambda}}$ a rational map). There is a notion of slope-stability that depends on a choice of a parabolic weight. Concretely, the weight $\vec{\alpha}$ is a sequence $\alpha_1, \dots, \alpha_n$ of real numbers with $0 < \alpha_i \le \frac{1}{2}$. A quasiparabolic bundle $(F; V_1, \dots, V_n)$ is an $\vec{\alpha}$-stable (resp. semistable) parabolic bundle if and only if every line subbundle $L \subset F$ satisfies the *slope inequality*

$$k + \sum_{i \in I} \alpha_i < \frac{1}{2} \sum_{i=1}^{n} \alpha_i \quad (\text{resp. } \le), \tag{5.7.1}$$

where $k = \deg L$ and $I \subset \{1, \dots, n\}$ is a subset of indices such that $L|_{z_i} = V_i$. We denote the corresponding moduli space by $\mathrm{Bun}_{\vec{\alpha}}(\mathbb{P}^1; z_1, \dots, z_n)$ or simply by $\mathrm{Bun}_{\alpha}(\mathbb{P}^1; z_1, \dots, z_n)$ if $\alpha_1 = \cdots = \alpha_n = \alpha$. Here is a summary of wall-crossing with chambers given by inequalities (5.7.1).

5.8 First we consider the *standard case* $\sum_{i=1}^{n} \alpha_i > 2$ as in [Bauer 1991; Mukai 2003; Araujo and Casagrande 2017; Biswas et al. 2010; Araujo et al. 2021]. If $\vec{\alpha}$ is strictly semistable, then

$$\mathrm{Pic}\, \mathrm{Bun}_{\vec{\alpha}}(\mathbb{P}^1; z_1, \dots, z_n) = \mathbb{Z}^{n+1}.$$

The Fano model (ie the model with $-K$ ample) is

$$\mathrm{Bun}_{\frac{1}{2}}(\mathbb{P}^1; z_1, \dots, z_n), \tag{5.8.1}$$

which is a smooth variety if n is odd, and has isolated singularities if n is even. As α increases from $2/n$ to $\frac{1}{2}$, $\mathrm{Bun}_{\alpha}(\mathbb{P}^1; z_1, \dots, z_n)$ undergoes the anticanonical minimal model program, ie the sequence of birational transformations that makes $-K$ more and more positive at every step. It proceeds as follows [Bauer 1991]:

(1) $\mathrm{Bun}_{2/n} = \mathbb{P}^{n-3}$ with $(\mathbb{P}^1; z_1, \dots, z_n)$ embedded into $\mathbb{P}^{n-3}$ as a rational normal curve of degree $n-3$. The MMP starts with $\mathrm{Bun}_{(2/n)+\varepsilon} = \mathrm{Bl}_{z_1,\dots,z_n} \mathbb{P}^{n-3}$.

(2) The first birational transformation "antiflips" several $\mathbb{P}^1$'s, namely lines connecting points $z_1, \dots, z_n$ pairwise and the rational normal curve. Each of these $\mathbb{P}^1$'s is blown-up and the exceptional divisor contracted onto $\mathbb{P}^{n-5}$.

(3) On the following steps, we antiflip certain $\mathbb{P}^k$'s analogously.

(4) MMP stops when $-K$ becomes big and nef on $\mathrm{Bun}_{\frac{1}{2}-\varepsilon}$, in fact even ample when n is odd. If n is even, the anticanonical model $\mathrm{Bun}_{\frac{1}{2}}$ is obtained by contracting certain K-trivial $\mathbb{P}^{(n-4)/2}$'s in $\mathrm{Bun}_{\frac{1}{2}-\varepsilon}$ to singular points.

5.9 The *special case* $\sum_{i=1}^n \alpha_i < 2$ was studied in [Moon and Yoo 2016], in which case

$$\operatorname{Pic} \mathrm{Bun}_{\vec{\alpha}}(\mathbb{P}^1; z_1, \dots, z_n) = \mathbb{Z}^n$$

if $\vec{\alpha}$ is strictly semistable. The Fano model is the symmetric GIT quotient

$$(\mathbb{P}^1)^n /\!/ \mathrm{PGL}_2,$$

which is smooth if n is odd and with isolated singularities if n is even. More generally, in the special case $\mathrm{Bun}_{\vec{\alpha}}(\mathbb{P}^1; z_1, \dots, z_n)$ is the GIT quotient $(\mathbb{P}^1)^n /\!/_{\vec{\alpha}} \mathrm{PGL}_2$ with respect to the fractional polarization $\vec{\alpha}$. The map

$$\Xi^{-1} \colon M_{0,n} \dashrightarrow \mathrm{Bun}(\mathbb{P}^1; z_1, \dots, z_n)$$

is equivalent to the natural embedding $\Xi^{-1} \colon M_{0,n} \hookrightarrow (\mathbb{P}^1)^n /\!/_{\vec{\alpha}} \mathrm{PGL}_2$.

5.10 The transition from the special (2) to the standard (1) cases goes as follows.

(2) All stable parabolic bundles have splitting type $\mathcal{O} \oplus \mathcal{O}$. The product $\mathbb{P}^1 \times \mathbb{P}^1$ with points $(z_1, z_1), \dots, (z_n, z_n)$ is stable, giving the point $o \in M_{0,n}$.

(1) The product $\mathbb{P}^1 \times \mathbb{P}^1$ above is destabilized by $\mathcal{O}(-1)$ embedded by the sequence $0 \to \mathcal{O}(-1) \to \mathcal{O} \oplus \mathcal{O} \to \mathcal{O}(1) \to 0$. The point o is blown-up. The exceptional divisor parametrizes parabolic bundles of type $\mathcal{O}(-1) \oplus \mathcal{O}(1)$.

We summarize the discussion by the following diagram:

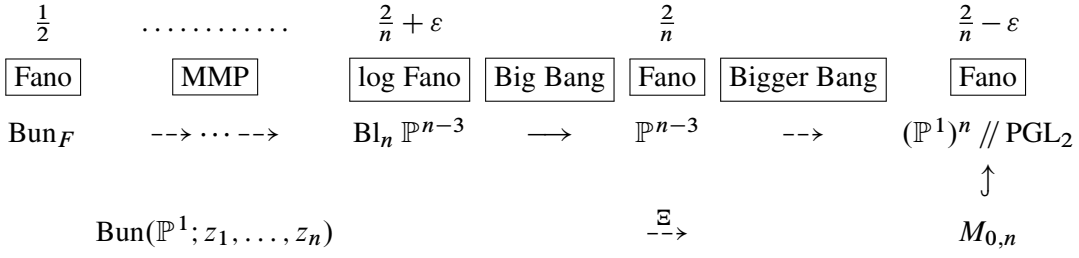

5.11 Example Suppose $g = 2$, $n = 5$. Apart from $\mathbb{P}^2$ there are only two models:

$$\mathrm{Bun}_{\frac{2}{5}+} = \mathrm{Bun}_{\frac{1}{2}} \simeq \mathrm{Bl}_{z_1,\dots,z_5} \mathbb{P}^2 = \mathbf{dP}_4 \quad \text{(standard)},$$
$$\mathrm{Bun}_{\frac{2}{5}-} \simeq \mathrm{Bl}_4 \mathbb{P}^2 = \mathbf{dP}_5 \quad \text{(special)},$$

the quartic and quintic del Pezzo surfaces. The morphism

$$\Xi \colon \mathbf{dP}_4 \to \mathbf{dP}_5 \simeq \overline{M}_{0,5}$$

contracts the conic through $z_1, \dots, z_5$ to the point $o = (z_1, \dots, z_5) \in M_{0,5}$. This morphism can also be described as projection of $z_1, \dots, z_5 \in \mathbb{P}^2$ to $\mathbb{P}^1$ from a varying point of $\mathbb{P}^2$; see [Castravet and Tevelev 2012]. We will further study this example in Section 7.

Enhancing $\mathbf{\Lambda}$ by $\overline{\mathbf{\Lambda}}$ corresponds to the transition from the special (2) to the standard (1) case of projective moduli of parabolic bundles. In the case of the Fano model, we have the following description of the indeterminacy locus of $\overline{\mathbf{\Lambda}}$.

5.12 Theorem *Consider the induced map* $\overline{\mathbf{\Lambda}} : \operatorname{Pic}^{g+1} C \dashrightarrow \operatorname{Bun}_{\frac{1}{2}}(\mathbb{P}^1; z_1, \dots, z_n)$.

(1) $\overline{\mathbf{\Lambda}}$ *is regular away from loci* $U(k, I)$ (*of codimension at least* 2) *of line bundles*

$$\mathbb{O}\left(kh + \sum_{i \in I} p_i + x_1 + \cdots + x_j\right) \subset \operatorname{Pic}^{g+1} C \quad \text{for } x_1, \dots, x_j \in C, \\ \text{where } g + 1 = 2k + |I| + j,\ j < \tfrac{1}{2}(g-1).$$

The loci $U(k, I)$ *with equality* $j = \frac{1}{2}(g-1)$ *give strictly semistable parabolic bundles.*

(2) $\overline{\mathbf{\Lambda}}^*(-K) \equiv 4\Theta$.

Proof First we check (1) using an argument from [Biswas et al. 2010]. Suppose $F = \overline{\mathbf{\Lambda}}(L)$ is unstable (resp. strictly semistable) and take its destabilizing line subbundle on $\mathbb{P}^1$ of degree k that contains V_i for $i \in I$. Pulling this line bundle back to C and using adjointness gives an injection

$$f : \mathbb{O}_C(kh) \hookrightarrow L$$

such that $f(\mathbb{O}_C(kh))$ vanishes at each point p_i for $i \in I$. Thus we can write

$$L = \mathbb{O}\left(kh + \sum_{i \in I} p_i + x_1 + \cdots + x_j\right)$$

for some points $x_1, \dots, x_j \in C$. Equating degrees gives

$$g + 1 = 2k + |I| + j.$$

The slope inequality gives $j < \frac{1}{2}(g-1)$ (equal for strictly semistable). This gives loci listed in the theorem. To show (2), notice that the ramification locus of $\overline{\mathbf{\Lambda}}$ and $\mathbf{\Lambda}$ is the same by (1), namely the divisor R. By Riemann–Hurwitz and Amplification 2.4,

$$\overline{\mathbf{\Lambda}}^*(-K) \sim -K_{\operatorname{Pic}^{g+1} C} + R \equiv 4\Theta.$$

This finishes the proof.[7] □

[7]The papers [Biswas et al. 2010; Araujo et al. 2021] contain a formula equivalent to $\overline{\mathbf{\Lambda}}^*(-K) \equiv 4^g\Theta$, which is different from our formula. But there is a mistake in the last line of the proof of Lemma 3.1 in [Biswas et al. 2010]. Formulas (3.19) and (3.20) there are both correct, but the conclusion is wrong; in fact the correct conclusion is exactly that $\overline{\mathbf{\Lambda}}^*(-K) \equiv 4\Theta$. This mistake does not affect any of the main results in these papers.

5.13 Corollary *The image of the divisor $E \subset \mathrm{Pic}^{g+1} C$ of Amplification 2.4 under $\overline{\Lambda}$ is a divisor that parametrizes parabolic bundles of splitting type $\mathcal{O}(-1) \oplus \mathcal{O}(1)$. This divisor is contracted by Ξ to the point $o \in M_{0,n}$.*

Proof The first statement is clear from the proof of Lemma 5.6. For the second, notice that $L \in F$ if and only if $L = h \otimes \mathcal{O}(x_1 + \cdots + x_{g-1})$ for some points on C. Generically along E, $\{x_1, \ldots, x_{g-1}\}$ is the base locus of L and therefore $\varphi_L = \varphi_h$. Thus $\Lambda(E) = (\varphi_h(p_1), \ldots, \varphi_h(p_n)) = o$. □

Next we study the dependence of scattering amplitude on marked points.

5.14 Notation Consider the Weil group $W(D_n) = S_n \ltimes (\mathbb{Z}_2)^{n-1}$, where we identify $(\mathbb{Z}_2)^{n-1}$ with the set of subsets of $\{1, \ldots, n\}$ of even cardinality. The Weil group acts on the stack $\mathrm{Bun}(\mathbb{P}^1, z_1, \ldots, z_n)$ as follows: the symmetric group acts by permuting marked points and the group $(\mathbb{Z}_2)^{n-1}$ acts by *elementary transformations*: for every subset $I \subset \{1, \ldots, n\}$ of even cardinality, consider an exact sequence

$$0 \to F' \xrightarrow{\alpha} F \to \bigoplus_{i \in I} (F|_{z_i})/V_i \to 0. \tag{5.14.1}$$

F' is a rank-2 vector bundle of degree $-|I|$ with parabolic lines defined as

$$V_i' = \begin{cases} \alpha^{-1} V_i & \text{if } i \notin I, \\ \mathrm{Ker}\, \alpha|_{z_i} & \text{if } i \in I. \end{cases}$$

To force the degree to be 0, the elementary transformation is defined as

$$\mathrm{el}_I(F) = F'\big(\tfrac{1}{2}|I|\big).$$

In the language of ruled surfaces, elementary transformations are given by blowing up an even number of parabolic points in fibers and blowing down proper transforms of fibers. $W(D_n)$ acts on the Fano model $\mathrm{Bun}_F(\mathbb{P}^1; z_1, \ldots, z_n)$ by elementary transformations, in fact it is its full automorphism group [Araujo et al. 2021].

5.15 Proposition *Let $C_0^n \subset C^n$ be the configuration space of points $p_1, \ldots, p_n \in C$ such that $p_i \neq p_j$ and $p_i \neq \tau(p_j)$ for $i \neq j$. Consider a commutative diagram*

$$\begin{array}{ccccc} \mathrm{Pic}^{g+1} C \times C_0^n & \xrightarrow{\overline{\Lambda}} & \mathit{Bun}_F(\mathbb{P}^1) & \xrightarrow{\Xi} & M_{0,n} \\ \downarrow & & \downarrow \zeta & & \\ C_0^n & \xrightarrow{o} & M_{0,n} & & \end{array}$$

where top arrows are rational maps and where

$$\mathit{Bun}_F(\mathbb{P}^1) \xrightarrow{\zeta} M_{0,n}$$

is the universal moduli space of parabolic vector bundles:

$$\zeta^{-1}(z_1, \ldots, z_n) = \mathrm{Bun}_F(\mathbb{P}^1, z_1, \ldots, z_n).$$

The map o is defined in (5.2.1). *The action of $W(D_n)$ has the following compatibility*:

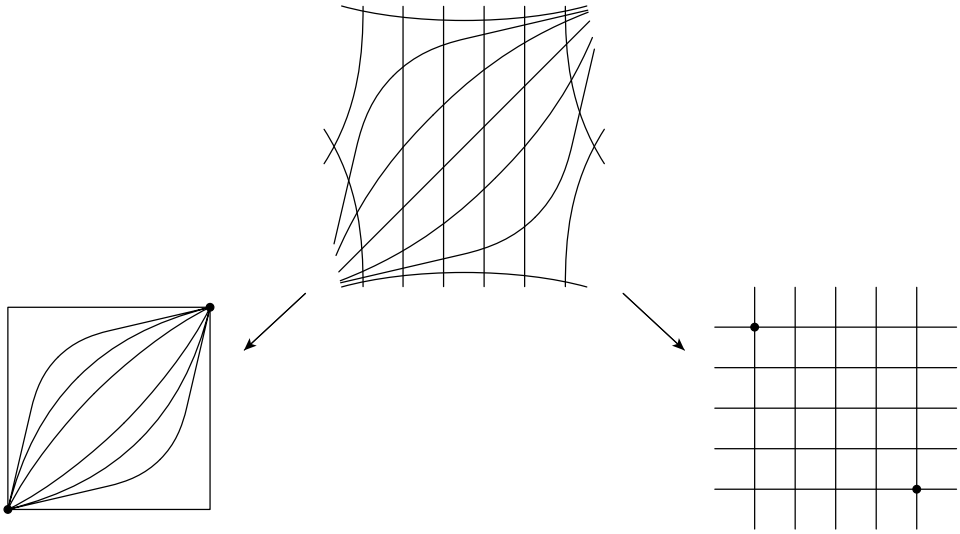

Figure 10

(1) *The map* $\Xi : \mathrm{Bun}_F(\mathbb{P}^1; z_1, \dots, z_n) \dashrightarrow M_{0,n}$ *is* S_n*-equivariant. Elementary transformations* el_I *give birational involutions of* $M_{0,n}$ *that depend on* $z_1, \dots, z_n$.

(2) *The square of the diagram is* $W(D_n)$ *equivariant. The action is defined as follows*:
   (a) S_n *acts everywhere by permuting marked points.*
   (b) $(\mathbb{Z}_2)^{n-1}$ *acts trivially*[8] *on* $M_{0,n}$.
   (c) *Every* $I \in (\mathbb{Z}_2)^{n-1}$ *acts on* $(D; p_1, \dots, p_n) \in \mathrm{Pic}^{g+1} C \times C_0^n$ *as follows*:

$$p_i \mapsto \begin{cases} \tau(p_i) & \text{if } i \in I, \\ p_i & \text{if } i \notin I, \end{cases} \qquad D \mapsto D - \sum_{i \in I} p_i + \tfrac{1}{2}|I|h. \tag{5.15.1}$$

Proof For (1), everything follows from definitions except for the remark about birational involutions on $M_{0,n}$. Note that $\mathbb{P}(F) = \mathbb{P}^1_z \times \mathbb{P}^1_q$, and $\mathrm{el}(I)$ amounts to an elementary transformation of this $\mathbb{P}^1$ bundle (over $\mathbb{P}^1_z$) in points (z_i, q_i) for $i \in I$. It suffices to consider the case when $I = \{1, n\}$. We change coordinates so that $z_1 = q_1 = 0$ and $z_n = q_n = \infty$. In these coordinates, proper transforms of lines $q = \lambda z$ after the elementary transformation become horizontal rulings. Thus

$$(0, q_2, \dots, q_{n-1}, \infty) \mapsto \left(\infty, \frac{q_2}{z_2}, \dots, \frac{q_{n-1}}{z_{n-1}}, 0\right) \sim \left(0, \frac{z_2}{q_2}, \dots, \frac{z_{n-1}}{q_{n-1}}, \infty\right).$$

This is a Cremona transformation with center that depends on $z_1, \dots, z_n$. See Figure 10.

For (2), notice that the sequence (5.14.1) is the pushforward of the sequence

$$0 \to \mathcal{O}\left(D - \sum_{i \in I} p_i\right) \to \mathcal{O}(D) \to \bigoplus_{i \in I} \mathcal{O}_{p_i} \to 0,$$

which gives the formula for F' after tensoring with a multiple of $\mathcal{O}(h)$. □

[8]Warning: this $M_{0,n}$ is different from $M_{0,n}$ in the top right corner!

6 Scattering using the matrix model

We continue to use notation of Section 5. In particular, C is a smooth hyperelliptic curve of genus $g \geq 2$ that satisfies Assumption 5.2, ie points $p_1, \dots, p_n \in C$ are different and no pair is in hyperelliptic involution. Let $z_1, \dots, z_n \in \mathbb{P}^1$ be their projections and $\overline{\mathbf{\Lambda}}\colon \mathrm{Pic}^{g+1} C \to \mathrm{Bun}(\mathbb{P}^1; z_1, \dots, z_n)$ is the standard morphism to the stack of quasiparabolic vector bundles. We first review the Jacobi's description of the Jacobian of a hyperelliptic curve as the space of conjugacy classes of 2×2 matrices following [Mumford 1984] and [Beauville 1990].

6.1 The curve C has equation $y^2 = f(z)$, where $f \in \mathbb{O}_{\mathbb{P}^1}(2g+2)$ is a polynomial without multiple roots. The map $\pi := \varphi_h\colon C \to \mathbb{P}^1$ is the projection $(z, y) \mapsto z$. The points $(z_0, 0)$ with z_0 a root of $f(z)$ are the Weierstrass points. As the sheaf of $\mathbb{O}_{\mathbb{P}^1}$-modules, we have

$$\pi_* \mathbb{O}_C = \mathbb{O}_{\mathbb{P}^1}(-g-1) \oplus \mathbb{O}_{\mathbb{P}^1}.$$

The sheaf of algebras structure of $\pi_* \mathbb{O}_C$ is completely determined by the map $\mathrm{Sym}^2 \mathbb{O}_{\mathbb{P}^1}(-g-1) \to \mathbb{O}_{\mathbb{P}^1}$, which is simply multiplication by $f \in \mathbb{O}_{\mathbb{P}^1}(2g+2)$. By Lemma 5.6, when $L \in \mathrm{Pic}^{g+1} C$ is away from the theta-divisor E, we have

$$\pi_* L = \mathbb{O}_{\mathbb{P}^1} \oplus \mathbb{O}_{\mathbb{P}^1}.$$

The action of $\pi_* \mathbb{O}_C$ on $\pi_* L$ is determined by a 2×2 matrix

$$M = \begin{bmatrix} V & U \\ W & V' \end{bmatrix} \in \mathrm{Hom}\big(\mathbb{O}_{\mathbb{P}^1}(-g-1) \otimes (\mathbb{O}_{\mathbb{P}^1} \oplus \mathbb{O}_{\mathbb{P}^1}), \mathbb{O}_{\mathbb{P}^1} \oplus \mathbb{O}_{\mathbb{P}^1}\big) \tag{6.1.1}$$

of polynomials U, V, V', W in z of degree at most $g+1$. Applying M twice should be a multiplication by the polynomial $f(z)$, which gives equations on polynomials

$$\begin{aligned} V' &= -V, \\ -\det(M) &= V^2 + UW = f(z). \end{aligned} \tag{6.1.2}$$

Let $S(f) \subset \mathbb{A}^{3(g+2)}$ be the affine subvariety given by equations (6.1.2), where $\mathbb{A}^{3(g+2)}$ parametrizes U, V, W. Then $S(f)$ is smooth for any polynomial $f(z)$ without multiple roots. Moreover, the group PGL_2 acts on $S(f)$ (with elements viewed as 2×2 matrices) by conjugation freely and the quotient is, by [Beauville 1990, Theoreme 1.4],

$$S(f)/\mathrm{PGL}_2 \simeq \mathrm{Pic}^{g+1} C \setminus E. \tag{6.1.3}$$

6.2 Theorem *The map $\overline{\mathbf{\Lambda}}$ (and thus the scattering amplitude map $\mathbf{\Lambda}$) has degree 2^g.*

Proof To determine the degree of $\overline{\mathbf{\Lambda}}$, we fix a general point in $\mathrm{Bun}_F(\mathbb{P}^1, z_1, \dots, z_n)$ and count the number of preimages of this point in $\mathrm{Pic}^{g+1} C$. A general parabolic bundle has splitting type $\mathbb{O} \oplus \mathbb{O}$ and the parabolic structure is the set of points $(z_1, q_1), \dots, (z_n, q_n)$, so essentially we choose general points $q_1, \dots, q_n \in \mathbb{P}^1$. The corresponding bundle $L \in \mathrm{Pic}^{g+1} C$ is away from the theta-divisor E, so we can locate it using (6.1.3).

6.3 Suppose that neither of the points $p_1, \dots, p_n$ is a Weierstrass point. Then $(\pi_* L)|_{z_i} = L|_{p_i} \oplus L|_{\tau(p_i)}$ and thus the 2×2 matrix $M(z_i)$ has two distinct eigenspaces, one corresponds to the parabolic structure given by p_i and another by $\tau(p_i)$. The point $q_i \in \mathbb{P}^1$ gives the slope of this eigenspace. Thus we need to do the following:

(1) Count the number of solutions in $S(f)$ such that each matrix $M(z_i)$ has an eigenspace with a fixed general slope q_i.

(2) Divide this number by 2^n. Indeed, using p_i or $\tau(p_i)$ gives the scattering amplitude of the same degree by Proposition 5.15.

Note that taking conjugacy classes of matrices by the PGL_2 action is not necessary: fixing three different slopes of eigenspaces eliminates the conjugacy action.

6.4 The smooth solution set $S(f) \subset \mathbb{C}^{3g+6}$ of dimension $g+3$ is the intersection of $2g+3$ affine quadrics, one for each coefficient of the degree-$(2g+2)$ polynomial $f(z)$. Solutions at infinity $\mathbb{P}^{3g+5}$ are given by the homogeneous equation $V^2 = UW$, which has expected dimension $g+2$. Indeed, if $V = 0$ then either $U = 0$ or $W = 0$, which gives a union of two projective subspaces of dimension $g+1$ each. If $V \neq 0$ then the solution is determined by V up to reordering of terms in the polynomial factorization and rescaling U by λ and W by λ^{-1}. Imposing the slope q_i at z_i is a linear equation on U, V, W. Since $\det M(z_i) \neq 0$ but $\operatorname{Tr} M(z_i) = 0$, no matrix $M(z_i)$ has more than two eigenspaces, and so these linear equations have no base locus on $S(f)$. By Bertini's theorem, the intersection is transversal and has expected dimension. We claim that there are no solutions at infinity. Indeed, the solution set of the homogeneous system of equations $V^2 = UW$ can be thought of as 2×2 matrices and is covered by n open charts where $M(z_i) \neq 0$. Since $\det M(z_i) = \operatorname{Tr} M(z_i) = 0$, $M(z_i)$ is a nonzero nilpotent matrix and thus have only one eigenspace. Thus the base locus of the solution set is empty and so it has an expected dimension by Bertini's theorem, which means it is empty.

6.5 The space of matrices of polynomials with fixed slopes q_i is a linear space of dimension $3(g+2)-n = 2g+3$ and we are counting intersection points of $2g+3$ quadrics under the assumption that intersection is transversal and does not run away to infinity. Thus we have 2^{2g+3} intersection points and therefore

$$\deg \overline{\mathbf{\Lambda}} = \frac{2^{2g+3}}{2^n} = 2^g.$$

6.6 If some of the points z_i are Weierstrass points, ie $p_i = \tau(p_i)$, the argument goes as before, except for two issues:

(1) We don't have to divide the number of solutions by 2, as in Section 6.3(2).

(2) By Claim 6.7, $M(z_i)$ is a nonzero nilpotent matrix. The subvariety of nilpotent 2×2 matrices is a quadric cone and fixing the slope q_i gives a ruling of this cone (intersection with the tangent plane of multiplicity 2). Thus fixing the slope is not equivalent to pulling back a general hyperplane by a morphism to projective space as in Section 6.4. The correct application of Bertini's theorem is to project this cone onto a conic (isomorphic to $\mathbb{P}^1$) and count this solution only once.

Thus issues (1) and (2) cancel each other and we get the same count.

6.7 Claim *$M(z_i)$ is a nonzero matrix.*

If $M(z_i)=0$ then U, V and W have a root at z_i. But then f has a double root at z_i, a contradiction. □

6.8 [Mumford 1984] In the model (6.1.3), one can eliminate the PGL_2-action by making

- f a monic polynomial of degree $2g+1$ (one of the roots is moved to ∞),
- U a monic polynomial of degree g,
- V a polynomial of degree $g-1$,
- W a monic polynomial of degree $g+1$.

Under these conditions, the solution set M of equations (6.1.2) in $\mathbb{A}^{3g+1}$ is isomorphic to $\mathrm{Pic}^{g+1} C \setminus E$. Solutions look as follows. Suppose $U(z)=(z-t_1)\cdots(z-t_g)$ has no multiple roots. Choose $s_i=\pm\sqrt{f(t_i)}$ for $i=1,\dots,g$ and use Lagrange interpolation to find $V(z)$ such that $V(t_i)=s_i$ for $i=1,\dots,g$. Then $U(z)$ divides $f(z)-V(z)^2$ and we can define

$$W(z)=\frac{f(z)-V(z)^2}{U(z)}.$$

For any $c\in\mathbb{P}^1$, the Lax pair differential equation gives a translation-invariant vector field $\dot{F}=(\dot{U}(z),\dot{V}(z),\dot{W}(z))$ on M with components

$$\begin{aligned}\dot{U}(z)&=\frac{V(c)U(z)-U(c)V(z)}{z-c},\\ \dot{V}(z)&=\frac{1}{2}\frac{U(c)W(z)-W(c)U(z)}{z-c}-U(c)U(z),\\ \dot{W}(z)&=\frac{W(c)V(z)-V(c)W(z)}{z-c}+U(c)V(z).\end{aligned}$$

General points $c_1,\dots,c_g$ give linearly independent translation-invariant vector fields $\dot{F}_1,\dots,\dot{F}_g$ and thus a translation-invariant polyvector field $A^\vee=\dot{F}_1\wedge\cdots\wedge\dot{F}_g$, which is dual to the translation-invariant volume form A on $\mathrm{Pic}^{g+1} C$. Applying $d\mathbf{\Lambda}$ to $A^\vee$ and dualizing gives the value of the branch of the scattering amplitude form that corresponds to the point (U,V,W). More concretely, we can factor the scattering amplitude map $\mathbf{\Lambda}\colon M\to M_{0,n}$ into maps

$$E\colon M \dashrightarrow (\mathbb{P}^1)^n \quad\text{and}\quad Q\colon (\mathbb{P}^1)^n \dashrightarrow M_{0,n},$$

where Q is the quotient by the PGL_2 action and E is the map that assigns to a matrix of polynomials (6.1.1) the slopes of its eigenspaces

$$\frac{y_1-V(z_1)}{U(z_1)},\dots,\frac{y_n-V(z_n)}{U(z_n)}$$

at marked points $p_i=(z_i,y_i)$ for $i=1,\dots,n$.

7 Bypassing the Kummer surface

We will make results of the previous section more explicit for genus 2 curves.

7.1 Notation Fix a smooth pointed genus 2 curve $(C; p_1, \dots, p_5)$.

(1) Let $P := p_1 + \cdots + p_5$.

(2) We view C as a degree-5 curve in $\mathbb{P}^3$ using the embedding $\varphi_P : C \hookrightarrow \mathbb{P}^3$.

(3) K is a canonical divisor, $\varphi_K : C \xrightarrow{2:1} \mathbb{P}^1$ is a hyperelliptic double cover.

(4) We introduce 16 points in $\mathrm{Pic}^3 C$,

$$\delta = P - K, \quad \delta_i = K + p_i, \quad \delta_{ij} = P - p_i - p_j,$$

where the indices are $1 \le i \le 5$ and $1 \le i < j \le 5$, respectively.

(5) Special loci in $\mathrm{Pic}^3 C$ defined in Amplification 2.4 are as follows:

$$W = \varnothing, \quad R = \{D \mid 2D \in P + C\} \equiv 4\Theta, \quad E = K + C, \quad E_{ij} = C + p_i + p_j.$$

(6) We introduce another useful theta-divisor on $\mathrm{Pic}^3 C$ for $i = 1, \dots, 5$,

$$E_i = P - p_i - C.$$

Here and elsewhere we don't distinguish between line bundles and linear equivalence classes of divisors; for example, $E = K + C$ denotes the locus in $\mathrm{Pic}^3 C$ of line bundles of the form $\mathcal{O}(K + p)$ for $p \in C$. Hopefully this won't cause confusion.

7.2 Lemma *In genus* 2, *Assumption 5.2 is equivalent to any of the following*:

(1) *No two points of* $p_1, \dots, p_5$ *are related by the hyperelliptic involution.*

(2) *No three points of* $p_1, \dots, p_5 \in \mathbb{P}^3$ *are colinear.*

(3) 16 *divisors* E, E_i, E_{ij} *are pairwise different.*

(4) 16 *points* δ, δ_i, δ_{ij} *are pairwise different.*

(5) *We have that* $\delta \notin E_{ij}$ *for any* $i \neq j$.

Proof Left as a fun exercise for the reader. The hint is $C = K - C \subset \mathrm{Pic}^1 C$. □

A special feature of the genus-2 case is that divisors of degree 2 are effective. This can be used to study divisors $D \in \mathrm{Pic}^3 C$ and their linear systems by associating to D a residual divisor $P - D$ of degree 2. This gives the following proposition.

7.3 Proposition *Let $\mathbb{P}^2 \subset \mathbb{P}^3$ be the plane passing through $p_1, \dots, p_5$. Let*

$$\mathbf{dP}_4 = \mathrm{Bl}_{p_1,\dots,p_5} \mathbb{P}^2$$

be the del Pezzo surface of degree 4. Recall that $\overline{M}_{0,5}$ is the del Pezzo surface of degree 5. The scattering amplitude map can be extended to a commutative diagram

$$\begin{array}{ccc} \mathrm{Sym}^2 C & \xrightarrow{\overline{\mathbf{\Lambda}}} & \mathbf{dP}_4 \\ {\scriptstyle a}\downarrow & & \downarrow{\scriptstyle \Xi} \\ \mathrm{Pic}^3 C & \xrightarrow{\mathbf{\Lambda}} & \overline{M}_{0,5} \end{array}$$

where horizontal arrows are rational maps. The maps can be described as follows:

(1) *For any $(x, y) \in \mathrm{Sym}^2 C$, consider the secant line $\ell_{xy} \subset \mathbb{P}^3$ connecting x and y (or the tangent line to C at x if $x = y$). Then $\overline{\mathbf{\Lambda}}(x, y) = \ell_{xy} \cap \mathbb{P}^2$.*

(2) *The map Ξ is given by projecting $p_1, \dots, p_5$ from a varying point of $\mathbb{P}^2$*; *see* [Castravet and Tevelev 2012]. *It blows down the conic passing through $p_1, \dots, p_5$ to the point*

$$o := \big(\varphi_K(p_1), \dots, \varphi_K(p_5)\big) \in M_{0,5}.$$

(3) *We have $a(x, y) = \mathbb{O}(P - x - y)$. The map a gives $\mathrm{Sym}^2 C$ as the blow-up of $\mathrm{Pic}^3 C$ at δ.*

Proof Indeed, for $x, y \in C$, $|P - x - y|$ is the pencil of planes in $\mathbb{P}^3$ through ℓ_{xy}. Projecting $p_1, \dots, p_5$ from ℓ is equivalent to projecting them from $\ell \cap \mathbb{P}^2$. □

7.4 Corollary *The scattering amplitude map $\mathbf{\Lambda} : \mathrm{Pic}^3 C \dashrightarrow M_{0,5}$ has degree 4.*

If course this follows from Theorem 6.2, but here is an independent proof.

Proof It suffices to check this for $\overline{\mathbf{\Lambda}}$. We have to count how many secant lines ℓ_{xy} pass through a general point of $\mathbb{P}^2$. By dimension count, projection of C from a general point of $\mathbb{P}^2$ is a nodal curve of degree 5 and therefore has arithmetic genus 6. Thus there will be $6-2=4$ nodes, each produced by a secant line. □

7.5 Lemma *We have divisors $\mathcal{D}, \mathcal{D}_i, \mathcal{D}_{ij} \subset C^5 \setminus \bigcup_{i<j} \Delta_{ij}$ that parametrize configurations of marked points $p_1, \dots, p_5 \in C$ satisfying any of the following equivalent conditions*:

(1) *$\delta \in E$, $\delta_i \in E_i$ and $\delta_{ij} \in E_{ij}$, respectively.*

(2) *$\delta \in R$, $\delta_i \in R$ and $\delta_{ij} \in R$, respectively.*

(3) *Each of $\delta - K$, $P - K - 2p_i$ and $P - 2p_i - 2p_j$, respectively, is an effective divisor.*

Divisors $\mathcal{D}$, $\mathcal{D}_i$ and $\mathcal{D}_{ij}$ can also be characterized using geometric conditions:

($\mathcal{D}$) *The unique quadric surface in $\mathbb{P}^3$ containing C is singular.*

($\mathcal{D}_i$) *The tangent line at p_i to $C \subset \mathbb{P}^3$ intersects C at another point.*

($\mathcal{D}_{ij}$) *Tangent lines at p_i and p_j intersect.*

Proof Left as a fun exercise for the reader. □

7.6 Theorem *Let X be the blow-up of $\mathrm{Pic}^3 C$ in 16 points δ, δ_i and δ_{ij} with exceptional divisors Δ, Δ_i and Δ_{ij}, respectively. Let $\mathbb{E}$, $\mathbb{E}_i$ and $\mathbb{E}_{ij}$ be the respective proper transforms of divisors E, E_i and E_{ij}.*

The scattering amplitude rational map $\boldsymbol{\Lambda}$ induces a finite $4:1$ morphism $X \xrightarrow{\bar{\boldsymbol{\Lambda}}} \mathbf{dP}_4$. The preimages of sixteen (-1)-curves of $\mathbf{dP}_4$ are the following pairs:

$$\begin{aligned}\bar{\boldsymbol{\Lambda}}^{-1}(\text{conic through } p_1,\dots,p_5) &= \Delta \cup \mathbb{E},\\ \bar{\boldsymbol{\Lambda}}^{-1}(\text{exceptional divisor over } p_i) &= \Delta_i \cup \mathbb{E}_i,\\ \bar{\boldsymbol{\Lambda}}^{-1}(\text{line through } p_i,\, p_j) &= \Delta_{ij} \cup \mathbb{E}_{ij}.\end{aligned}$$

The restriction of $\bar{\boldsymbol{\Lambda}}$ to each "$\Delta \cup E$" pair depends on whether $(p_1,\dots,p_5)$ is contained in the corresponding configuration divisor "$\mathcal{D}$" in C^5:

(yes) *$\bar{\boldsymbol{\Lambda}}$ is ramified (of order 2) along Δ'' and has degree 2 along "$\mathbb{E}$".*

(no) *$\bar{\boldsymbol{\Lambda}}$ is an isomorphism along "Δ" and has degree 3 along "$\mathbb{E}$".*

Proof We draw special curves on X and how they intersect; see Figure 11. We use that $\Theta^2 = 2$ and check how special curves pass through the special points. In Figure 11 we draw the special curves when the configuration $(p_1,\dots,p_5)$ is away from (top) and along (bottom) the corresponding $\mathcal{D}$ divisors. In the latter case, the inverse image of an "E" divisor in $\mathrm{Pic}^3 C$ is the union "$\Delta \cup \mathbb{E}$" and the ramification divisor on X is the union of the proper transform of R and the "Δ" divisor. Note that the configuration $(p_1,\dots,p_5)$ can be on some $\mathcal{D}$ divisors and not on the others, so the actual picture could be a mixture of the top and the bottom of Figure 11.

Next we study the map $\mathrm{Sym}^2 C \to \mathbb{P}^2$, $(x,y) \mapsto \ell_{xy} \cap \mathbb{P}^2$, of Proposition 7.3. It is well-defined unless $\ell_{xy} \subset \mathbb{P}^2$, which happens at points δ_{ij}. So the map $X \to \mathbb{P}^2$ induced by $\bar{\boldsymbol{\Lambda}}$ is regular away from Δ_{ij}, in particular it is regular along $\Delta \cup \mathbb{E}$.

What is the preimage of p_i? In $\mathrm{Sym}^2 C$, there are two possibilities, one is the curve (p_i, C), ie E_i. Another is a point (x,y) such that $P - (p_i + x + y)$ is a degree-2 pencil, which should be K. So another option is the point $P - p_i - K = \delta_i$. Thus on X away from the Δ_{ij}, the preimage of p_i is $\mathbb{E}_i \cup \Delta_i$.

What is the preimage of the conic Q through 5 points? This conic is the intersection of $\mathbb{P}^2$ with the unique quadric $\mathbb{Q}$ that contains C. Thus a secant ℓ_{xy} must be contained in $\mathbb{Q}$. If $\mathbb{Q}$ is smooth, C has bidegree $(2,3)$. One ruling is cut by points in the hyperelliptic involution, which is the curve Δ. Another ruling is cut by triples of points contained in the line, ie such that $P - x - y - K$ is effective, which is the curve $\mathbb{E}$. If $\mathbb{Q}$ is singular then these two rulings are the same, given by the vertex of the quadratic cone $\sim P - 2K$ and pairs of points in the hyperelliptic involution. This shows that the rational map $X \dashrightarrow \mathbf{dP}_4$ is regular along $\Delta \cup \mathbb{E}$, and maps this divisor to the proper transform of the conic passing through five points.

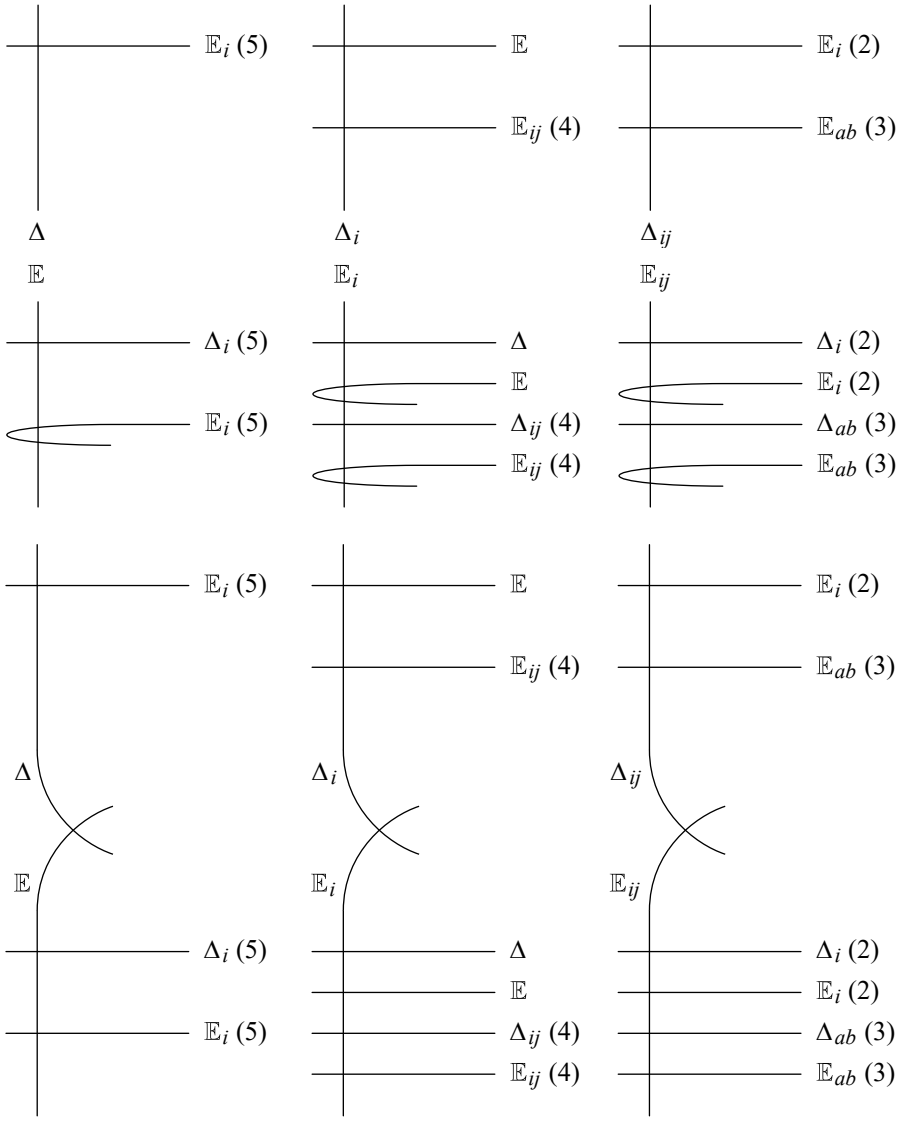

Figure 11: "Double sixteen" configuration on X away from (top) and along (bottom) the corresponding $\mathcal{D}$ divisors.

Analysis of other "$\Delta \cup \mathbb{E}$" pairs can be done similarly. However, this is not necessary. By Proposition 5.15, the map $X \dashrightarrow \mathbf{dP}_4$ can be extended to a $W(D_5)$-equivariant map

$$\coprod_{I \subset \{1,\dots,5\},\ |I| \equiv 0 \bmod 2} X_I \dashrightarrow \mathbf{dP}_4,$$

where X_I corresponds to a 5-tuple (5.15.1). Since the action permutes "$\Delta \cup \mathbb{E}$" pairs, if the map is regular along one pair (for all X_I), it is regular along all pairs. □

When does $(p_1, \dots, p_5)$ belong to all configuration divisors $\mathcal{D}, \mathcal{D}_i, \mathcal{D}_{ij}$?

7.7 Theorem *We have $(p_1,\dots,p_5)\in\mathcal{D}\cap\bigcap_i\mathcal{D}_i\cap\bigcap_{ij}\mathcal{D}_{ij}$ if and only if $p_1,\dots,p_5$ are Weierstrass points of C, ie ramification points of φ_K. Suppose that this is the case.*

(1) *Let p_6 be the remaining Weierstrass point. The* 16 *special points are*

$$\delta = K+p_6,\quad \delta_i = K+p_i,\quad \delta_{ij}=p_i+p_j+p_6.$$

Equivalently, this is the set of 2-torsion points in $\mathrm{Pic}^0 C$ *shifted by* δ.

(2) *Let τ be the involution of* $\mathrm{Pic}^3 C$ *induced by the hyperelliptic involution of C. Let* $\mathrm{Kum}=\mathrm{Pic}^3/\tau$ *be the Kummer surface with* 16 *double points, and let* K3 *be its minimal resolution. Then τ lifts to $X=\mathrm{Bl}_{\delta,\delta_i,\delta_{ij}}\mathrm{Pic}^3$, and* $\mathrm{K3}=X/\tau$.

(3) *The scattering amplitude* $4:1$ *cover $\overline{\mathbf{\Lambda}}: X\to\mathbf{dP}_4$ factors as*

$$X\xrightarrow{2:1}\mathrm{K3}\xrightarrow{2:1}\mathbf{dP}_4.$$

(4) *The images of "Δ" and "$\mathbb{E}$" type divisors give two configurations of* 16 *rational curves in* K3. *Their images in* Kum *are the* 16 *nodes and* 16 *conics called "tropes". The image of R is a genus-5 "Humbert" curve.*

Proof Suppose that $p_1,\dots,p_5$ are Weierstrass points. Assumption 5.2 is satisfied. We have $P\sim 3K-p_6$ by the Riemann–Hurwitz formula. Thus

$$P-2K\sim P-K-2p_i\sim P-2p_i-2p_j\sim p_6$$

is effective, and the configuration belongs to all divisors.

In the opposite direction, let $(p_1,\dots,p_5)\in\mathcal{D}\cap\bigcap_i\mathcal{D}_i$. Define

$$P-2K\sim z\in C\quad\text{and}\quad P-K-2p_i\sim z_i\in C.$$

Then $z-z_i\sim 2p_i-K$, ie $z+\tau(p_i)\sim p_i+z_i$ for every i, where τ denotes the hyperelliptic involution. There are two cases, either p_i is a Weierstrass point or $z=p_i$ and $z_i=\tau(p_i)$. Thus either all five points are Weierstrass points, which is what we are trying to prove, or 4 of them are, say p_2, p_3, p_4, p_5, and $P-2K\sim p_1$. But then $p_2+p_3+p_4+p_5\sim 2K$, ie $p_2+p_3\sim p_4+p_5$, which is impossible.

The rest is also easy: (1) is immediate to verify, (2) and (4) are classical and well-known [Dolgachev 2012; Skorobogatov 2010]. To prove (3) it suffices to notice that $\overline{\mathbf{\Lambda}}$ is τ-invariant if all marked points are Weierstrass points. □

8 Scattering measures of M-curves

8.1 We refer to [Gross and Harris 1981] for the basic theory of real algebraic curves and Jacobians. Let C be a smooth projective complex algebraic curve of genus g. We view the set of complex points $C(\mathbb{C})$ as a Riemann surface. The curve C endowed with a real structure (equivalently, an anti-holomorphic involution) is called an *M-curve*[9] if the set of real points $C(\mathbb{R})\subset C(\mathbb{C})$ has $g+1$ (the maximal possible

[9]M stands for "maximal".

number) connected components $C_1, \dots, C_{g+1}$. These ovals separate $C(\mathbb{C})$ into two connected subsets interchanged by the complex conjugation $p \mapsto \bar{p}$. Recall from Theorem 2.3 that all smooth curves with $n = g + 3$ marked points are MHV curves. In this section we will study the scattering amplitude of M-curves.

8.2 Definition A smooth *MHV M-curve* is a pointed M-curve such that its divisor of marked points $p_1 + \cdots + p_n$, where $n = g + 3$, is preserved by the complex conjugation. Moreover, we assume that we have one of the following two cases:

(A) All marked points are real and all components of $C(\mathbb{R})$ contain one marked point each except for one component, which contains three marked points.

(B) All but two marked points are real, one on each component of $C(\mathbb{R})$. The two remaining marked points are complex-conjugate.

8.3 It is well-known [Gross and Harris 1981] that the set of real points

$$\mathrm{Pic}^d\,\mathbb{R} \subset \mathrm{Pic}^d\,\mathbb{C}$$

of every component of the Picard group of an M-curve C is a union of 2^g connected components denoted by $\mathrm{Pic}^d_I\,\mathbb{R}$ and indexed by subsets $I \subset \{1, \dots, g+1\}$ such that $|I| \equiv d \mod 2$. Namely, if a divisor $D = \bar{D}$ is preserved by the complex conjugation, then the following conditions are equivalent:

(1) $\mathbb{O}(D) \in \mathrm{Pic}^d_I\,\mathbb{R}$.

(2) The divisor $D \cap C_i$ has odd degree if and only if $i \in I$.

Each component $\mathrm{Pic}^d_I\,\mathbb{R} \subset \mathrm{Pic}^d\,\mathbb{R}$ is a torsor of the real Lie group

$$\mathrm{Pic}^0_\varnothing\,\mathbb{R} \simeq \mathrm{U}(1)^g \simeq (\mathbb{R}/\mathbb{Z})^g.$$

In what follows we mostly focus on the MHV component $\mathrm{Pic}^d\,C$, so that $d = g + 1$.

8.4 Definition Let $M^{(k,l)}_{0,n}(\mathbb{R})$ be the moduli space of n-tuples of distinct points in $\mathbb{P}^1(\mathbb{C})$ such that there are k real points and l pairs of complex conjugate points. We will need the cases $(k,l) = (n,0)$ and $(n-2,1)$:

(A) $M^A_{0,n}(\mathbb{R})$, or simply $M_{0,n}(\mathbb{R})$, the moduli space of n real points in $\mathbb{P}^1(\mathbb{C})$.

(B) $M^B_{0,n}(\mathbb{R})$, the moduli space of $n-2$ real and two complex-conjugate points.

See [Ceyhan 2007] for compactifications of real forms of $M_{0,n}$.

8.5 By Amplification 2.4, the scattering amplitude map $\mathbf{\Lambda} : \mathrm{Pic}^{g+1}\,C \dashrightarrow M_{0,n}$ is well-defined away from the divisors E, E_{ij} and is unramified away from the divisor R. Since all components $\mathrm{Pic}^{g+1}_I\,\mathbb{R}$ of an MHV M-curve are Zariski dense in $\mathrm{Pic}^{g+1}\,\mathbb{C}$, $\mathbf{\Lambda}$ is defined and unramified generically along them. Moreover,

$$\mathbf{\Lambda}(\mathrm{Pic}^{g+1}\,\mathbb{R}) \subset M^?_{0,n}(\mathbb{R}),$$

where $? = A$ or B depending on the type of the curve C. Indeed, if $L \in \mathrm{Pic}^{g+1}\mathbb{R}$ then we can choose $\varphi_L \in \mathbb{R}(C)$ a real meromorphic function and the marked points will be mapped to points of the Riemann sphere according of type A or B.

8.6 Theorem *Let $? = A$ or B depending on the type of the MHV M-curve C. Then*

$$\mathbf{\Lambda}^{-1}(M^{?}_{0,n}(\mathbb{R})) \subset \mathrm{Pic}^{g+1}\mathbb{R}.$$

Moreover, restriction of $\mathbf{\Lambda}$ to any of the 2^g connected components $\mathrm{Pic}^{g+1}_I\mathbb{R}$ is injective.

Proof Let $(q_1, \dots, q_n) \in M^{?}_{0,n}(\mathbb{R})$. Let $f \in \mathbb{C}(C)$ be a rational function of degree $g+1$ such that $f(p_i) = q_i$ for every $i = 1, \dots, n$. First we claim that $f \in \mathbb{R}(C)$. We argue by contradiction and suppose that this is not the case. Then

$$g(z) = if(z) - i\,\overline{f(\overline{z})} \in \mathbb{R}(C)$$

is a nonzero real rational function. Thus $g(z)$ has finitely many zeros on $C(\mathbb{R})$, and so $f(C(\mathbb{R})) \cap \mathbb{P}^1(\mathbb{R})$ is a finite union of points. By applying a transformation from $\mathrm{PGL}_2(\mathbb{R})$, we can assume that $\infty \notin f(C(\mathbb{R}))$. Thus g also doesn't have any poles on $C(\mathbb{R})$. On the other hand, $g(p_i) = 0$ for every i and $\mathrm{div}(g) \cap C_i$ is even for every i, which is true for any real rational function; see [Gross and Harris 1981, Lemma 4.1]. Thus g has at least one additional zero on each C_i and therefore has degree at least $2g+4$. This is a contradiction: zeros of g are intersection points of the diagonal in $\mathbb{P}^1 \times \mathbb{P}^1$ with the image of C under the map $(f(z), \overline{f(\overline{z})})$ which has homology class $(g+1, g+1)$. Thus we have at most $2g+2$ intersection points.

Next we show injectivity of the restriction of $\mathbf{\Lambda}$ to any connected component $\mathrm{Pic}^{g+1}_I\mathbb{R}$. We argue by contradiction and suppose that $\mathbf{\Lambda}(L) = \mathbf{\Lambda}(L')$ for two different line bundles in the same component. We can find rational functions $f, f' \in \mathbb{R}(C)$ in the corresponding linear systems such that $f(p_i) = f'(p_i) = q_i$ for every $i = 1, \dots, n$ (because $\mathbf{\Lambda}(L) = \mathbf{\Lambda}(L')$) and such that $f^{-1}(\infty) \cap C_i$ and $f'^{-1}(\infty) \cap C_i$ have the same parity for every i (because they are in the same component Pic_I). We can also apply a projective transformation from $\mathrm{PGL}_2(\mathbb{R})$ so that f and f' have disjoint poles. Then $f - f'$ has an even number of poles on every C_i. Therefore $f - f'$ has an even number of zeros on every C_i. One of these zeros is p_i, so there must be at least one additional zero on each C_i. Thus $f - f'$ has at least $2g+4$ zeros total, and we finish as in the first part. □

8.7 Corollary *The scattering amplitude map of a generic MHV curve has degree 2^g.*

Proof By Theorem 8.6, every point in $M^{?}_{0,n}(\mathbb{R})$ has at most 2^g preimages by $\mathbf{\Lambda}$. Since $M^{?}_{0,n}(\mathbb{R})$ is a real form of $M_{0,n}$ of real dimension $n-3$, it is Zariski dense in it. Thus the scattering amplitude map $\mathbf{\Lambda}$ of any MHV M-curve has degree at most 2^g in both types (A) and (B). Let $D \le 2^g$ be the maximum of these degrees.

Since the locus of MHV M-curves $(C; p_1, \dots, p_n)$ of either of these types is a connected component of the real form of the moduli space $M_{g,n}$ of real dimension $3g-3+n$ (see [Seppälä and Silhol 1989]), it

is Zariski dense in $M_{g,n}$. It follows that the degree of the scattering amplitude is bounded above by D for a Zariski dense subset in $M_{g,n}$.

We claim that the degree of $\mathbf{\Lambda}$ is bounded above by D for all smooth curves. Indeed, let $\mathcal{P}ic^{g+1} \to M_{g,n}$ be the universal Jacobian and let

$$\mathbf{\Lambda} : \mathcal{P}ic^{g+1} \dashrightarrow M_{g,n} \times M_{0,n}$$

be the universal scattering amplitude map (the reader uncomfortable with stacks can use a 1-parameter family of curves connecting two curves instead of $M_{g,n}$). Since $\mathbf{\Lambda}$ is generically finite and $M_{g,n} \times M_{0,n}$ is normal, the Stein factorization of $\mathbf{\Lambda}$ implies that cardinality of finite fibers can't be more than D.

Finally, by Theorem 6.2, the scattering amplitude map of a hyperelliptic curve has degree 2^g. Therefore, $D = 2^g$, which completes the proof. □

8.8 Definition There exists a distinguished connected component of $\mathrm{Pic}^{g+1}\mathbb{R}$,

$$\mathrm{Pic}_H^{g+1}\mathbb{R} := \mathrm{Pic}^{g+1}_{\{1,\dots,g+1\}}\mathbb{R},$$

which was studied in [Huisman 2001]. We call it the *Huisman component*. Every effective divisor from $\mathrm{Pic}_H^{g+1}\mathbb{R}$ is a union of $g+1$ points, one in each connected component $C_1, \dots, C_{g+1} \subset C(\mathbb{R})$. Here are some nice properties of $\mathrm{Pic}_H^{g+1}\mathbb{R}$:

8.9 Proposition [Huisman 2001] (1) *Every $L \in \mathrm{Pic}_H^{g+1}\mathbb{R}$ is nonspecial and globally generated.*

(2) *The map φ_L is unramified along $C(\mathbb{R}) = C_1 \cup \cdots \cup C_{g+1}$.*

(3) *The map $\varphi_L|_{C_i} : C_i \to \mathbb{P}^1(\mathbb{R})$ is a real-analytic isomorphism for any $i = 1, \dots, g+1$.*

(4) *Fix $z_{g+1} \in C_{g+1}$. The map*

$$C_1 \times \cdots \times C_g \to \mathrm{Pic}_H^{g+1}\mathbb{R}, \quad z_1, \dots, z_g \mapsto \mathcal{O}(z_1 + \cdots + z_g + z_{g+1}),$$

is a real-analytic isomorphism.

Here's the second main result of this section.

8.10 Theorem *In the notation of Amplification 2.4, $\mathrm{Pic}^{g+1}\mathbb{R}$ is disjoint from the ramification divisor R in both types (A) and (B). In particular, the scattering amplitude map*

$$\mathbf{\Lambda}_I : \mathrm{Pic}_I^{g+1}(\mathbb{R}) \setminus \left(E \cup \bigcup_{i<j} E_{ij} \right) \to M_{0,n}^?(\mathbb{R})$$

is a real-analytic isomorphism onto its image for every component $\mathrm{Pic}_I^{g+1}(\mathbb{R})$.

Proof Suppose $D \in \mathrm{Pic}^{g+1}(\mathbb{R}) \cap R$. By definition of R, this means that

$$2D \sim x_1 + \cdots + x_{g-1} + p_1 + \cdots + p_{g+3} \quad \text{for some } x_i \in C.$$

Since C has type (A) or (B), we can assume without loss of generality that either p_{g+2} and p_{g+3} are complex-conjugate points (type B), or additional points on one of the connected components of $C(\mathbb{R})$ (type A). Let

$$G = x_1 + \cdots + x_{g-1} + p_{g+2} + p_{g+3} \sim 2D - p_1 - \cdots - p_{g+1}.$$

Since $O(2D) \in \mathrm{Pic}^{2g+2}_{\varnothing} \mathbb{R}$ and $O(p_1 + \cdots + p_{g+1}) \in \mathrm{Pic}^{g+1}_{H} \mathbb{R}$, it follows that $\mathbb{O}(G) \in \mathrm{Pic}^{g+1}_{H} \mathbb{R}$, and therefore it is basepoint-free and $h^0(G) = 2$ by Proposition 8.9. On the other hand, it has a complex-conjugate section $\overline{x}_1 + \cdots + \overline{x}_{g-1} + p_{g+2} + p_{g+3}$, which also contains p_{g+2} and p_{g+3}. So this must be the same section, otherwise p_{g+2} and p_{g+3} are in the base locus of $\mathbb{O}(G)$. It follows that G is invariant under complex conjugation. But then it can't be in $\mathrm{Pic}^{g+1}_{H} \mathbb{R}$ since either p_{g+2} and p_{g+3} are complex-conjugate or belong to the same connected component of $C(\mathbb{R})$; in either case the degree of $G \cap C_i$ can't be odd for all i. Since $\mathbf{\Lambda}_I$ is injective by Theorem 8.6 and its domain is disjoint from R, it is an analytic immersion where it is defined. □

8.11 Amplification By Corollary 8.7, for smooth *complex* curves, the scattering amplitude map $\mathbf{\Lambda} \colon \mathrm{Pic}^{g+1} C \to M_{0,n}$ has large degree 2^g. However, Theorems 8.6 and 8.10 show that for smooth *real* M-curves line bundles in every fiber "localize" into different connected components $\mathrm{Pic}^{g+1}_{I} \mathbb{R}$ of $\mathrm{Pic}^{g+1} \mathbb{R}$. In other words, $\mathbf{\Lambda}$ is determined by open immersions (in the domain of $\mathbf{\Lambda}$)

$$\mathbf{\Lambda}_I \colon \mathrm{Pic}^{g+1}_{I} \mathbb{R} \dashrightarrow M^{?}_{0,n}(\mathbb{R}).$$

Each component $\mathrm{Pic}^{g+1}_{I} \mathbb{R}$ carries a uniform probability measure $|A_I|$ given by the real-valued volume form A_I translation-invariant under the real g-dimensional torus $\mathrm{Pic}^{0}_{\varnothing} \mathbb{R}$. Viewed on $M^{?}_{0,n}(\mathbb{R})$, this gives a differential form A_I and a probability measure $|A_I|$ that we call a *scattering amplitude probability measure*. We will typically compactify $M^{?}_{0,n}(\mathbb{R})$ in some way and extend Λ to its domain of definition (so that, in particular, it will be determined at least generically along E and E_{ij}). Since not every reasonable compactification of $M^{?}_{0,n}(\mathbb{R})$ is an orientable manifold, one has to remember (from calculus) that in this case the integral of a form is not well-defined, however one can always integrate probability measures. The scattering measure of the Huisman's component is especially well-behaved.

8.12 Theorem *Let C be a smooth MHV M-curve with ovals $C(\mathbb{R}) = C_1 \cup \cdots \cup C_{g+1}$. Furthermore, we assume that $p_i \in C_i$ for $i = 1, \ldots, g+1$ and that $p_{g+2}, p_{g+3} \in C_{g+1}$ (type A) or $p_{g+2} = \overline{p}_{g+3}$ (type B). We compactify $M_{0,n}$ by $(\mathbb{P}^1)^g \simeq (\overline{M}_{0,4})^g$ using the product of forgetful maps*

$$\pi_{i,g+1,g+2,g+3} \colon M_{0,n} \to M_{0,4}$$

for $i = 1, \ldots, g$. The scattering amplitude map induces a real-analytic isomorphism

$$\mathbb{R}^g / \mathbb{Z}^g \simeq \mathrm{Pic}^{g+1}_{H} \mathbb{R} \xrightarrow{\mathbf{\Lambda}} (\mathbb{RP}^1)^g$$

and gives a positive real-analytic scattering amplitude probability measure on $(\mathbb{RP}^1)^g$.

Proof By Theorem 8.10, $\mathrm{Pic}^{g+1}_{H} \mathbb{R}$ does not intersect the ramification divisor R. As an easy reformulation of Definition 8.8(1), $\mathrm{Pic}^{g+1}_{H} \mathbb{R}$ does not intersect E either. Indeed, let $D = z_1 + \cdots + z_{g+1}$ with $z_i \in C_i$.

Arguing by contradiction, suppose D is linearly equivalent to a divisor in E, ie $D \sim K + x_0 - x_1 - \cdots - x_{g-2}$ for some $x_i \in C$. Then $h^0(D) = 2$ by 8.8 but since $h^0(x_1 + \cdots + x_{g-2}) \geq 1$,

$$h^0(D - x_0) = h^0(K - x_1 - \cdots - x_{g-2}) = h^1(x_1 + \cdots + x_{g-2}) \geq 2$$

by the Riemann–Roch formula, which contradicts the global generation of D.

For every $L \in \operatorname{Pic}_H^{g+1} \mathbb{R}$, $\varphi_L(p_{g+1})$, $\varphi_L(p_{g+3})$ and $\varphi_L(p_{g+3})$ are different. In type (A) this follows from Definition 8.8(3). In type (B), this follows because points $\varphi_L(p_{g+2})$ and $\varphi_L(p_{g+3})$ are not real (the preimage of every real point under φ_L is real). By Lemma 2.7, the map $\operatorname{Pic}_H^{g+1} \mathbb{R} \dashrightarrow (\mathbb{RP}^1)^g$ is a regular real-analytic immersion at every point. On the other hand, it is injective by Theorem 8.10. □

8.13 Example (genus 1) Let C be an elliptic M-curve with two ovals, X and Y. We can use a point $x \in X$ to identify $C(\mathbb{R})$ with $\operatorname{Pic}^2 \mathbb{R}$ by tensoring with $\mathcal{O}(x)$. We denote the corresponding ovals of $\operatorname{Pic}^2 \mathbb{R}$ by $X^{(2)}$ and $Y^{(2)}$. It is clear that $X + X = X^{(2)}$, where the left-hand side denotes the locus of line bundles $\mathcal{O}(x + x')$ for $x, x' \in X$. It is also clear that $X + Y = Y^{(2)}$. We claim that $Y + Y = X^{(2)}$. Indeed, we have a continuous map $C \to \operatorname{Pic}^2(\mathbb{R})$, which sends z to $\mathcal{O}(z + \overline{z})$. By continuity, the image of this map has to be equal to $X^{(2)}$. In the notation of Section 8.3,

$$X^{(2)} = \operatorname{Pic}^2_{\varnothing} \mathbb{R} \quad \text{and} \quad Y^{(2)} = \operatorname{Pic}^2_{\{1,2\}} \mathbb{R} = \operatorname{Pic}^2_H \mathbb{R}$$

is the Huisman component of $\operatorname{Pic}^2 \mathbb{R}$. If $L \in X^{(2)}$ then the map

$$\varphi_L \colon C(\mathbb{R}) \to \mathbb{P}^1(\mathbb{R})$$

represents $C(\mathbb{R})$ in the form $y^2 = f_4(x)$, where $f_4(x)$ is a real polynomial with four real roots (the left side of Figure 12). By tradition, one of these roots is usually moved to infinity. Here φ_L is projection onto the x-axis. Note that restriction of φ_L to either X or Y is neither surjective nor injective. By contrast, if $L \in Y^{(2)}$, the map φ_L represents the same curve in the form $y^2 = f_4(x)$, where $f_4(x)$ is a real polynomial with two pairs of complex conjugate roots (the right side of Figure 12). In accordance with Definition 8.8, the restriction of φ_L to both X and Y is a real-analytic isomorphism with inverses given by

$$x \mapsto (x, \sqrt{f_4(x)}), \quad x \mapsto (x, -\sqrt{f_4(x)}).$$

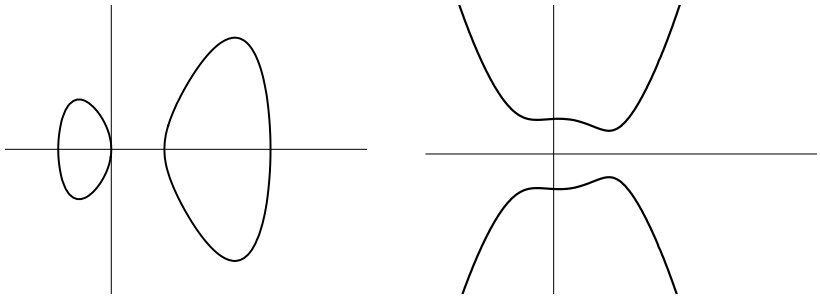

Figure 12: Two types of double covers $C(\mathbb{R}) \to \mathbb{P}^1(\mathbb{R})$ of an elliptic M-curve C. A double cover from the Huisman component is on the right.

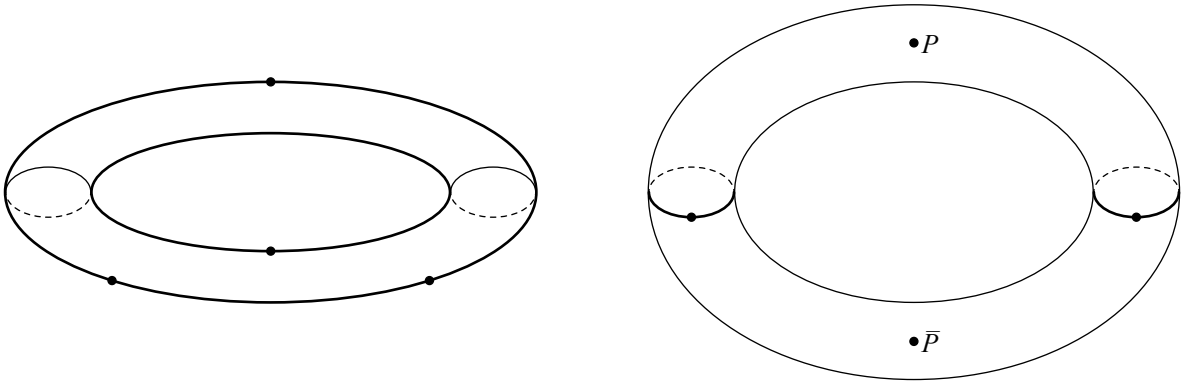

Figure 13: MHV elliptic M curves of Type A, left, and type B, right.

Next we suppose that C is an MHV elliptic M-curve of type A or B. In other words, we add 4 marked points so that, depending on the type,

(A) $p_1, p_2, p_3 \in X$ and $p_4 \in Y$,

(B) $p_1 \in X$, $p_2 \in Y$ and $p_3 = \bar{p}_4$ are complex-conjugate points.

We have six special points $p_{ij} = \mathbb{O}(p_i + p_j) \in \mathrm{Pic}^2 C$. Depending on the type,

(A) $p_{12}, p_{13}, p_{23} \in X^{(2)}$ and $p_{14}, p_{24}, p_{34} \in Y^{(2)}$,

(B) $p_{34} \in X^{(2)}$, $p_{12} \in Y^{(2)}$ and $p_{13} = \bar{p}_{14}$, $p_{23} = \bar{p}_{24}$ are complex-conjugate.

The scattering amplitude map $\mathbf{\Lambda} : \mathrm{Pic}^2 C \to \mathbb{P}^1$ is given by the line bundle

$$\mathscr{L} = \mathbb{O}(p_{12} + p_{34}) \simeq \mathbb{O}(p_{13} + p_{24}) \simeq \mathbb{O}(p_{14} + p_{23}).$$

In both cases (A) and (B), $\mathscr{L} \in Y^{(4)}$, the Huisman component of $\mathrm{Pic}^2(\mathrm{Pic}^2 C)$. The restriction of $\mathbf{\Lambda}$ to both connected components $X^{(2)}$ and $Y^{(2)}$ of $\mathrm{Pic}^2 \mathbb{R}$ is an analytic isomorphism with $\mathbb{P}^1(\mathbb{R})$. In other words, the scattering amplitude map $\mathbf{\Lambda}$ of an elliptic M-curve of type (A) or (B) looks like the projection onto the x-axis as on the right side of Figure 12. We get a 4-parameter family of smooth scattering amplitude probability measures given (up to normalization) by

$$A = \frac{dx}{\sqrt{f_4(x)}},$$

where f_4 is a real polynomial with two pairs of complex conjugate roots. A familiar 2-parameter subfamily is given by

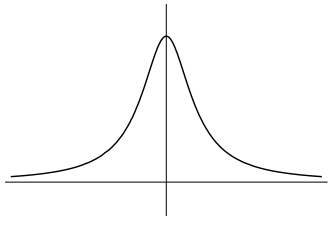

$$\frac{M(a,b)}{\pi} \frac{dx}{\sqrt{(x^2+a^2)(x^2+b^2)}},$$

where $a \neq b$ and $M(a,b)$ is the arithmetic–geometric mean of a and b.

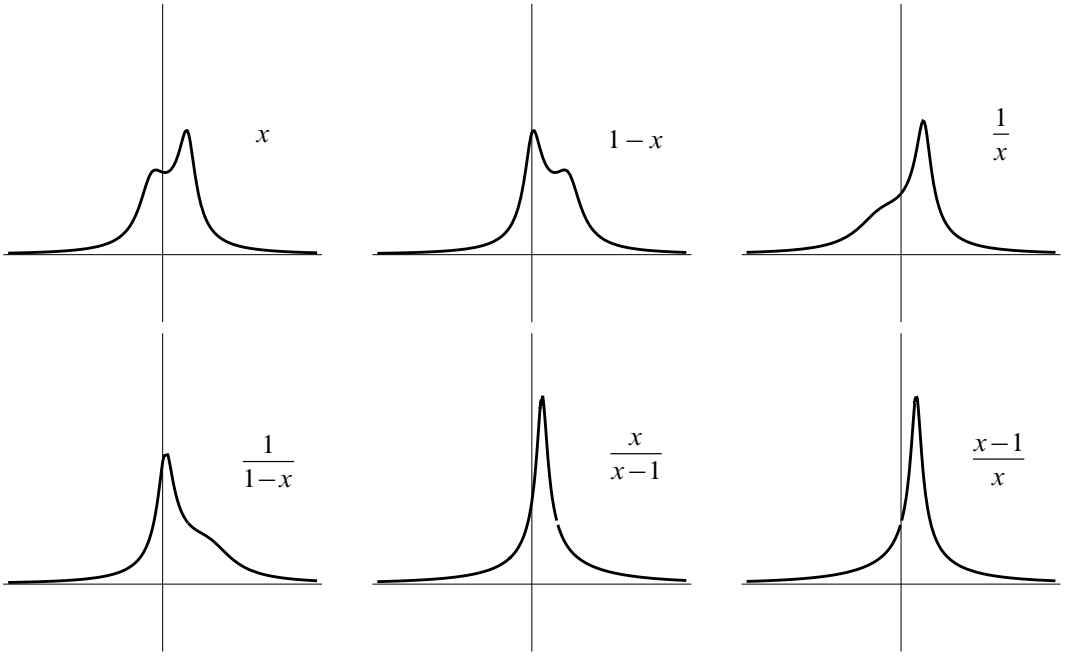

Figure 14

8.14 Remark The scattering probability measure $\rho(x)\,|dx|$ is a smooth measure on $\overline{M}_{0,4}(\mathbb{R}) \simeq \mathbb{RP}^1$ including the point at ∞, ie $\rho(1/x)/x^2$ is smooth at 0. In fact, presenting it as a probability measure on $\mathbb{R}$ depends on a specific choice of the identification $\overline{M}_{0,4}(\mathbb{R}) \simeq \mathbb{RP}^1$, and it is well-known that there are $|S_3| = 6$ possibilities, which can result in differently looking density graphs; see Figure 14.

8.15 Genus 1, continued In type (A), the real form of $M_{0,4}$ is $M^A_{0,4}(\mathbb{R}) = M_{0,4}(\mathbb{R})$, the configuration space of 4 points in $\mathbb{P}^1(\mathbb{R})$. Viewing $M_{0,4}(\mathbb{C})$ as a Riemann sphere punctured at $0, 1, \infty$ via the cross-ratio map, $M_{0,4}(\mathbb{R})$ is identified with the real axis without $0, 1, \infty$ and $\overline{M}_{0,4}(\mathbb{R})$ with $\mathbb{P}^1(\mathbb{R})$, the equator of the Riemann sphere. The scattering amplitude map $\mathbf{\Lambda}\colon \mathrm{Pic}^2\,\mathbb{R} \to \overline{M}_{0,4}(\mathbb{R})$ has the property that

$$\mathbf{\Lambda}(p_{14}) = \mathbf{\Lambda}(p_{23}) = 0, \quad \mathbf{\Lambda}(p_{13}) = \mathbf{\Lambda}(p_{24}) = 1, \quad \mathbf{\Lambda}(p_{12}) = \mathbf{\Lambda}(p_{34}) = \infty. \tag{8.15.1}$$

In type (B), the real form is $M^B_{0,4}(\mathbb{R})$, the configuration space of two real and two complex-conjugate points in $\mathbb{P}^1(\mathbb{C})$. If $\lambda = (p_1, p_2; p_3, p_4)$ is their cross-ratio then

$$\overline{\lambda} = (p_1, p_2; p_4, p_3) = 1 - \lambda.$$

Therefore,

$$M^{2,1}_{0,4}(\mathbb{R}) = \{\mathrm{Re}(z) = \tfrac{1}{2}\} \subset \mathbb{C},$$

and the compactification $\overline{M}^{2,1}_{0,4}(\mathbb{R})$ is obtained by adding a single point (at ∞). The scattering amplitude map $\mathbf{\Lambda}\colon \mathrm{Pic}^2\,\mathbb{R} \to \overline{M}^{2,1}_{0,4}(\mathbb{R})$ still has property (8.15.1), but now only ∞ is part of the real locus $\overline{M}^{2,1}_{0,4}(\mathbb{R})$. This corresponds to the fact that points $p_{13} = \bar{p}_{14}$ and $p_{23} = \bar{p}_{24}$ are not in $\mathrm{Pic}^2\,\mathbb{R}$.

8.16 Real planar locus W Recall from Section 2.8 that the planar locus $W \subset \mathrm{Pic}^{g+1} C$ has codimension 3 and (for a general curve) parametrizes realizations of C as a degree-$(g+1)$ plane curve with $\frac{1}{2}g(g-3)$ nodes away from the marked points $p_1, \dots, p_n$. Generically along W, the scattering amplitude map is resolved by the blow-up (2.8.2) of W with exceptional divisor $\widehat{W}$, and the scattering amplitude form vanishes along $\widehat{W}$ with multiplicity 2. Suppose that C is a generic real MHV M-curve. Then line bundles in $W(\mathbb{R})$ give realizations of C as *Harnack curves*, more precisely real plane curves of degree $g+1$ and genus g with $g+1$ real components. These curves have $\frac{1}{2}g(g-3)$ acnodes, ie isolated real points (where two complex-conjugate branches of the complex plane curve intersect transversally). If g is odd then all $g+1$ components are ovals (separate $\mathbb{RP}^2$ into a disk and a Möbius strip). If g is even, there are g ovals and one pseudoline (a generator of $\pi_1(\mathbb{RP}^2)$); see [Gross and Harris 1981]. It follows that a general real line in $\mathbb{RP}^2$ has even degree on all components of $C(\mathbb{R})$ if g is odd, and on all but one if g is even. So for a general real MHV M-curve,

$$W(\mathbb{R}) \subset \mathrm{Pic}^{g+1}_{\varnothing} \mathbb{R}$$

if g is odd. If g is even, $W(\mathbb{R})$ is contained in the union of $\mathrm{Pic}^{g+1}_{I} \mathbb{R}$ for $|I| = 1$. It follows that the scattering amplitude probability measures $|A_{\varnothing}|$ (g odd) and $|A_I|$ for $|I| = 1$ (g even) are the only ones that vanish to the order 2 along $\widehat{W}(\mathbb{R})$.

In the rest of the section we study scattering measures of genus 2 curves.

8.17 Let C be a smooth MHV M-curve of genus 2 given by the equation $y^2 = f(x)$, where f is a real polynomial of degree 5 with 5 distinct real roots. We denote the ovals of $C(\mathbb{R})$ by C_1, C_2 and C_3. Like in Theorem 8.12, we assume that

$$p_i \in C_i \quad \text{for } i = 1, 2, 3,$$

and that

$$p_4, p_5 \in C_3 \ \text{ (type A)} \quad \text{or} \quad p_4 = \overline{p}_5 \ \text{ (type B)}.$$

See Figure 3. We follow the notation of Section 7 for special points and divisors. In particular,

$$K \in \mathrm{Pic}^2_{\varnothing} \mathbb{R} \quad \text{and} \quad P = p_1 + \cdots + p_5 \in \mathrm{Pic}^5_{\{1,2,3\}} \mathbb{R}.$$

The special points $\delta = P - K$, $\delta_i = K + p_i$ and $\delta_{ij} = P - p_i - p_j$ are distributed among four components of $\mathrm{Pic}^3 \mathbb{R}$ as follows:

type	$\mathrm{Pic}^3_H \mathbb{R}$	$\mathrm{Pic}^3_{\{1\}} \mathbb{R}$	$\mathrm{Pic}^3_{\{2\}} \mathbb{R}$	$\mathrm{Pic}^3_{\{3\}} \mathbb{R}$
A	$\delta, \delta_{45}, \delta_{34}, \delta_{35}$	$\delta_1, \delta_{23}, \delta_{24}, \delta_{25}$	$\delta_2, \delta_{13}, \delta_{14}, \delta_{15}$	$\delta_3, \delta_4, \delta_5, \delta_{12}$
B	δ, δ_{45}	δ_1, δ_{23}	δ_2, δ_{13}	δ_3, δ_{12}

The map φ_P embeds $C(\mathbb{R})$ into $\mathbb{P}^3(\mathbb{R})$. Let $\mathbb{P}^2 \subset \mathbb{P}^3$ be the plane passing through $p_1, \dots, p_5$. Let $\mathbf{dP}_4 = \mathrm{Bl}_{p_1,\dots,p_5} \mathbb{P}^2$ be the quartic del Pezzo surface. Depending on the type of the MHV M-curve C, there are two possibilities for its real form,

$$\mathbf{dP}_4^A(\mathbb{R}) = \mathrm{Bl}_{p_1,\dots,p_5} \mathbb{P}^2(\mathbb{R}) \quad \text{or} \quad \mathbf{dP}_4^B(\mathbb{R}) = \mathrm{Bl}_{p_1,p_2,p_3} \mathbb{P}^2(\mathbb{R}).$$

	curve in $\mathbf{dP}_4(\mathbb{R})$	$\mathrm{Pic}^3_H(\mathbb{R})$	$\mathrm{Pic}^3_{\{1\}}(\mathbb{R})$	$\mathrm{Pic}^3_{\{2\}}(\mathbb{R})$	$\mathrm{Pic}^3_{\{3\}}(\mathbb{R})$
A	conic	Δ	$E(C_1)$	$E(C_2)$	$E(C_3)$
	exceptional	$E_1(C_1)$	Δ_1	$E_1(C_3)$	$E_1(C_2)$
		$E_2(C_2)$	$E_2(C_3)$	Δ_2	$E_2(C_1)$
		$E_k(C_3)$	$E_k(C_2)$	$E_k(C_1)$	Δ_k
	line	Δ_{kl}	$E_{kl}(C_1)$	$E_{kl}(C_2)$	$E_{kl}(C_3)$
		$E_{2k}(C_1)$	Δ_{2k}	$E_{2k}(C_3)$	$E_{2k}(C_2)$
		$E_{1k}(C_2)$	$E_{1k}(C_3)$	Δ_{1k}	$E_{1k}(C_1)$
		$E_{12}(C_3)$	$E_{12}(C_2)$	$E_{12}(C_1)$	Δ_{12}
B	conic	Δ	$E(C_1)$	$E(C_2)$	$E(C_3)$
	exceptional	$E_1(C_1)$	Δ_1	$E_1(C_3)$	$E_1(C_2)$
		$E_2(C_2)$	$E_2(C_3)$	Δ_2	$E_2(C_1)$
		$E_3(C_3)$	$E_3(C_2)$	$E_3(C_1)$	Δ_3
	line	Δ_{45}	$E_{45}(C_1)$	$E_{45}(C_2)$	$E_{45}(C_3)$
		$E_{23}(C_1)$	Δ_{23}	$E_{23}(C_3)$	$E_{23}(C_2)$
		$E_{13}(C_2)$	$E_{13}(C_3)$	Δ_{13}	$E_{13}(C_1)$
		$E_{12}(C_3)$	$E_{12}(C_2)$	$E_{12}(C_1)$	Δ_{12}

Table 1

8.18 By Theorem 8.10, $\mathrm{Pic}^3\,\mathbb{R}$ is disjoint[10] from the ramification divisor R. This implies by Theorem 7.6 that the degree-4 morphism

$$\overline{\mathbf{\Lambda}}\colon \mathrm{Bl}_{16}\,\mathrm{Pic}^3\,C(\mathbb{R}) \to \mathrm{Bl}_{p_1,\dots,p_5}\,\mathbb{P}^2(\mathbb{R}) \quad \text{in type (A)},$$
$$\overline{\mathbf{\Lambda}}\colon \mathrm{Bl}_{8}\,\mathrm{Pic}^3\,C(\mathbb{R}) \to \mathrm{Bl}_{p_1,p_2,p_3}\,\mathbb{P}^2(\mathbb{R}) \quad \text{in type (B)},$$

induced by the scattering amplitude map is a real-analytic isomorphism on each connected component $\mathrm{Pic}^3_I\,C(\mathbb{R})$ blown up at four (in type A) or two (in type B) points. Note that topologically each of these components is a connected sum of a torus T^2 with four (in type A) or two (in type B) $\mathbb{RP}^2$'s, while $\mathbf{dP}_4(\mathbb{R})$ is a connected sum of six (in type A) or four (in type B) $\mathbb{RP}^2$'s. The scattering amplitude map $\overline{\mathbf{\Lambda}}$ provides a real-analytic isomorphism between these (nonorientable) surfaces.

8.19 By Theorem 7.6, the preimage of each (-1)-curve in $\mathbf{dP}_4$ is the union of the Δ and E-type divisors, where the former is a $\mathbb{P}^1$ and the latter is a copy of C. In Table 1 we give the preimages under $\overline{\mathbf{\Lambda}}$ of real (-1)-curves in $\mathbf{dP}_4(\mathbb{R})$. Recall that the E-type divisors are

$$E = K + C, \quad E_i = P - p_i - C, \quad E_{ij} = C + p_i + p_j.$$

The range of indices k, l in the table is $3, 4, 5$. We use notation

$$E(C_i) = K + C_i, \quad E_i(C_j) = P - p_i - C_j, \quad E_{ij}(C_k) = C_k + p_i + p_j.$$

[10] Since $\delta \in \mathrm{Pic}^3\,\mathbb{R}$, this has a curious geometric consequence: the unique quadric surface in $\mathbb{P}^3$ containing C is smooth (by Lemma 7.5).

8.20 Remark The scattering amplitude measure on each connected component $\mathrm{Pic}^3_I(\mathbb{R})$ is a probability measure on a real algebraic surface that in any real-analytic chart U has form $\rho(x,y)|dx\,dy|$, where $\rho(x,y)>0$ is a smooth, in fact real-analytic, function. The behavior of the probability measure under the blow-up is as follows. Locally, we blow up the origin $(0,0)$ of the chart,

$$\pi : \mathrm{Bl}_{(0,0)}\, U \to U.$$

The surface $\mathrm{Bl}_{(0,0)}\, U$ is nonorientable and contains an exceptional curve $\mathbb{RP}^1$, the preimage of $(0,0)$; see the cover artwork of [Shafarevich 2013]. A tubular neighborhood of the curve $\mathbb{RP}^1$ is covered by two charts that correspond to standard charts of $\mathbb{RP}^1$. In each chart, π has the form $(u,v)\mapsto(u,uv)$ and thus the probability measure is

$$\rho(u,uv)|u||du\,dv|. \tag{8.20.1}$$

Note that $u=0$ is the local equation of the exceptional curve. The probability measure (8.20.1) vanishes along it to the order of $|u|$. More generally, if $|A|$ is a probability measure on a real-analytic manifold X which is smooth and nonvanishing generically along a submanifold Y of codimension c, then the same measure on the blow-up $\mathrm{Bl}_Y X$ vanishes along the exceptional divisor generically to the order of $|u|^{c-1}$.

8.21 Back in our situation, the scattering amplitude measure on $\mathbf{dP}_4(\mathbb{R})$ is smooth and positive away from four (in type A) or two (in type B) projective lines that correspond to Δ-divisors in the Section 8.19. Along these lines, the scattering amplitude form vanishes like in (8.20.1). These disjoint (-1)-curves can always be contracted to points giving morphisms $\mathbf{dP}_4(\mathbb{R})\to(\mathbb{RP}^1)^2$. Combining everything together gives a commutative diagram

$$\begin{array}{ccc} \mathrm{Bl}\,\mathrm{Pic}^3_I(\mathbb{R}) & \xrightarrow{\bar{\mathbf{\Lambda}}} & \mathbf{dP}_4(\mathbb{R}) \\ \downarrow & & \downarrow \\ \mathrm{Pic}^3_I(\mathbb{R}) & \xrightarrow{\simeq} & (\mathbb{RP}^1)^2 \end{array}$$

where vertical arrows are blow-downs of four (type A) or two (type B) projective lines, and the bottom arrow is a real-analytic isomorphism — note that algebraically these varieties can't be more different! It follows that we can view the scattering amplitude measure on $\mathbf{dP}_4(\mathbb{R})$ as a smooth positive probability measure on $(\mathbb{RP}^1)^2$, subject to Möbius transformations of coordinates as in Remark 8.14.

8.22 So far we have treated the Huisman component and the other connected components of $\mathrm{Pic}^3(\mathbb{R})$ on an equal footing, but there is an important difference. For simplicity, we consider Type A only. Recall that the space $\mathbf{dP}_4$ is an artifact of the hyperelliptic case; the actual observable is not this surface but $\mathbf{dP}_5=\overline{M}_{0,5}$. The map $\mathbf{dP}_4\to\mathbf{dP}_5$ is a contraction of the conic that corresponds to the exceptional divisor Δ only for the Huisman component (see Section 8.19), in which case the scattering amplitude map gives a real-analytic isomorphism

$$\mathbf{\Lambda} : \mathrm{Bl}_{\delta_{45},\delta_{34},\delta_{35}}\,\mathrm{Pic}^3_H(\mathbb{R}) \to \mathbf{dP}_5 = \overline{M}_{0,5}(\mathbb{R}).$$

The 10 exceptional divisors of $\mathbf{dP}_5$ (the "Petersen graph") are images of the 10 proper transforms l_{ij} in $\mathbf{dP}_4$ of lines in $\mathbb{P}^2$ connecting points p_i and p_j of the conic pairwise. The lines l_{34}, l_{35}, l_{45} are images of the exceptional divisors Δ_{34}, Δ_{35}, Δ_{45} on $\mathrm{Bl}_{\delta_{45},\delta_{34},\delta_{35}}\mathrm{Pic}^3_H$. These three lines on $\mathbf{dP}_5$ are contracted by the map

$$\overline{M}_{0,5} \to (\mathbb{P}^1)^2 = (\overline{M}_{0,4})^2$$

given by cross-ratios 1345 and 2345. This gives a diagram of Theorem 8.12

$$\begin{array}{ccc} \mathrm{Bl}_{\delta_{45},\delta_{34},\delta_{35}}\mathrm{Pic}^3_H(\mathbb{R}) & \xrightarrow[\simeq]{\mathbf{\Lambda}} & \overline{M}_{0,5}(\mathbb{R}) \\ \downarrow & & \downarrow{\scriptstyle \begin{matrix}1345\\2345\end{matrix}} \\ \mathrm{Pic}^3_H(\mathbb{R}) & \xrightarrow{\simeq} & (\overline{M}_{0,4}(\mathbb{R}))^2 \end{array}$$

where horizontal arrows are real-analytic isomorphisms. To summarize, for the Huisman component we have a preferred choice of cross-ratios that gives a smooth positive scattering amplitude probability measure on $(\mathbb{R}\mathbb{P}^1)^2$. For the reader's amusement, we include a few pretty examples of these probability density functions in Figure 15, rendered using Section 6.8.

```
Roots:-1, 0, 1, 2, 3
Marked points:
(-0.7, 1.8885)
(1.3, 1.03317)
(3.3, 3.56769)
(3.45, 4.95408)
(4.2, -13.5832)
```

```
Roots:-1, 0, 1, 2, 3
Marked points:
(-0.1, 0.802801)
(1.9, 0.738573)
(3.9, 9.73481)
(4.35, 15.727)
(6.6, -68.2029)
```

```
Roots:-2, -0.2, 0.2, 2, 7
Marked points:
(-1.28, 5.59063)
(0.92, 3.93215)
(7.4, 33.3322)
(7.6, 43.1488)
(8.6, -90.9632)
```

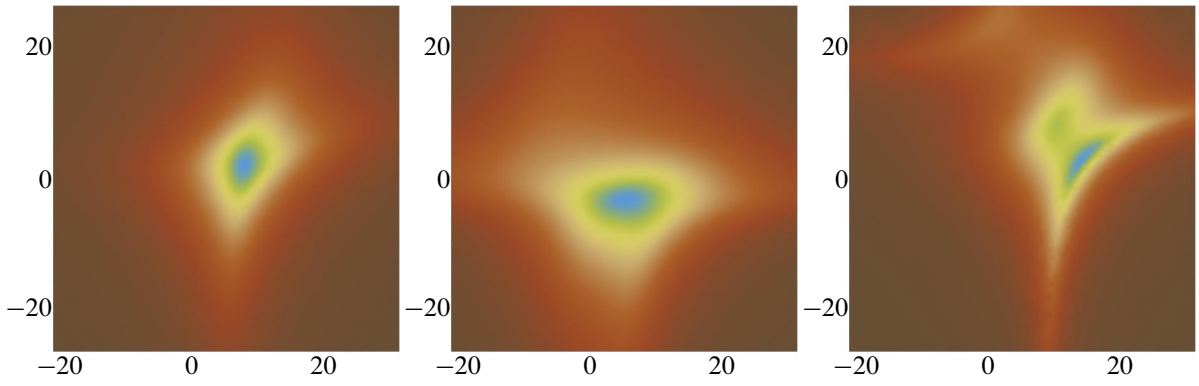

Figure 15: Scattering amplitudes in genus 2, Huisman's component.

9 Forest behind the hypertrees

9.1 Let C be a *maximally degenerate* stable curve: every irreducible component is a $\mathbb{P}^1$ with three special points (either nodes or marked points). Equivalently, an on-shell diagram is trivalent. We will characterize MHV curves of this type.

9.2 Lemma *If C is an MHV curve, then L has degree 0 or 1 on every component of C. The on-shell diagram is a trivalent graph with d black circles (where L has degree 1) and the remaining white circles (where L has degree 0).*

Proof We argue by contradiction and suppose that the degree of L on some irreducible component B is at least 2. By Lemma 3.10, the remaining part of the curve A is connected. Let g_A be its genus and let d_A be the degree of L on A. Then $d_A \le d-2 = g-1$. On the other hand, $g_A \ge g-2$. If $g_A > 0$ then, by Lemma 3.5(1), $d_A = g-1$ and $d_A = g_A+1$. If $g_A = 0$ then $g = 2$ and so again $d_A = g_A+1$. In both cases, by Lemma 3.5(2), A contains at most $g_A+3 = n-2$ marked points. Thus B contains at least two marked points. This contradicts Lemma 3.10. □

9.3 Assumption By Lemma 3.2 and Remark 3.3, if C is an MHV curve then every connected component of a subgraph of white circles of the on-shell diagram is a tree with at most one marked point. In addition, by Lemma 3.5, a connected subcurve $A \subset C$ of arithmetic genus p should satisfy the following conditions:

(1) If $p > 0$, then $\deg L|_A \ge p+1$.

(2) If $\deg L|_A = p+1$, then A contains at most $p+3$ marked points.

From now on we will assume that all these conditions hold.

The precise shape of these subtrees is not important for the calculation of the scattering amplitude map and form and there are two ways to ignore them.

9.4 Definition Let C be a maximally degenerate curve satisfying Assumption 9.3.

(1) For each maximal connected subtree of white circles of the on-shell diagram, contract all interior edges of the tree so that it shrinks to a point. We call this point a white *megacircle*. It is possible for it to have more than three outgoing edges. A similar operation appears in [Arkani-Hamed et al. 2015]. Geometrically, this corresponds to a curve C_s obtained by smoothing some nodes of C.

(2) Contract each component of C where L has degree 0 to a singular point of a *hypertree curve* Σ [Castravet and Tevelev 2013, Definition 1.8]. Σ is not a stable curve: it has singularities worse than nodes and marked points at singularities. But it is convenient: every morphism to $\mathbb{P}^1$ given by a line bundle in $\mathrm{Pic}^{\vec{d}}\, C$ factors through Σ.

The following lemma was essentially proved in [Arkani-Hamed et al. 2015].

9.5 Lemma *Let C be a maximally degenerate curve satisfying Assumption 9.3. Then its on-shell diagram has the following properties*:

(1) *Black circles are only connected to white megacircles and marked points.*

(2) *Each white megacircle is connected to exactly one marked point.*

(3) *The data of the on-shell diagram is equivalent to the data of triples in $\{1,\dots,n\}$*:

$$\Gamma = \{\Gamma_1,\dots,\Gamma_d\}.$$

Each Γ_i is associated to one of the d black circles of the on-shell diagram. For such a circle, the associated Γ_i consists of the markings that are either attached directly at that black circle, or sit on a white megacircle connected to it.

Proof The first step is to place a dummy white megacircle with two edges between every marked point and a black circle directly connected to it. After this operation, no black circle is connected directly to a marked point. Let r be the total number of white megacircles. The on-shell diagram can be built step by step as follows: start with r white megacircles connected to marked points. The Euler characteristic of this graph is r. Now add black circles one by one. Every time we add a new black (trivalent!) circle, the Euler characteristic goes down by at most 2, and exactly by 2 only if the black circle is connected to an already constructed graph at three points. It follows that at the end of the construction the Euler characteristic will be at least $r-2(g+1)$, on the other hand it should be equal to $1-g$. Thus $r \le g+3 = n$. On the other hand, $n \le r$ because each white megacircle is connected to at most one marked point. Thus we have all the conclusions: $r = n$, all white megacircles are connected to marked points and black vertices are not connected to each other. It remains to note that every black vertex is connected to three different marked points. Indeed, otherwise a black vertex is connected to a white vertex by two paths, producing a subcurve of arithmetic genus 1 and degree 1, which contradicts Assumption 9.3. □

Not every maximally degenerate curve satisfying Assumption 9.3 is an MHV curve. The precise condition is as follows:

9.6 Theorem [Castravet and Tevelev 2013, Theorems 2.4 and 3.2] *A maximally degenerate stable curve C is an MHV curve if and only if it is give by triples Γ as in Lemma 9.5 that form a CT hypertree*,[11] *ie satisfy equation* (‡),

$$\left|\bigcup_{j\in S}\Gamma_j\right| \ge |S|+2 \quad \text{for every } S\subset\{1,\dots,d\}.$$

The scattering amplitude map is birational, with inverse map (*called v in* [loc. cit.])

$$\mathbf{\Lambda}^{-1}\colon M_{0,n}\to \mathrm{Pic}^{\vec{d}}\, C,\quad \mathbf{\Lambda}^{-1}(q_1,\dots,q_n) = v^*\mathbb{O}_{\mathbb{P}^1}(1), \tag{9.6.1}$$

where $v\colon C\to\mathbb{P}^1$ is a unique morphism such that $v(p_i)=q_i$ and $v^*\mathbb{O}_{\mathbb{P}^1}(1)\in \mathrm{Pic}^{\vec{d}}\, C$.

[11] See [Castravet and Tevelev 2013] for motivation and a more general definition for subsets other than triples. There are other notions of hypertree in literature, so to distinguish our case we use the terminology "CT hypertree".

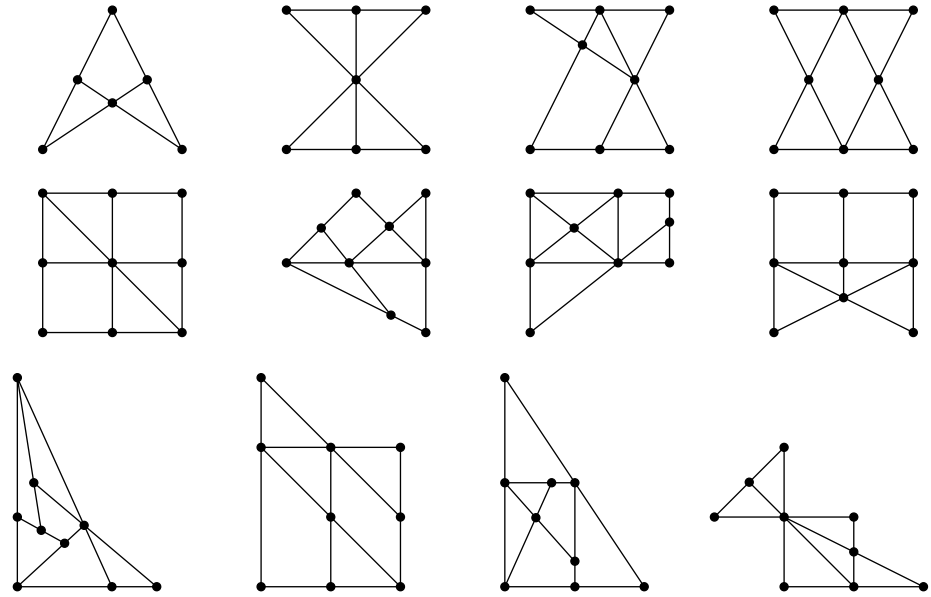

Figure 16

9.7 Definition [Castravet and Tevelev 2013] A CT hypertree Γ is called irreducible if (‡) is a strict inequality for every S such that $1 < |S| < d$.

9.8 Example In genus 0 and 1, irreducible CT hypertrees are Examples 1.10 and 4.10, respectively. In genus 2, there are none. See Figure 16 for irreducible hypertrees in genus $3, 4, 5, 6$. The database of irreducible CT hypertrees in genus at most 8 up to symmetries along with equations and classes of the corresponding hypertree divisors was created by Opie and Scheidwasser [2009].

9.9 The main goal of [Castravet and Tevelev 2013] was to construct *hypertree divisors* $D_\Gamma \subset M_{0,n}$ with good properties. Suppose that Γ is an irreducible CT hypertree and $g \geq 3$. Then $\mathbf{\Lambda}^{-1}$ contracts a unique divisor $D_\Gamma \subset M_{0,n}$ given by

- choosing a configuration of different points $p_1, \dots, p_n \in \mathbb{P}^2$ such that different points p_i, p_j, p_k are colinear if and only if $\{i, j, k\} \in \Gamma$,
- projecting points $p_1, \dots, p_n$ from a point $p \in \mathbb{P}^2$ to points $q_1, \dots, q_n \in \mathbb{P}^1$, and
- representing the datum $(\mathbb{P}^1; q_1, \dots, q_n)$ by a point of $M_{0,n}$.

See Figure 17. The reader will notice a parallel with Section 2.8: the image $W_\Gamma := \mathbf{\Lambda}^{-1}(D_\Gamma) \subset \mathrm{Pic}^{\vec{d}}\, C$ is the analogue of the planar locus $W \subset \mathrm{Pic}^{g+1}\, C$ of a smooth MHV curve C that parametrizes its presentations as a plane curve of degree $g+1$. Like in the smooth case, the scattering amplitude form on $\mathrm{Pic}^{\vec{d}}\, C$ (when pulled back to $M_{0,n}$) vanishes along D_Γ with multiplicity 2 because W_Γ has codimension 3. This was noticed in [Castravet and Tevelev 2013] and [Arkani-Hamed et al. 2015], which both contain (the same) determinantal equation for D_Γ.

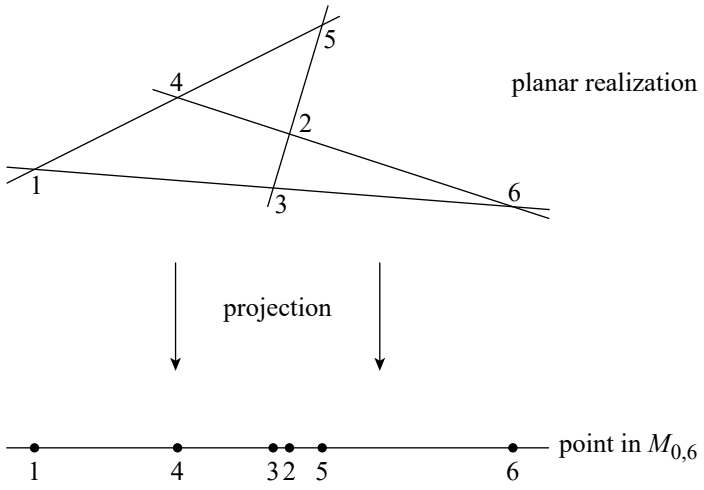

Figure 17

9.10 Remark The same stable curve can give many hypertrees by changing a vector $\vec{d}$ of multidegrees. It is a nontrivial question to understand all MHV curves with the same underlying stable maximally degenerate curve C.

We finish this section by studying geometry of spherical CT hypertrees. Recall that every checkerboard triangulation of a 2-sphere as in Figure 5 gives a CT hypertree: vertices of the triangulation give the indexing set $\{1,\dots,n\}$ and black triangles give triples (another CT hypertree is given by white triangles).

9.11 Theorem *Let Γ be a CT hypertree and let C be the corresponding maximally degenerate stable MHV curve. Then Γ is spherical if and only if C does not have a 2-channel factorization (see Definition 3.11) and admits a real algebraic structure such that*:

(1) *C is a stable limit of smooth pointed M-curves C_t of type A; see Definition 8.2. Let $C(\mathbb{R}) = W_1 \cup \cdots \cup W_{g+1}$ be the union of images of $g+1$ ovals of $C_t(\mathbb{R})$.*

(2) *No W_i is an acnode, ie a real node which is a connected component of $C(\mathbb{R})$.*

(3) *No W_i is contained in a degree-0 component of C (white circle of the on-shell diagram). Equivalently, W_i is not contracted to a point by the morphism $C \to \Sigma$.*

Proof Let C be a maximally degenerate stable MHV curve without 2-channel factorization that satisfies properties (1)–(3). By Theorem 9.6, it corresponds to a CT hypertree Γ. We need to show that Γ is spherical. According to [Seppälä 1991], we can obtain C as follows.[12] Start with a smooth pointed M-curve C_t of type A. Topologically, C_t is obtained by gluing two identical discs D and $\bar{D}$ with g holes removed. In C_t, these disks are interchanged by the complex conjugation. They are glued along the

[12]More precisely, [Seppälä 1991] is restricted to curves without marked points. But there is a trick, a morphism from $\overline{M}_{g,n}$ to the "flag stratum" of $\overline{M}_{g+n}$, which attaches a nodal genus-1 curve to every marking. All results that we need about the stable reduction follow from the corresponding results for $\overline{M}_{g+n}$.

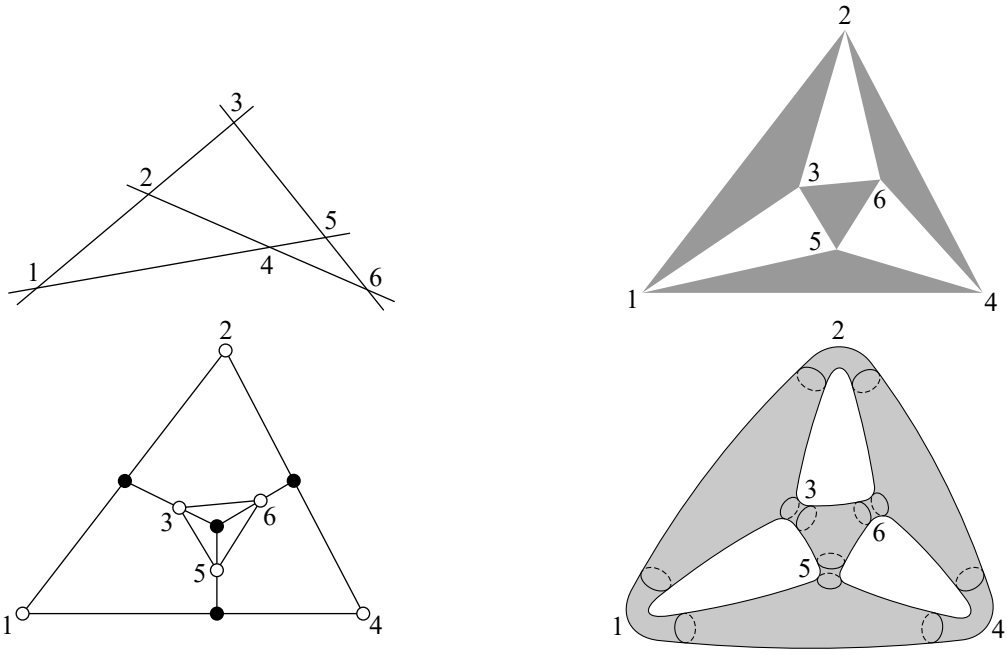

Figure 18: A hypertree curve (top left) of a spherical CT hypertree (top right) with an on-shell diagram (bottom left) is a degeneration of a real algebraic M-curve (bottom right).

real locus $C(\mathbb{R}) = D \cap \bar{D}$, which is the union of the outside oval of D and g inside ovals. Of course we can turn any oval into an "outside" oval by turning D inside out. But there is a good choice: we choose the oval with 3 marked points as an outside one, and the remaining ovals (with one marked point each) as the inside ovals.

Next we fix a hyperbolic metric on $C_t \setminus \{p_1, \dots, p_n\}$, remove small conjugation-invariant discs around marked points with geodesic boundaries and choose a conjugation-invariant pair-of-pants decomposition of the remaining surface, with geodesic boundaries. The stable curve C is obtained by shrinking the boundaries of pairs of pants to nodes, except for the boundaries around marked points.

We investigate the structure of this pair-of-pants decomposition. Since C does not contain acnodes by condition (2), no real oval of C_t is the boundary of a pair of pants. We claim that no boundary B is entirely contained in D (or $\bar{D}$) either. Indeed, if this were the case then by Jordan's lemma B separates D into two connected components. Shrinking B (and $\bar{B}$) creates a pair of complex-conjugate nodes of C. Neither of these nodes is a separating node because C does not admit a one-channel factorization by Lemma 3.10. Thus these nodes separate C into two connected components. But this contradicts the fact that C does not admit a two-channel factorization[13] and satisfies condition (3).

[13]Interestingly, if this two-channel factorization by complex-conjugate nodes does occur, the resulting curve is of the easy type (I), completely described in Theorem 3.16.

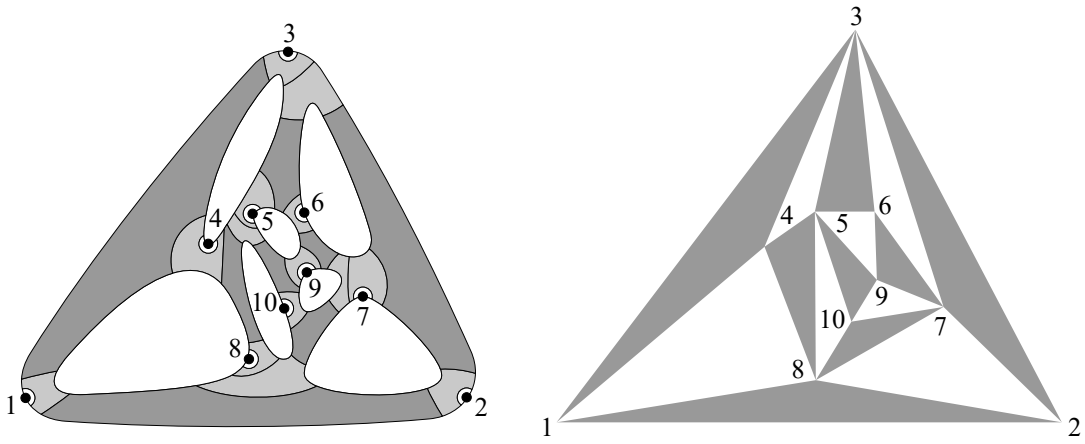

Figure 19: Decomposition of the disk D and the corresponding triangulation.

It follows that every pair of pants, a Riemann sphere with three discs removed, is in fact conjugation-invariant, moreover isomorphic to $\mathbb{P}^1(\mathbb{C})$ with the usual complex conjugation and three removed discs are centered at three points of $\mathbb{P}^1(\mathbb{R})$. The quotient of C_t with the pair-of-pants decomposition by the complex conjugation is the original disc D with g holes, and the quotient of each pair of pants is a curved hexagon with alternating sides that are either arcs of real ovals of $C(\mathbb{R})$ or arcs connecting the ovals. The pairs of pants arising from the marked points look as follows: an arc around the marked point connecting two points of the same real oval Z, then two arcs of Z, then two sides of the hexagon connecting Z to an oval Z', then an arc of Z'. Other pairs of pants connect three real ovals. We claim that in fact in the first case $Z \neq Z'$, and in the second case all three real ovals are different. Indeed, if one of the sides of the hexagon (not around the marked point) connects a real oval to itself, then the corresponding border of the pair of pants is shrunk to a node of C that separates C into two connected components, which is impossible by Lemma 3.10. We illustrate the decomposition of D into hexagons in Figure 19, where we shade in gray the components of C of degree 0.

Finally, we produce a checkerboard decomposition of the sphere, as follows. We shrink pairs of pants arising from the marked points to points. Furthermore, we shrink hexagons that correspond to other degree 0 components of C to points. Furthermore, we shrink arcs connecting real ovals of degree-1 components of C to points. This gives $g+1$ black triangles. We glue $g+1$ white polygons to the real ovals of C along the arcs of black triangles. This gives a checkerboard decomposition of the sphere into $g+1$ black triangles and $g+1$ white polygons. A priori, some of these white polygons may have two sides; however, if that were the case then two adjacent black triangles would produce a two-channel factorization of C, which is impossible. Thus all white polygons have at least three edges, and therefore they are all triangles since the total number of edges of black and white triangles is the same. Therefore, the CT hypertree is spherical. We illustrate the pair-of-pants decomposition and the corresponding triangulation in Figure 19.

It remains to prove that every spherical CT hypertree gives a maximally degenerate stable MHV curve that can be obtained as a limit of smooth pointed M-curves C_t of type A. The construction of the

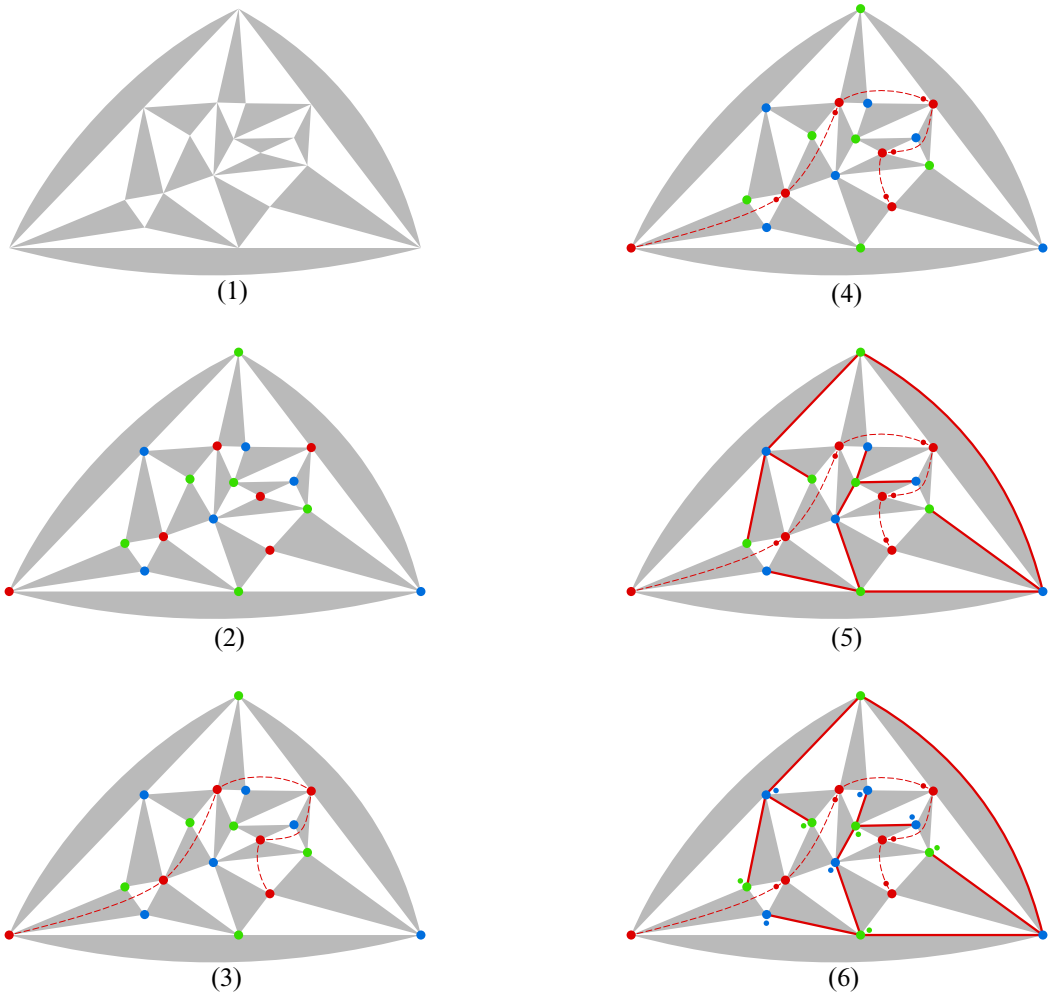

Figure 20: Tutte matching algorithm [1975].

conjugation-invariant pair-of-pants decomposition should be obvious at this point. The only nontrivial remaining part of the argument is to explain how to distribute points among the real ovals of $C_t(\mathbb{R})$. Concretely, we start with a checkerboard triangulation of the sphere, attach three marked points to the "outside" white triangle, and now have to distribute the remaining g marked points in g inside white triangles so that every triangle contains exactly one marked point as in Figure 19. In other words, we have to construct a perfect matching between nonexterior vertices of the triangulation and interior white triangles. This nontrivial matching has been constructed by Tutte [1975] in his famous trinity theorem. The algorithm goes as follows, as illustrated in Figure 20:

(1) Start with any checker-board triangulation.

(2) It is easy to see that the vertices of the triangulation can be colored red, green and blue so that every triangle has vertices of all colors.

(3) There always exists at least one red *arborescence*: a directed connected tree connecting an outside red vertex to all inside red vertices with one arrow pointing into each inside red vertex. Every arrow first crosses a black and then a white triangle. In our illustration the red arborescence is just a path but it can of course be a more complicated tree.

(4) At this point we can already construct a partial Tutte matching: match interior red vertices to white triangles right before them in the arborescence. We indicate this by small red dots in these white triangles.

(5) Construct another connected red tree by connecting blue and green vertices by edges which are not intersected by the red arborescence.

(6) Shrink the red tree leaf-by-leaf and on every step match a vertex from which the leaf is removed to a white triangle adjacent to the leaf. We indicate the matching by small green and blue dots in these white triangles.

This completes construction of the matching and the proof of the theorem. □

10 Further remarks

Returning to the general case of factorization $\omega_C(p_1+\cdots+p_n)=L\otimes\widetilde{L}$, we write $d=\deg L=g+k-1$, where k is an expected dimension of $H^0(C,L)$, known in the physical context as helicity. When $k>2$, the line bundle L itself does not determine a map $C\to\mathbb{P}^1$; one also needs to choose a two-dimensional subspace in $H^0(C,L)$, ie a pencil of divisors. There are several ways to turn this set-up into a problem about geometry of linear systems. One approach is to consider a diagram

$$\begin{array}{ccc} \mathcal{G} & \xrightarrow{\ \mathbf{\Lambda}\ } & M_{0,n} \\ \downarrow & & \\ \mathrm{Pic}^d\, C & & \end{array}$$

where all arrows are rational maps, the vertical map is generically a Grassmannian fibration with fiber $G(2,H^0(C,L))$, and the horizontal map sends a pencil into images of marked points in $\mathbb{P}^1$. While there is no natural probability distribution on $\mathcal{G}$, one can still ask about properties of the map $\mathbf{\Lambda}$, for example about its degree if it is generically finite, which happens if $g+2(k-2)=n-3$, ie $n=g+2k-1$.

Another approach is to consider maps $\varphi_L: C\to\mathbb{P}^{k-1}$ given by complete linear systems instead of maps to $\mathbb{P}^1$ given by pencils. This gives a rational map

$$\mathrm{Pic}^d\, C \overset{\Lambda}{\dashrightarrow} X(k,n),$$

where $X(k,n)$ is the moduli space of n points in $\mathbb{P}^{k-1}$ modulo PGL_k; see [Keel and Tevelev 2006; Schaffler and Tevelev 2022; Tevelev 2007] for the background on this space and its compactifications.

With this definition, we can again view the volume form on $\mathrm{Pic}^d C$ as a multivalued meromorphic scattering amplitude form on $X(k,n)$, at least if the map Λ is generically finite, which happens if $g = n(k-1)-k^2+1$, ie if $n = g/(k-1)+k+1$. Another advantage is that the duality between bundles L and $\widetilde{L}$ is manifest: we have

$$\widetilde{d} = \deg \widetilde{L} = (2g-2+n)-(g+k-1) = g+(n-k)-1 = g+\widetilde{k}-1,$$

where $\widetilde{k} = n-k$. In fact we have a commutative diagram

$$\begin{array}{ccc} \mathrm{Pic}^d C & \xrightarrow{\simeq} & \mathrm{Pic}^{\widetilde{d}} C \\ {\scriptstyle\Lambda}\downarrow & & \downarrow{\scriptstyle\widetilde{\Lambda}} \\ X(k,n) & \xrightarrow{\simeq} & X(n-k,n) \end{array}$$

with rational vertical arrows. Indeed, the Gale duality $X(k,n) \simeq X(n-k,n)$ corresponds to the pairing $(U \subset V) \longleftrightarrow (U^\perp \subset V^*)$ between subspaces of $\mathbb{C}^n$, and global sections of L and $\widetilde{L}$ are indeed perpendicular, due to the residue theorem.

10.1 Example The first non-MHV case is the following "666 puzzle". Let C be a genus-4 curve with 6 marked points $p_1, \dots p_6$. A choice of a degree-6 line bundle $L \in \mathrm{Pic}^6 C$ realizes C as a 6-nodal sextic in $\mathbb{P}^2$ with 6 marked points. This gives a generically finite rational map Λ from $\mathrm{Pic}^6 C$ to $X(3,6)$, which has dimension 4. What is the degree of Λ? An easier case for $k=3$ would be to consider nodal genus 2 quartics in $\mathbb{P}^2$ with 5 marked points, but by the Gale duality this case is equivalent to the MHV case $g=k=2$, so the degree of Λ will be 4.

In the rest of this section we show that, in the maximally degenerate case, our scattering amplitude form on $X(k,n)$ (which is isomorphic to $M_{0,n}$ in the MHV case $k=2$) is equivalent to the leading singularity form of the scattering amplitude on the Grassmannian $G(k,n)$ as described in [Arkani-Hamed et al. 2016]. It is convenient to pass to the $(\mathbb{C}^*)^{n-1}$-torsor $\widehat{\mathrm{Pic}}\, C \to \mathrm{Pic}\, C$, which parametrizes line bundles L along with trivializations $t_i : L|_{p_i} \simeq \mathbb{C}$ for $i = 1, \dots, n$. This automatically gives trivializations $\widetilde{t}_i : \widetilde{L}|_{p_i} \simeq \mathbb{C}$ such that $t_i \otimes \widetilde{t}_i$ is the canonical trivialization $\omega_C(p_1+\cdots+p_n)|_{p_i} \simeq \mathbb{C}$ given by the residue. The choice of global sections $s_\alpha \in H^0(C,L)$ and $\widetilde{s}_{\widetilde{\alpha}} \in H^0(C,\widetilde{L})$ for $\alpha, \widetilde{\alpha} = 1,2$ gives spinor 2-vectors $\lambda_i = t_i(s_\alpha|_{p_i})$ and $\widetilde{\lambda}_i = \widetilde{t}_i(\widetilde{s}_\alpha|_{p_i})$ such that each (external) momentum can be written as $\boldsymbol{p}_i = \lambda_i \widetilde{\lambda}_i^T$. The change of trivializations corresponds to the action of the little torus $(\mathbb{C}^*)^n$ by $\lambda_i \mapsto t_i \lambda_i$ and $\widetilde{\lambda}_i \mapsto t_i^{-1}\widetilde{\lambda}_i$.

We have a commutative diagram

$$\begin{array}{ccc} \widehat{\mathrm{Pic}}^{\vec{d}}\, C & \overset{\hat{\Lambda}}{\dashrightarrow} & G(k,n) \\ \downarrow & & \downarrow{\scriptstyle\pi} \\ \mathrm{Pic}^{\vec{d}}\, C & \overset{\Lambda}{\dashrightarrow} & X(k,n) \end{array}$$

Here $\hat{\Lambda}(L, t_1, \dots, t_n)$ is the row space of the matrix $\big(t_i(s_j|_{p_i})\big)_{i=1,\dots,n;\, j=1,\dots,k}$, where $s_1, \dots, s_k$ is a basic of $H^0(C,L)$, and π is a (rational) quotient map by the little torus acting on the Grassmannian. Being

a torsor over $\mathrm{Pic}^{\vec{d}}\, C$, $\widehat{\mathrm{Pic}}^{\vec{d}} C$ also carries a canonical volume form, and writing it down as a multivalued form on $G(k,n)$ in Plücker coordinates is equivalent to writing a scattering amplitude form on $X(k,n)$.

We specialize to the maximally degenerate case. Let v be the number of irreducible components of C, ie the number of vertices of the on-shell diagram, and let i be the number of internal edges. Then $\dim \widehat{\mathrm{Pic}}^{\vec{d}} C = g+n-1 = 2v-i$. Furthermore, $\widehat{\mathrm{Pic}}^{\vec{d}} C$ has a presentation as a quotient torus

$$\widehat{\mathrm{Pic}}^{\vec{d}} C \simeq \widehat{\mathrm{Pic}}^{\vec{d}} C^{\nu}/(\mathbb{C}^*)^i \simeq (\mathbb{C}^*)^{2v}/(\mathbb{C}^*)^i,$$

defined as follows. The restriction of L to every irreducible component of C (equivalently, every connected component of the normalization C^{ν}) is either $\mathbb{O}_{\mathbb{P}^1}(1)$ (for black vertices) or $\mathbb{O}_{\mathbb{P}^1}$ (for white vertices). In either case, choose its trivialization at three special points of that component and use these trivializations to glue a line bundle on C from the line bundle on the normalization. The action of the torus $(\mathbb{C}^*)^i$ comes from simultaneously rescaling trivializations at two points of C^{ν} that glue to the same node of C. The standard dlog form on $(\mathbb{C}^*)^{2v}/(\mathbb{C}^*)^i$ then gives the formula [Arkani-Hamed et al. 2016, (4.41)] for the leading singularity of the scattering amplitude. Various delta-functions in this formula simply encode the fact that choosing the spinor variables λ_i (resp. $\widetilde{\lambda}_i$) corresponds to choosing a two-dimensional subspace in $H^0(C,L)$ (resp. in the Gale-dual $H^0(C,\widetilde{L})$, orthogonal of $H^0(C,L)$).

References

[Alexeev 2004] **V Alexeev**, *Compactified Jacobians and Torelli map*, Publ. Res. Inst. Math. Sci. 40 (2004) 1241–1265 MR

[Araujo and Casagrande 2017] **C Araujo**, **C Casagrande**, *On the Fano variety of linear spaces contained in two odd-dimensional quadrics*, Geom. Topol. 21 (2017) 3009–3045 MR

[Araujo et al. 2021] **C Araujo**, **T Fassarella**, **I Kaur**, **A Massarenti**, *On automorphisms of moduli spaces of parabolic vector bundles*, Int. Math. Res. Not. 2021 (2021) 2261–2283 MR

[Arbarello et al. 1985] **E Arbarello**, **M Cornalba**, **P A Griffiths**, **J Harris**, *Geometry of algebraic curves, I*, Grundl. Math. Wissen. 267, Springer (1985) MR

[Arkani-Hamed et al. 2015] **N Arkani-Hamed**, **J L Bourjaily**, **F Cachazo**, **A Postnikov**, **J Trnka**, *On-shell structures of MHV amplitudes beyond the planar limit*, J. High Energy Phys. 2015 (2015) art. id. 179 MR

[Arkani-Hamed et al. 2016] **N Arkani-Hamed**, **J Bourjaily**, **F Cachazo**, **A Goncharov**, **A Postnikov**, **J Trnka**, *Grassmannian geometry of scattering amplitudes*, Cambridge Univ. Press (2016) MR

[Bauer 1991] **S Bauer**, *Parabolic bundles, elliptic surfaces and* SU(2)*–representation spaces of genus zero Fuchsian groups*, Math. Ann. 290 (1991) 509–526 MR

[Beauville 1990] **A Beauville**, *Jacobiennes des courbes spectrales et systèmes hamiltoniens complètement intégrables*, Acta Math. 164 (1990) 211–235 MR

[Biswas et al. 2010] **I Biswas**, **Y I Holla**, **C Kumar**, *On moduli spaces of parabolic vector bundles of rank* 2 *over* $\mathbb{CP}^1$, Michigan Math. J. 59 (2010) 467–475 MR

[Buch and Pandharipande 2021] **A S Buch**, **R Pandharipande**, *Tevelev degrees in Gromov–Witten theory*, preprint (2021) arXiv 2112.14824

[Castravet and Tevelev 2012] **A-M Castravet**, **J Tevelev**, *Rigid curves on $\overline{M}_{0,n}$ and arithmetic breaks*, from "Compact moduli spaces and vector bundles" (V Alexeev, A Gibney, E Izadi, J Kollár, E Looijenga, editors), Contemp. Math. 564, Amer. Math. Soc., Providence, RI (2012) 19–67 MR

[Castravet and Tevelev 2013] **A-M Castravet**, **J Tevelev**, *Hypertrees, projections, and moduli of stable rational curves*, J. Reine Angew. Math. 675 (2013) 121–180 MR

[Cela 2023] **A Cela**, *Quantum Euler class and virtual Tevelev degrees of Fano complete intersections*, Ark. Mat. 61 (2023) 301–322 MR

[Cela and Lian 2023] **A Cela**, **C Lian**, *Generalized Tevelev degrees of $\mathbb{P}^1$*, J. Pure Appl. Algebra 227 (2023) art. id. 107324 MR

[Cela et al. 2022] **A Cela**, **R Pandharipande**, **J Schmitt**, *Tevelev degrees and Hurwitz moduli spaces*, Math. Proc. Cambridge Philos. Soc. 173 (2022) 479–510 MR

[Ceyhan 2007] **Ö Ceyhan**, *Graph homology of the moduli space of pointed real curves of genus zero*, Selecta Math. 13 (2007) 203–237 MR

[Ciocan-Fontanine and Kim 2010] **I Ciocan-Fontanine**, **B Kim**, *Moduli stacks of stable toric quasimaps*, Adv. Math. 225 (2010) 3022–3051 MR

[Dolgachev 2012] **I V Dolgachev**, *Classical algebraic geometry: a modern view*, Cambridge Univ. Press (2012) MR

[Farkas and Lian 2023] **G Farkas**, **C Lian**, *Linear series on general curves with prescribed incidence conditions*, J. Inst. Math. Jussieu 22 (2023) 2857–2877 MR

[Farkas et al. 2003] **G Farkas**, **M Mustaţă**, **M Popa**, *Divisors on $\mathcal{M}_{g,g+1}$ and the minimal resolution conjecture for points on canonical curves*, Ann. Sci. École Norm. Sup. 36 (2003) 553–581 MR

[Gross and Harris 1981] **B H Gross**, **J Harris**, *Real algebraic curves*, Ann. Sci. École Norm. Sup. 14 (1981) 157–182 MR

[Halphen 1882] **G H Halphen**, *Mémoire sur la classification des courbes gauches algébriques*, Gauthier, Paris (1882)

[Hartshorne 1977] **R Hartshorne**, *Algebraic geometry*, Grad. Texts in Math. 52, Springer (1977) MR

[Huisman 2001] **J Huisman**, *On the geometry of algebraic curves having many real components*, Rev. Mat. Complut. 14 (2001) 83–92 MR

[Jacobi 1846] **C G J Jacobi**, *Über eine neue Methode zur Integration der hyperelliptischen Differentialgleichungen und über die rationale Form ihrer vollständigen algebraischen Integralgleichungen*, J. Reine Angew. Math. 32 (1846) 220–226 MR

[Keel and Tevelev 2006] **S Keel**, **J Tevelev**, *Geometry of Chow quotients of Grassmannians*, Duke Math. J. 134 (2006) 259–311 MR

[Lian 2023] **C Lian**, *Asymptotic geometric Tevelev degrees of hypersurfaces*, Michigan Math. J. (online publication December 2023)

[Lian and Pandharipande 2021] **C Lian**, **R Pandharipande**, *Enumerativity of virtual Tevelev degrees* (2021) arXiv 2110.05520 To appear in Ann. Sc. Norm. Super. Pisa Cl. Sci.

[Marian et al. 2011] **A Marian**, **D Oprea**, **R Pandharipande**, *The moduli space of stable quotients*, Geom. Topol. 15 (2011) 1651–1706 MR

[Moon and Yoo 2016] **H-B Moon**, **S-B Yoo**, *Birational geometry of the moduli space of rank* 2 *parabolic vector bundles on a rational curve*, Int. Math. Res. Not. 2016 (2016) 827–859 MR

[Mukai 2003] **S Mukai**, *An introduction to invariants and moduli*, Cambridge Stud. Adv. Math. 81, Cambridge Univ. Press (2003) MR

[Mumford 1984] **D Mumford**, *Tata lectures on theta, II: Jacobian theta functions and differential equations*, Progr. Math. 43, Birkhäuser, Boston (1984) MR

[Oda and Seshadri 1979] **T Oda**, **C S Seshadri**, *Compactifications of the generalized Jacobian variety*, Trans. Amer. Math. Soc. 253 (1979) 1–90 MR

[Opie and Scheidwasser 2009] **M Opie**, **I Scheidwasser**, *Hypertree divisor database*, electronic reference (2009) Available at `https://people.math.umass.edu/~tevelev/HT_database/database.html`

[Pauly 1996] **C Pauly**, *Espaces de modules de fibrés paraboliques et blocs conformes*, Duke Math. J. 84 (1996) 217–235 MR

[Schaffler and Tevelev 2022] **L Schaffler**, **J Tevelev**, *Compactifications of moduli of points and lines in the projective plane*, Int. Math. Res. Not. 2022 (2022) 17000–17078 MR

[Seppälä 1991] **M Seppälä**, *Moduli spaces of stable real algebraic curves*, Ann. Sci. École Norm. Sup. 24 (1991) 519–544 MR

[Seppälä and Silhol 1989] **M Seppälä**, **R Silhol**, *Moduli spaces for real algebraic curves and real abelian varieties*, Math. Z. 201 (1989) 151–165 MR

[Shafarevich 2013] **I R Shafarevich**, *Basic algebraic geometry, I: Varieties in projective space*, 3rd edition, Springer (2013) MR

[Simpson 1994] **C T Simpson**, *Moduli of representations of the fundamental group of a smooth projective variety, I*, Inst. Hautes Études Sci. Publ. Math. 79 (1994) 47–129 MR

[Skorobogatov 2010] **A Skorobogatov**, *del Pezzo surfaces of degree* 4 *and their relation to Kummer surfaces*, Enseign. Math. 56 (2010) 73–85 MR

[Tevelev 2007] **J Tevelev**, *Compactifications of subvarieties of tori*, Amer. J. Math. 129 (2007) 1087–1104 MR

[Tutte 1975] **W T Tutte**, *Duality and trinity*, from "Infinite and finite sets, III" (A Hajnal, R Rado, V T Sós, editors), Colloq. Math. Soc. János Bolyai 10, North-Holland, Amsterdam (1975) 1459–1472 MR

Department of Mathematics and Statistics, University of Massachusetts
Amherst, MA, United States

`tevelev@umass.edu`

Proposed: Richard P Thomas
Seconded: Mark Gross, Jim Bryan

Received: 16 October 2020
Revised: 8 August 2023

GEOMETRY & TOPOLOGY

msp.org/gt

See inside back cover or msp.org/gt for submission instructions.

The subscription price for 2025 is US $865/year for the electronic version, and $1210/year (+$75, if shipping outside the US) for print and electronic. Subscriptions, requests for back issues and changes of subscriber address should be sent to MSP. Geometry & Topology is indexed by Mathematical Reviews, Zentralblatt MATH, Current Mathematical Publications and the Science Citation Index.

Geometry & Topology (ISSN 1465-3060 printed, 1364-0380 electronic) is published 9 times per year and continuously online, by Mathematical Sciences Publishers, c/o Department of Mathematics, University of California, 798 Evans Hall #3840, Berkeley, CA 94720-3840. Periodical rate postage paid at Oakland, CA 94615-9651, and additional mailing offices. POSTMASTER: send address changes to Mathematical Sciences Publishers, c/o Department of Mathematics, University of California, 798 Evans Hall #3840, Berkeley, CA 94720-3840.

GT peer review and production are managed by EditFLOW® from MSP.

PUBLISHED BY

mathematical sciences publishers

nonprofit scientific publishing

http://msp.org/

GEOMETRY & TOPOLOGY

Volume 29 Issue 6 (pages 2783–3343) 2025